GLAVNOE UPRAVLENIE GIDROMETEOROLOGICHESKOI SLUZHBY PRI
SOVETE MINISTROV SSSR · VYSOKOGORNYI GEOFIZICHESKII INSTITUT

Main Administration of the Hydrometeorological Service, USSR Council of Ministers ·
High-Altitude Geophysics Institute

G. K. Sulakvelidze, N. I. Glushkova
and L. M. Fedchenko

FORECASTING OF HAIL, THUNDERSTORMS AND SHOWERS

(Prognoz grada, groz i livnevykh osadkov)

Gidrometeorologicheskoe Izdatel'stvo
Leningrad 1970

Translated from Russian

Israel Program for Scientific Translations
Jerusalem 1977

Cat. No. 61218 6
ISBN 0 7065 1563 2

Translated by IPST staff

Printed and bound by Keterpress Enterprises, Jerusalem

CONTENTS

PREFACE

In the late 1950s, a team of researchers at the High-Altitude Geophysics Institute began to investigate the formation of convective clouds, the ultimate goal being to develop methods for the modification of hail processes.

A specific feature of the project was its combined approach to the subject, thanks to which it was possible to cope not only with the above-mentioned problem but also with many other interesting topics in the physics of the atmosphere and related areas. Among these were radar techniques for the detection of hail cells, estimation of rainfall by radar, fall speeds of systems of particle in viscous media, determination of the coefficient of capture for particles of commensurate dimensions, design of a non-fragmenting anti-aircraft shell, artificial crystallization of supercooled drops, and so on.

The investigations finally produced a model of a shower-producing cloud which, though it may not describe the whole complex of processes involved in the formation and occurrence of convective precipitation, does at any rate provide a satisfactory answer to many of the questions with which we were concerned, regarding the origin of hail and heavy showers.

To test this model, a hail-prediction technique was worked out. The high accuracy of the technique permitted further research progress, including a number of short-range forecasts.

The book consists of five chapters. Chapter 1 considers the thermodynamic conditions for the onset of convection, which lead to the formation and fall of shower-type precipitation and hail. Chapter 2 describes a hail-forecasting method, Chapter 3 a method for forecasting showers, and Chapter 4 a method for forecasting thunderstorm phenomena. Finally, in Chapter 5 we present some practical recommendations for the preparation of forecasts, as well as results of tests of the various methods, carried out in various Soviet institutions.

Section 1.6 was written by G. K. Sulakvelidze, Section 3.8 by N. M. Mal'bakhova and Section 3.9 by Ya. G. Sulakvelidze. Chapter 4 makes use of material kindly made available by V. A. Belentsova.

The authors take this opportunity to express their gratitude to one of the pioneers of cloud research in the Soviet Union, B. V. Kiryukhin, for his invaluable comments, which were largely responsible for the publication of this book. Thanks are also due to N. L. Lebedeva of the Moscow State University, to three senior workers at Gidromet-tsentr SSSR, A. A. Bachurina, N. P. Luzhnaya and S. I. Ponomarenko, for their useful remarks, and to all our colleagues at the High-Altitude Geophysics Institute who participated in the preparation of the monograph.

This book is intended for meteorology students at hydrometeorological institutes, universities and other institutes of learning, scientific workers, graduate students and specialists working in cloud physics and artificial weather control.

The authors hope that the book will be of assistance to practical meteorologists in actual forecasting work, and also to researchers engaged in the study of convective clouds and the thermodynamics of the atmosphere.

INTRODUCTION

The prediction of hail, shower-type precipitation and thunderstorms is of essential importance for the national economy of the Soviet Union. Unfortunately, the methods currently available for this purpose cannot always meet the increasing demands of the economy.

Extensive research in cloud physics, conducted at the High-Altitude Geophysics Institute, has produced new methods for the prediction of these phenomena. Historically speaking, the origin of this research and the impetus for its development lie in the need for techniques to combat hail damage.

The considerable losses inflicted by hail on agriculture in the southern regions of the USSR presented meteorologists with the task of working out some method to modify the natural process. In contradistinction to most other countries engaged in this problem, Soviet researchers first concentrated their attention on the mechanism of formation of shower-type precipitation and hail. Since 1965, investigations have been under way at the High-Altitude Geophysics Institute under the supervision of one of the present authors /88/. A specific feature of this research is the interdisciplinary approach to the project, which called for the participation of workers in various specialized fields. Special attention was also paid to a highly diversified complex of terrestrial and airborne observations of the development of shower- and hail-producing clouds, made under field conditions.

In the course of this work, an attempt was made to determine the dependence between stratification, which determines the thermodynamic conditions, and the formation of precipitation. That the latter depends on the energy of air instability due to high lapse rates and humidities was established back in the 19th century /41, 42, 43/. Various attempts have been made to discern a correlation between the magnitude of the instability energy and the type of precipitation. Investigations have shown that positive instability energy, as established by morning radiosonde, does not necessarily imply the occurrence of precipitation.

Researches carried out at our Institute /24, 91/ have shown that in order to establish a correlation between instability energy and precipitation one should consider not the entire instability energy, defined on the emagram by the area between the curve of state and the stratification curve, but only the instability energy of what is known as the active cloud-formation layer (that is to say, the layer of air between the condensation level and the level at which the updrafts attain maximum speed).

By analyzing the instability energy of the active cloud-formation layer and atmospheric stratification, one can estimate the kind of precipitation forming in a cloud and also predict the fall to earth of hail and shower-type precipitation.

In 1960, the first attempts were made to corroborate the hail-formation mechanism evolved at the Institute on the basis of atmospheric stratification data. It was found that these data provide not only an answer to the question of whether hail can form in a cloud, but also an estimate of the size of the hailstones that will reach the ground. Afterwards, this method for the prediction of potential hail formation was developed by one of the present authors into a method for the prediction of hailstorms.

It is extremely difficult to work out a method predicting the amount of shower-type precipitation, as its origin and evolution is conditioned by a host of factors, all of which must be taken into account. Attempts on the part of several investigators to solve this problem by establishing a correlation between the amount of precipitation and vertical velocities have failed to yield reliable results.

Current techniques for predicting the amount of shower-type precipitation schematically reflect conceptions as to the accumulation of moisture and its resolution as rain. In view of the complexity of the process whereby moisture accumulates in a cloud, the structure of cumulonimbus clouds and the distribution in time and space of updrafts, one cannot hope for a practically acceptable method unless more detailed consideration is taken of the interaction between the various factors that produce and maintain the process.

A method for predicting the amount of shower-type precipitation has been worked out in connection with the need to estimate the resolution time of air instability. It was the solution of the latter problem, combined with data of atmospheric stratification and certain ideas as to the formation mechanism of shower-type precipitation, that enabled one of the present authors to propose a method to this end.

Both of the above-mentioned methods are based on our conceptions as to the origin of shower-type precipitation and hail and as to the thermodynamic conditions that must prevail in the air for these phenomena to begin and develop.

Belentsova, in her method of storm prediction, adopted a slightly different approach. The high reliability of the previous two methods suggested that all processes associated with convective clouds are conditioned primarily by thermodynamic conditions. On this basis, Belentsova tried to identify the atmospheric conditions most favorable for storm formation. She found that in middle latitudes storms can be predicted unambiguously on the basis of atmospheric stratification data.

For clouds to form the air must contain condensation nuclei, while hail formation requires crystallization nuclei and storm formation implies the presence of electrical charges. It seems that in middle latitudes the conditions necessary for any of these processes, that is to say, the requisite amounts of the relevant cloud, hail- or storm-producing elements, depend solely on the prevailing thermodynamic conditions. Formulas for hailstone size or amount of precipitation are derived using data on the initial and terminal thermodynamic state of the atmosphere. The quality of the practical results obtained has shown that this approach yields high accuracy in predicting hail, storms, and the amount of shower-type precipitation. It has now gained wide acceptance in practical work at Gidrometsluzhba.*

* [Main Administration of the Hydrometeorological Service, USSR Council of Ministers.]

True, this principle is useless if one wishes to describe how the air changes from one state to another or, consequently, to demonstrate the mechanisms of moisture accumulation and electric-charge formation. However, the present authors were not concerned with this formulation of the problem.

Many investigators, such as List and Braham, hold that an exhaustive systematic model of the shower cloud must include both the microphysical and the thermodynamic processes that take place in the cloud. Without disputing this obvious truth, we would nevertheless point out that many data on shower-type precipitation may be obtained by a more detailed analysis of the thermodynamic processes occurring in shower clouds. For example, apart from the above-mentioned successes, a knowledge of the change in the overall energy of the atmosphere before and after the development of convection enables one to calculate the amount of precipitation reaching the ground, to estimate the total quantity of water generated by the cloud, and so on.

Particular attention should be paid to the role of water vapor in the development of convection, as its condensation causes rapid ascent of air in convective clouds.

Chapter 1

CONDITIONS FOR FORMATION OF CONVECTIVE CLOUDS

1.1. CRITERIA OF AIR STABILITY

A convective cloud forms in the atmosphere as a result of updrafts. The ascent of bodies of air may be highly localized in a homogeneous air mass (intra air-mass processes), or it may extend over considerable territories, incorporating air masses possessing properties other than those of the original one (frontal processes).

There are two principal methods of treating the ascent of air masses; the first, the "parcel" method, determines whether ascent is at all possible, while the "slice" method considers the actual ascent. The parcel method considers the vertical adiabatic displacement of an air "parcel," that is to say, an elementary volume of air, unmixed with the surrounding air which is in static equilibrium. If the forces acting on the parcel after displacement tend to return it to its former position, the air is in stable equilibrium. If the forces accelerate the vertical motion of the parcel, the air is in unstable equilibrium; and if the net total force acting on the parcel is zero one has a state of neutral equilibrium. Since friction comes into play only after the onset of motion, it may be neglected to a first approximation in stability calculations. The assumption that the environment is in static equilibrium implies that the vertical components of the force of gravity and the pressure gradient are in equilibrium, according to the equation

$$-g-\frac{1}{\rho}\frac{\partial P}{\partial z}=0. \tag{1.1}$$

If the air parcel is not in static equilibrium, it follows from Newton's second law that the resultant of the two forces induces a vertical acceleration dw/dt:

$$\frac{dw}{dt}=-g-\frac{1}{\rho}\frac{\partial P}{\partial z}, \tag{1.2}$$

where ρ is the density of the displaced parcel. One considers quasistatic processes in which $P'=P$, i. e., the pressure acting on the accelerated parcel is equal to the pressure of the environment at that level. Eliminating the pressure gradient from the equation and expressing ρ in terms of temperature, we obtain

$$\frac{dw}{dt}=\frac{g(T_w-T)}{T}. \tag{1.3}$$

The right-hand side of Eq. (1.3) may be expressed in terms of the lapse rate /181/:

$$\frac{dw}{dt} = \frac{g}{T}\left[(T_0 - T_{w_0}) + (\gamma - \gamma_w)(z - z_0)\right], \tag{1.4}$$

where γ_w and γ are the lapse rates for the rising particle and the surrounding air, respectively, w is the vertical speed of displacement of the parcel, g the acceleration of gravity, T_0 and T_{w_0} the temperatures of the surrounding air and the rising parcel at the initial level, and z the height which the parcel attains from height z_0.

If the parcel is displaced from the level $z=0$, where it is in thermal equilibrium with the surrounding air ($T_0=T_{w_0}$), then

$$\frac{dw}{dt} = \frac{gz(\gamma - \gamma_w)}{T}. \tag{1.5}$$

Hence the medium is in unstable equilibrium if $\gamma>\gamma_w$, in neutral equilibrium if $\gamma=\gamma_w$, and in stable equilibrium if $\gamma<\gamma_w$.

The parcel method provides a certain estimate of the vertical stability of the air. However, it presupposes that the surrounding air is undisturbed; this assumption is undoubtedly artificial, since the updraft will necessarily create a compensating subsidence in the environment.

This downdraft is taken into consideration in the slice method, first proposed by Bjerknes /116/ and further developed by Peterssen /156/ and Shishkin /94—101/. The basic assumptions of the method are as follows: the downdraft occurs along the dry adiabat, the updraft along the wet adiabat; the quantity of rising air is equal to the quantity of falling air, $\frac{\partial T}{\partial x} = \frac{\partial T}{\partial y} = 0$, and there are no horizontal movements of air.

According to the slice method, the possible onset of convection depends on the ratio of the mass M' of rising air to the mass M'' of falling air /116, 63/.

The stratification is stable if

$$\frac{\gamma - \gamma_w}{\gamma_d - \gamma} < \frac{M'}{M''}, \tag{1.6}$$

neutrally stable if

$$\frac{\gamma - \gamma_w}{\gamma_d - \gamma} = \frac{M'}{M''}, \tag{1.7}$$

and unstable if

$$\frac{\gamma - \gamma_w}{\gamma_d - \gamma} > \frac{M'}{M''}, \tag{1.8}$$

where γ_d is the dry adiabatic rate.

Thus:

a) If $\gamma - \gamma_w < 0$, $\gamma_d - \gamma > 0$, i. e., $\gamma < \gamma_w$ the air is stable irrespective of the horizontal extent of the motion (masses M' and M'').

b) If $\gamma > \gamma_d$, then, whatever the horizontal extent of the motion (i.e., for any mass M'), the air is unstable. In these two cases the slice method yields the same conclusions as the parcel method.

c) If $\gamma = \gamma_w$, the air is stably stratified. Here the slice method implies a stability criterion other than that of the parcel method.

d) If $\gamma_w < \gamma < \gamma_d$, which occurs quite commonly, stability depends not only on the magnitudes of γ, γ_w and γ_d but also on the mass ratio M'/M''. If the air is originally at rest and subsequently an updraft is triggered, kinetic energy of vertical motion will develop only if the masses of rising and falling air satisfy the inequality

$$\frac{\gamma - \gamma_w}{\gamma_d - \gamma} > \frac{M'}{M''}. \tag{1.9}$$

If γ is close to γ_w, the air is unstable only to small disturbances (mass M'). Isolated cumulus clouds will be observed, with weak vertical development. If γ is much larger than γ_w, the air is unstable for a wide range of parcel sizes. Cumulus clouds will cover a large portion of the sky, showing both weak and strong vertical development.

Research at the High-Altitude Geophysics Institute has provided some additional insight on the development of convection when $\gamma_w < \gamma < \gamma_d$. Two new concepts were introduced. First, the "cloud-formation layer" is defined to be the layer between the condensation level z_c and the convection level z_v. The boundaries of the layer may be determined by the air pressure P_c and P_v at these levels. The "active cloud-formation layer" is that between the condensation level z_c and the level at which the temperature difference between the stratification curve T_m and the curve of state T_{wm} is a maximum. This is the level of maximum updraft speed w_m in the cloud and we therefore call it the "maximum speed level." The boundaries of this layer are also determined by the appropriate pressures P_c and P_m.

It was found that a criterion for the development of convection may be based not only on the ratio of masses of ascending and descending air currents, but also on the mass ratio of the air layers participating in convection, which in turn are determined from stratification data.

When $\gamma \geqslant \gamma^*$, where

$$\gamma^* = \gamma_w + (\gamma_d - \gamma_w) \frac{P_m - P_v}{P_c - P_v}, \tag{1.10}$$

convection may develop; when

$$\gamma < \gamma^* \tag{1.11}$$

the air is stably stratified.

It is clear from (1.10) that if the vertical thickness of the layer between the maximum speed and convection layers is small, i. e., the mass m_2 of this layer approaches 0, then γ^* is approximately equal to the wet adiabatic lapse rate; in other words, the condition for development of convection may be determined by the "parcel" method, provided the "parcel" is assumed to be rising in saturated air.

Another consequence of (1.10) is that if the lower (active) and upper layers contain equal masses of air, i. e., $P_m - P_v = P_0 - P_m$, then

$$\gamma' = \gamma_w + \frac{(\gamma_d - \gamma_w)}{2} = \frac{\gamma_d + \gamma_w}{2}, \tag{1.12}$$

since $P_c - P_v = P_c - P_m + P_m - P_v$, so that the criterion for convection is

$$\gamma \geqslant \frac{\gamma_w + \gamma_d}{2}. \tag{1.13}$$

A similar convection criterion was worked out by Shishkin /98/: the special case of (1.10) with $m_1 = m_2$. In the great majority of cases $m_2 < m_1$, so Shishkin's inequality is a sufficient but by no means necessary condition for convection to occur. Convective clouds will form whenever the lapse rate γ satisfies inequality (1.10). Thus inequality (1.10) provides an unambiguous answer to the question of when a convective cloud may form, regardless of the horizontal extent of the convection cell.

One of the present authors had previously obtained slightly different expressions for the equilibrium lapse rate; these formulas were essentially the same as (1.10), though more cumbersome.

1.2. DISTRIBUTION OF UPDRAFT SPEED IN A CONVECTIVE CLOUD

The main factors in formation of convective clouds are updrafts, which determine both hail size and the amount of shower-type precipitation from the cloud. Investigations of vertical air currents at the High-Altitude Geophysics Institute since 1956 have produced some quite detailed material, providing a good basis for a model of the updraft distribution in time and space. When a cumulus cloud begins to form, the masses of air ascend in separate thermals (bubbles). The size of the bubbles and their internal temperature distribution have been studied in detail by Vul'fson. Typical of this early stage of convection are Cu hum. and Cu med. clouds. As the cloud grows, the thermals overtake one another and aggregate in the central region of the cloud, forming an updraft. If the air is highly unstable, thermals may aggregate below the condensation level, and the updraft occupies the central portion of the cloud, from its base to the upper levels (Cu cong., Cb).

In thick convective clouds, beginning approximately from the cloud base, the speed of the updraft increases almost linearly with height, reaching a maximum before the cloud top and then decreasing linearly to the top /8, 11/ (Figure 1). According to observational data, the maximum updraft speed in a cumulonimbus cloud is 25—60 m/sec /102/. Downdrafts appear in the cloud when precipitation begins.

The level at which the updraft speed w_m reaches its maximum is denoted by z_m. Experimental data show that the updraft speed is the following function of z:

$$w(z) = w_0 + (w_m - w_0)\frac{z}{z_m} \quad \text{at} \quad 0 \leqslant z \leqslant z_m; \tag{1.14}$$

$$w(z) = w_m\left(1 - \frac{z - z_m}{z_t - z_m}\right) \quad \text{at} \quad z_m \leqslant z \leqslant z_t, \tag{1.15}$$

where w_0 is the updraft speed at the condensation level $z=0$ (the cloud base) and z_t the height of the cloud top.

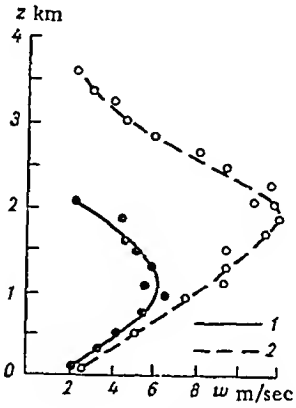

FIGURE 1. Distribution according to height of updraft speed in a convective cloud.

1) Cu and Cu med., 2) Cu cong. and Cb.

Calculations have shown that w_m may be derived from stratification data by either parcel or slice method; later we shall discuss this in more detail. The updraft speed depends on the instability energy of the air. It is worth mentioning that Eqs. (1.14) and (1.15) are in good agreement with theoretical calculations of Gutman /31/ and Lebedev /55/, and they have also been corroborated by data from experimental observations in middle latitudes (Caucasus, Transcaucasia, Middle Asia) and in the tropics (Cuba).

Data of some investigators /20, 21, 76, 120, 159/ have shown that updraft speed depends not only on height but also on the lateral distance from the cloud center. It also varies with time. In Cu the updraft speed w is at most several m/sec (Bibilashvili) or less, while some U. S. investigators have shown that in mature Cb it may reach as much as 65 m/sec /102, 103/.

Figure 2 is a plot of updraft speed vs. time (curve 1), based on data of Shishkin /98/, fitted to an analytical distribution curve (curve 2).

Analytically, the draft curve is a parabola:

$$w(t) = w_m - \frac{t^2}{2P}, \tag{1.16}$$

where t is the time, P a parameter whose value, as derived from boundary conditions, is $3.8 \cdot 10^3$ sec/cm.

The updraft speed decreases along the horizontal cross section from the center of the air jet to its boundary.

Vul'fson /20, 21/ has shown that the maximum updraft speed varies over the cloud cross section as follows (Figure 3):

$$w(x) = w_m\left(1 - \frac{x^2}{R^2}\right)^{\frac{1}{2}}, \qquad (1.17)$$

where x is the distance from the cloud center to the point at which the speed is measured and R is the cloud radius.

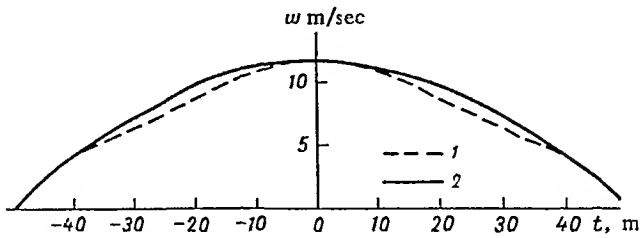

FIGURE 2. Updraft speed vs. time.

An analysis of data of Pinus (Figure 4) shows that the updraft speed may be expressed as a function of the horizontal cloud coordinate as follows (Figure 3):

$$w(x) = w_m e^{-ax^2}, \qquad (1.18)$$

where $a = 2 \cdot 10^{-12}$ cm^{-2}.

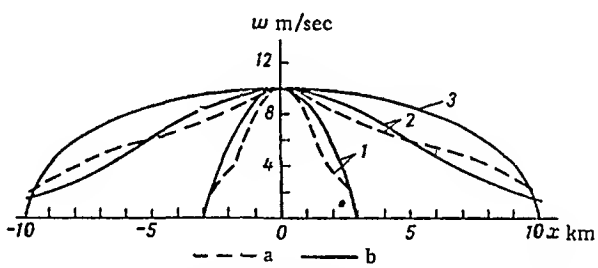

FIGURE 3. Updraft speed vs. horizontal cross section of cloud

a) experimental, b) analytical. Data of: 1) Byers and Braham, 2) Pinus, 3) Vul'fson.

Byers and Braham /120/, analysing experimental data, obtained the following equation for the updraft speed:

$$w(x) = w_m - \frac{x^2}{2P}, \qquad (1.19)$$

where $P = 4.5 \cdot 10^8$ cm/sec.

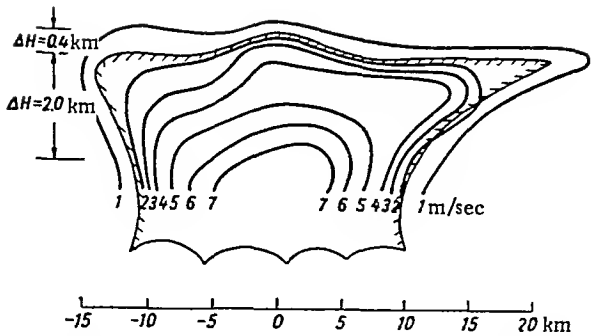

FIGURE 4. Distribution of updraft speed in upper part of cumulonimbus, after Pinus.

The updraft curves plotted in Figure 3 on the basis of Eqs. (1.17), (1.18) and (1.19) show that the updraft speed in a cloud is a complicated function of the parameters and of time, so the problem of the behavior of updraft speed still lacks a definitive solution.

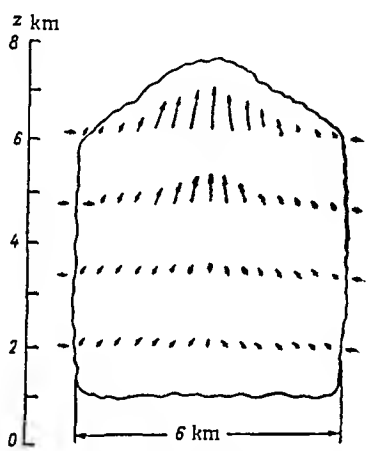

FIGURE 5. Distribution of updraft speed in cumulonimbus, after Byers and Braham.

1.3. ACTIVE CLOUD-FORMATION LAYER

Up to the present, no quantitative correlation has been determined between the instability energy and the process of cloud formation. Attempts to correlate the instability energy E with the amount of precipitation or with hailstone size have not been successful /4/. For this reason, many authors use updraft speed or cloud thickness rather than instability energy when calculating various cloud parameters.

The hailstone radius may be calculated from stratification data /87, 90/, according to the equation

$$r = \frac{w_m^2}{\beta^2}, \tag{1.20}$$

where β is a parameter depending on the density of the hailstone and on the density of the air at the fall-out level of the hail; a good average value for this parameter is $2.3 \cdot 10^3\ \text{cm}^{\frac{1}{2}} \cdot \text{sec}^{-1}$; w_m is the calculated updraft speed.

The maximum amount of precipitation from one convective cloud may be determined from the formula

$$Q_m \leqslant \frac{w_m^2}{2g} \rho_m. \tag{1.21}$$

where ρ_m is the air density at level w_m.

Equations (1.20) and (1.21) show that the hailstone radius and the amount of showery precipitation depend on the square of the maximum updraft speed, i. e., on the instability energy of the air masses.

The instability energy is defined as the work done by the buoyant force in displacing unit mass of air from one level to another. Its analytical expression is

$$E = -2.3R\int_{P_1}^{P_2}(T_w - T)\,d\ \log\ P. \tag{1.22}$$

where R is the specific gas constant of dry air, $T_w - T$ the temperature difference between the rising air and the surrounding air. The right-hand side of this equation is represented on the aerological diagram by the area between the isobars P_1 and P_2, the wet adiabat and the stratification curve.

Research at out Institute has revealed a clear-cut correlation not between the entire instability energy and the cloud parameters, but only between that part of the energy enclosed between the condensation level and the calculated maximum speed level, on the one hand, and the cloud parameters, on the other.

The thermal energy E_m convertible into kinetic energy when an air mass rises above the condensation level is given by

$$E_m = -2.3R\int_{P_c}^{P_m}(T_w - T)d\ \log\ P. \tag{1.23}$$

The difference between Eqs. (1.22) and (1.23) is that in the first the integration is performed in the pressure interval $[P_c, P_v]$, i. e., from the condensation level to the convection level, whereas in the second it extends from the condensation level to the level of maximum updraft speed, i. e., over the active cloud-formation layer. We now define the efficiency η by

$$\eta = \frac{T_c - T_{dm}}{T_c}. \tag{1.24}$$

where T_c is the temperature at the condensation level, T_{dm} the temperature at level w_m, rising along the dry adiabat from the condensation level. The equation then becomes

$$E_m = -2{,}3R\eta\int_{P_c}^{P_m}(T_w - T)\,d\log P. \qquad (1.25)$$

For water to accumulate in a convective cloud, creating conditions for shower-type precipitation, it is necessary that $w_m > v_d$, where v_d is the fall speed of a drop of radius $r = 2.5$ to 3.0 mm. A suitable value of v_d is 10^3 cm/sec. Thus the kinetic energy of a unit mass of air for which $w_m > v_d$ must be more than $5 \cdot 10^5$ erg. Consequently, the inequality

$$E_m > 5 \cdot 10^5 \text{ erg} \qquad (1.26)$$

is a precondition for shower-type precipitation. In order to establish a relationship between the instability energy, calculated from the emagram, and weather phenomena, it is convenient to introduce a dimensionless parameter Σ, defined as the ratio of the kinetic energy of the air mass between levels z_c and z_m to the critical kinetic energy necessary for formation and falling of shower-type precipitation:

$$\Sigma = \frac{E_m}{5 \cdot 10^5}. \qquad (1.27)$$

Summarizing the above discussion, we may now state that the condition for shower-type precipitation from a cumulonimbus cloud is

$$\Sigma \geqslant 1. \qquad (1.28)$$

It has been shown that in middle latitudes the energy condition for formation of hail in a convective cloud is that the updraft speed exceed 20 m/sec. This can happen only when

$$\Sigma \geqslant 2.5. \qquad (1.29)$$

This condition is necessary, but not sufficient, for hail to fall, since the hail may melt away as it falls through the warm layers of air if the hailstone radius is less than 1.5 cm. If the radius is larger, melting has a negligible effect on hailstone size, even when the zero isotherm is as much as 4 km above the surface. On the basis of these data, it has been concluded that a necessary and sufficient condition for hail to fall from cumulonimbus is

$$\Sigma \geqslant 5.5. \qquad (1.30)$$

Thus, when the instability energy of the air is positive, the correlation between the type of weather phenomenon and the instability energy may involve four cases:

a) $\Sigma < 1$: no shower-type precipitation formed;

b) $1 \leqslant \Sigma < 2.5$: rain;

c) $2.5 \leqslant \Sigma < 5.5$: shower-type precipitation, possible hail;

d) $\Sigma \geqslant 5.5$: hail.

In case (c) one must determine r from (1.20) and reckon with melting of hail below the zero isotherm /90/. Thus, the dimensionless parameter Σ

enables one to predict the type of precipitation reaching the surface. Analysis of the instability energy of the active layer in 28 actual hailstorms in the North Caucasus in 1966 and 1967 showed that in all cases $2.6 \leqslant \Sigma < 20$, in full agreement with conditions (c) and (d) above. However, we shall show below that the potential formation of storms and hail depends not only on the instability energy but on other parameters of convective clouds. Thus, the methods used in predicting these phenomena are based on their mechanism of formation, using data on atmospheric stratification. What is new here is the conclusion that all processes in the air are influenced by the instability energy of the active layer, not by that of the entire convection layer as believed till recently /4/.

1.4. CALCULATION OF MAXIMUM UPDRAFT SPEED

All processes taking place in a cloud depend on the instability energy of the active layer, and hence on the maximum updraft speed w_m. We calculate w_m by the slice method. As shown by Eq. (1.9), instability of the layer depends not only on the lapse rate but also on the mass ratio of rising and falling air. There are several methods to determine updraft speed; of these we mention those of Lebedeva /56, 57, 58/ and Shishkin /97/, and the parcel method /156, 181/.

In Lebedeva's method, one determines ΔT_{av}, that is, the average deviation of the curve of state from the stratification curve (Figure 6), on surfaces at steps of 100 mb. Using ΔT_{av}, one calculates the average speed of the convection current. At $\Delta T_{av} = 60°$, for example, $w_{av} = 13$ m/sec /56/. However, the occurrence of hail and other harmful phenomena depends not on the average of the updraft speed but on its maximum. The parcel method computes the updraft speed without allowance for heat lost due to the compensating subsidence of dry air /156, 181/. At each level, the force acting on a parcel of density different from that of the environment is the resultant of the Archimedes buoyant force and the force of gravity:

$$\frac{d^2z}{dt^2} = g\frac{T_w - T}{T}. \tag{1.31}$$

The work performed by this force in displacing the particle over an elementary distance dz is

$$dA = g\frac{T_w - T}{T}dz. \tag{1.32}$$

This work is converted into kinetic energy of the rising particle. Standard equations of statics yield an expression for the updraft speed:

$$d\frac{w^2}{2} = 2.3R(T_w - T)\,d(-\log P), \tag{1.33}$$

where the appearance of the factor 2.3 is due to the passage from natural to decimal logarithms.

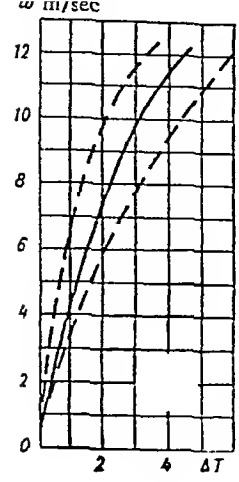

FIGURE 6. Average speed w of convection current vs. average deviation of curve of state from stratification curve.

On the aerological diagram, $d(\log P)$ is the differential of the ordinate:

$$-d(\log P) = dy. \tag{1.34}$$

Finally /63/,

$$\frac{w^2}{2} = B\int_{z_1}^{z_2}(T_w - T)\,dy, \tag{1.35}$$

where $B=2.3$ is a constant.

The equation for the kinetic energy per unit mass of cloud air is

$$\frac{w^2}{2} = \eta c_p\,|(T_w - T) - S_0(T_w - T_d)|. \tag{1.36}$$

If clouds develop at several atmospheric levels, with different lapse rates γ_k, the formula for the kinetic energy per unit mass cloud air may be written

$$\frac{w^2}{2} = \eta c_p \sum_{k=1}^{n} |(T_w - T)_k - S_0(T_w - T_d)_k|. \tag{1.37}$$

where T is the absolute temperature of the air at the cloud base, T_k the temperature at the upper boundary of the k-th layer, T_{a_k} and T_{d_k} the temperatures of the air rising from the lower boundary of the k-th layer to its upper boundary along the wet and dry adiabats, respectively, c_p the specific heat of air at constant pressure, η the efficiency of conversion of thermal to kinetic energy, S_0 the optimum cloudiness for maximum release of convective energy, calculated by Shishkin as

$$S_0 = 1 - \sqrt{\frac{\sum_{k=1}^{n}(T - T_d)_k}{\sum_{k=1}^{n}(T_w - T_d)_k}}\,. \tag{1.38}$$

However, Shishkin's formula was obtained for the speed at which the cloud tower grows and is the averaged speed of ascent of the cloud mass in the layer. A new formula for the maximum updraft speed has therefore been proposed /25, 26/. The kinetic energy of the layer is generated by the difference in heat content between rising and falling air. The temperature difference between rising and falling air may be calculated by Bjerknes' slice method, which reckons with the compensating subsidence of the surrounding air that accompanies the ascent of an air parcel. Bjerknes considers a horizontal layer of air which is large enough to include several rising and falling currents.

At the initial moment, the air temperature and pressure are assumed to be uniform in the horizontal plane. By assumption, the rising mass M' is equal to the falling mass M, in keeping with the law of mass conservation. Then $A'w' = -Aw$, where A' and A are the areas of the layers covered by masses M' and M, respectively, and w' and w their average vertical velocities. The rising mass follows the wet adiabat, the falling mass the dry adiabat. The temperature excess ΔT (Figure 7) of the rising mass over the falling mass is

$$\begin{aligned}\Delta T &= T_{t'} - T_t = (T_A - \gamma_w w' t) - (T_w - \gamma_d w' t) = \\ &= T_A - T_w + (\gamma_d w' - \gamma_w w') t = -\gamma (w - w') t + \\ &+ (-\gamma_w w' + \gamma_d w') t = w' t \left| (\gamma - \gamma_w) - \frac{A'}{A} (\gamma_d - \gamma) \right|. \end{aligned} \tag{1.39}$$

and since $w't = \Delta z$, we have

$$\Delta T = \Delta z \left| (\gamma - \gamma_w) - \frac{A'}{A} (\gamma_d - \gamma) \right|. \tag{1.40}$$

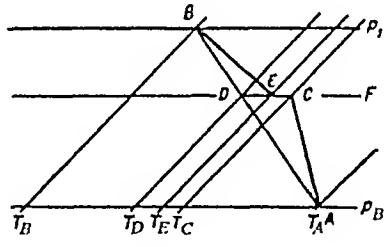

FIGURE 7. Effect of compensating currents in environment.

AB — initial temperature distribution; AC — adiabat of rising air; EB — adiabat of falling air; $T_C - T_E$ — temperature excess in rising air at pressure P /156/.

Investigations by Bjerknes, Peterssen and others have shown that thick convective clouds occupy from 0.1 to 0.2 of space, while the downdrafts w are distributed over an infinitely large area. Therefore, to determine the temperature difference between the rising and falling air, one assumes that the ratio $\frac{A'}{A}$ is equal to zero, and

$$\Delta T = T_c - T_w = \Delta z (\gamma - \gamma_w). \tag{1.41}$$

Thus, if the stratification curve is divided into several layers and the wet adiabat considered for each separately, the temperature difference between rising and falling air may be determined from Eq. (1.41).

The level of maximum updraft speed is identified with the level at which $\sum_{i=1}^{n}(T_w - T)_i = \Delta T_{max}$. Above this level the updraft speed decreases, owing to the penetration of air into layers of negative buoyancy. The energy accumulated in the lower active layer is consumed to overcome the resistance of the downdrafts above this level. The change of heat content per unit column of air in the layer from the surface to the maximum updraft speed level is

$$\Theta = c_p \int_{z_0}^{z_m} (T_w - T)\rho dz. \tag{1.42}$$

This integral may be expressed as a sum of two integrals:

$$\Theta = c_p \left[\int_{z_0}^{z_c} (T_w - T)\rho\, dz + \int_{z_c}^{z_m} (T_w - T)\rho\, dz_1 \right], \tag{1.43}$$

where z_c is the condensation level. Since

$$\int_{z_0}^{z_c} (T_w - T)\rho dz \ll \int_{z_c}^{z_m} (T_w - T)\rho\, dz, \tag{1.44}$$

we may assume that

$$\Theta = c_p \int_{z_c}^{z_m} (T_w - T)\rho\, dz \tag{1.45}$$

By standard equations,

$$\rho\, dz = -\frac{dP}{g}; \tag{1.46}$$

hence

$$\Theta = c_p \int_{P_c}^{P_m} (T_w - T)\left(-\frac{dP}{g}\right). \tag{1.47}$$

The development of a convective cloud is envisaged as a thermodynamic cycle, consisting of two adiabats (air rising in the cloud along the wet adiabat and a compensating subsidence of surrounding air along the dry adiabat) and two isobars (horizontal displacements completing the cycle). The efficiency of this process is $\eta = T_c - T_{dm}/T_c$.

The kinetic energy of a single air column taking part in the convection process, at the maximum speed level, is

$$E_{kin} = \bar{\rho} z_m \frac{w_m^2}{2}. \tag{1.48}$$

It is assumed that the pressure in the surrounding air is equal to that in the cloud — the process is quasistatic. The pressure at any level is given by a standard formula:

$$\int_{P_0}^{P_m} dP = -\int_{z_0}^{z_m} g\rho dz. \tag{1.49}$$

where z_0 is the absolute geopotential at sea level, which is zero; hence

$$z_m = \frac{P_0 - P_m}{g\rho}. \tag{1.50}$$

Inserting this into Eq. (1.48), we obtain

$$E_{kin} = \frac{P_0 - P_m}{g} \frac{w_m^2}{2}. \tag{1.51}$$

Comparing Eqs. (1.47) and (1.51), we obtain the following formula for the updraft speed of a single column of air:

$$\frac{w_m^2}{2} = \eta c_p \int_{P_c}^{P_m} (T_w - T)\left(-\frac{dP}{P_0 - P_m}\right). \tag{1.52}$$

Multiplying and dividing the integrand by P, we obtain

$$\frac{w_m^2}{2} = \eta c_p \int_{P_c}^{P_m} (T_w - T)\left[-\frac{P\,dP}{P(P_0 - P_m)}\right].$$

Taking the constant $\overline{P}$ through the integral sign and assuming that $(P_0 - P_m)$ and $\overline{P}$ are equal (for thick convective clouds this assumption causes a small error in the calculated updraft speed), we obtain

$$\frac{w_m^2}{2} = \eta c_p \int_{P_c}^{P_m} (T_w - T)\left(-\frac{dP}{P}\right). \tag{1.53}$$

The integral on the right of this equation may be solved using the aerological diagram. The geometrical representation of the integral is the area between the curve of state, the stratification curve, and the isobars P_c and P_m.

On the aerological diagram,

$$\int_{y_1}^{y_2} x\,dy = \int_{P_c}^{P_m} (T_w - T)\,d(-\log P) = \frac{g(z_2 - z_1)}{R \cdot 2.3}. \tag{1.54}$$

In view of (1.53) and (1.54), the formula for the maximum speed is

$$\frac{w_m^2}{2} = \eta c_p \Delta T_m (\log P_c - \log P_m). \tag{1.55}$$

where ΔT_m is the maximum deviation of the curve of state from the stratification curve.

Table 1 lists some maximum speeds as calculated by the different methods we have discussed. It is clear from the table that the w_m values calculated by Shishkin's formula and by Eq. (1.55) are almost the same. Nevertheless, there is a difference, which increases when the z_m level becomes lower. For example, if z_c is at 2000—2100 m and z_m at 4000 m, then Eq. (1.55) yields w_m as 3.5 m/sec, whereas Shishkin's formula gives 16 m/sec, which is close to the value given by the parcel method. This is probably because Shishkin's method disregards the mass of the convecting layer.

It should be noted that the calculation of maximum speed and temperature at this level is based on the stratification curve of the air mass in which the clouds are developing. For reliable prediction, therefore, it is highly important to extend the stratification curve in time right up to maximum cloud development. This may be done as described in the handbook /78/.

TABLE 1. Comparison of maximum speeds calculated by the slice method (1), the parcel method (2), and Eq. (1.55).

Date	Time, hrs	Height, m	Condensation level, m	w_m m/sec		
				(1)	(1.55)	(2)
24/V 1964	3	5600	2500	23	15.5	25.0
4/VI	15	7400	2100	33.2	33.0	42.0
11/VI	9	7400	1500	32	30	38
28/VI	3	4000	2100	16	3.5	14.9
2/VII	3	7400	2100	26	28	34.5
1/VIII	3	4000	1500	22,0	13.5	24.4
2/VIII	3	6200	1700	20	20	28.4
6/VI 1965	9	5600	1500	24,0	26.0	33.0

The updraft speed depends on the liquid water content of the surrounding air. If the environment air is dry, some of it will penetrate the developing cumulus cloud and move along with the cloud air. This entrainment changes the lapse rate. The mixed air is unsaturated and contains liquid water from the cloud. Upon saturation, some of this water evaporates and as a result the temperature of the cloud air falls. This temperature drop in the updraft may create negative buoyancy, which retards further growth of the cloud /74, 75/.

Slavin /85/, attempting to allow for the entrainment of surrounding air in the growing cloud when determining air instability, proposes the following formula for the terminal temperature of the rising air when cooled by entrainment of surrounding air, from the condensation level up to 500 mb:

$$\Delta T = k\Delta T_a \frac{S_{a\,av} - S_{0\,av}}{1 + 0.2S_{a\,av}}, \qquad (1.56)$$

where ΔT is the temperature difference between the surrounding air and the rising air (including the entrained air), $S_{0\,av}$ the specific humidity at the 700 mb surface, $S_{a\,av}$ the maximum specific humidity at the 700 mb surface,

ΔT_a the deviation of the temperature of the adiabatically rising air from the temperature of the surrounding air. The factor k depends on ΔT_a:

$$k \approx 0.6 - 0.02\Delta T_a, \tag{1.57}$$

$$\Delta T = \Delta T_a. \tag{1.58}$$

where ΔT is an indicator of the magnitude of convective instability, ΔT_a the temperature difference between the cloud air and the surrounding medium on the assumption that the convection process is adiabatic. In Slavin's method one assumes that the condensation level lies near the 850 mb surface and the temperature at the condensation level is given by

$$T_c = T_{850} + 1. \tag{1.59}$$

Eq. (1.59) was derived from statistical studies. Allowance is made for vertical currents caused by friction at the earth's surface by introducing a correction to the temperature of the 500 mb surface, depending on the curvature of the isobars near the ground. Faust has calculated that if the isobars show cyclonic curvature of radius 1000, 500 or 250 km, the temperature at the 500 mb level (during the period from 3 hours before maximum development of convection, corrected for isobar curvature) drops by 1.0, 1.4 or 2°, respectively; if the curvature is anticyclonic the temperature is raised by the same amount. When the isobars are straight the correction is $\Delta T'' = 0$.

Austin /113/ proposed a simple graphical method to allow for entrainment of air. This involves mixing of the rising air with the surrounding air at constant pressures, followed by saturation of the mixture in a wet-bulb thermometer process. Figure 8 illustrates the process. The point A corresponds to air in the cloud at a certain level P_1, where it is mixed with the surrounding air. Two parts of rising air are mixed with one part of environmental air. The unsaturated mixture is represented by the point B. The air is then saturated at constant pressure by evaporation of water previously condensed in the rising current. The saturated mixture is represented by the point C. Without entraining any air from the environment, the air rises along the wet adiabat CA'. After mixing with surrounding air EE' at pressure P_2, the state is represented by the point B', while C' represents the saturated mixture in terms of its wet-bulb temperature. Thus, instead of the wet adiabat AD, which would correspond to rising air in the absence of entrainment processes, the change of state of the air when these processes are included is represented by the curve CC'. The dryer the rising air, the lower is the instability energy of the air mass.

According to U. S. studies of storm structure in 1945 /117/, air is entrained by growing cumulus clouds at a rate of approximately 100% for an ascent of 400 mb, i. e., the mass of rising air is doubled for every 400 mb. The mixing process must fit these results. For example, in rising 100 mb, one part of surrounding air is mixed with four parts of rising air, but over 200 mb there is one part of surrounding air for two parts of rising air. The entrainment rates are derived from empirical data. It follows from this discussion that allowance must be made for entrainment of dry air into the cloud when calculating maximum updraft speeds.

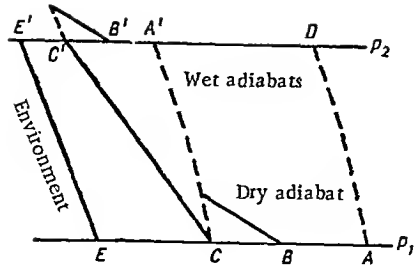

FIGURE 8. Entrainment of surrounding air into a cloud.

According to data of Stommel /166/ and Malkus /145 – 147/, the maximum entrainment for air bubbles of diameter 500 m ranges from $0.5 \cdot 10^{-5}$ to $1.0 \cdot 10^{-5}$ cm^{-1}; per 100 mb, this gives 0.8 parts of surrounding air to one part of rising air. Other entrainment figures are obtained for bubbles of different diameters. The best method seems to be Austin's since (among other things) Slavin's method allows for entrainment in the layer from 850 to 500 mb only, whereas maximum updraft speed may occur at any isobaric surface. Glushkova /25, 26/ calculates entrainment of the surrounding air by layers. The temperature difference ΔT_m in Eq. (1.55) is replaced by a parameter $\Delta T'_m$ including entrainment. The basic assumption is that, for each ascent of 200 mb, two parts of rising air are mixed with one part of surrounding air. The method is illustrated in Figure 9. Investigations of the development of cumulus clouds have shown that entrainment is maximal when the average relative humidity in the layer 850 – 500 mb is less than a certain critical value, taken to be 60%. Therefore, if the average relative humidity in the 850 – 500 mb layer is less than 60%, the construction of the curve of state must include entrainment (mixing adiabat), replacing ΔT_m in Eq. (1.55) by $\Delta T'_m$ – the maximum deviation of the curve of state from the stratification curve with allowance for entrainment. The magnitude and level of maximum updraft speed given by Eq. (1.55) agree with experimental data.

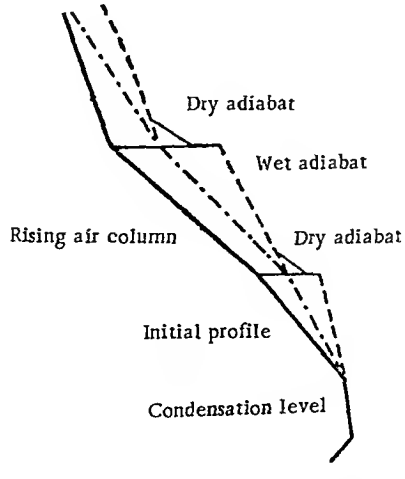

FIGURE 9. Construction of curve of state with allowance for entrainment of surrounding air into the cloud.

During a 1960 expedition to the Kabardino-Balkar Autonomous SSR, observations of the development of thick convective clouds were made at the village of Chegem (700 m above sea level). An artillery range-finder was used. The azimuth, angle of elevation and range were measured at 15–30 second intervals. The maximum growth rate of the cloud tower for the period from May 28 to June 15, 20 m/sec, was measured at 12 noon on June 14. As the updraft speed in the cloud is double the growth rate of the tower /169, 32/, it was possible to compare the observed maximum tower growth rate with the figure calculated by Eq. (1.55). The results are shown in Table 2.

TABLE 2. Comparison of measured maximum growth rate of cloud tower with calculated maximum updraft speed in cloud, 1964

Date	Time	w_m, m/sec	
		meas.	calc.
29/V	14 35	7.0	19.3
8/VI	9 00	11.0	19.7
10/VI	10 00	9.3	22.1
14/VI	12 00	20.0	42.8

In addition, during the 1964 anti-hail expedition to the Kabardino-Balkar Autonomous SSR, several observations were made of the zone of maximum radar reflection from the cloud, during a period extending from development up to beginning of precipitation. The level of maximum radar reflection was found to coincide with the level of maximum updraft speed (Table 3). It is thus reasonable to conjecture that measurement of radar reflection is a good way to calculate maximum updraft speed. Speeds calculated by this method are quite close to those observed in convective clouds.

TABLE 3. Comparison of calculated maximum speed level with measured level of maximum radar reflection, 1964

Date	Time	Level, m	
		meas.	calc.
31/V	11 54	5900	5600
	15 25	5800	
3/VI	13 20	5600	5600
	20 15	5700	
4/VI	14 05	5500	7400
	14 05	5500	
	15 00	7400	
5/VI	14 45	7200	7400
10/VI	17 21	7200	7400
12/VI	15 20	7000	7400
15/VI	17 16	5600	5000
2/VII	14 53	6000	5600

1.5. EFFECT OF VERTICAL WIND SHEAR ON DEVELOPMENT OF CONVECTION

A change of weather at any point is conditioned by diverse factors, which may be divided into three groups: 1) circulation, 2) transformation and 3) orographic factors /36/.

Circulation factors effect weather changes via movements of air masses, atmospheric fronts, cyclones and anticyclones, as well as evolution of the latter. It is these that cause the most significant weather changes. They may be classified as inertial, advective and dynamic factors. While advective changes of meteorological elements take place in both steady and unsteady (accelerated) air, dynamic factors are operative mainly in the latter, and also in the development of convective motion in the atmosphere.

Recent research has shown that convection may set in and develop not only as a result of nonuniform heating of different portions of the earth's surface (thermal convection), but also owing to dynamic causes (of a thermal and dynamic nature); the latter produce small-scale turbulence which, under certain conditions, will develop into organized convection. Major factors in this process are friction with the underlying surface and sharp changes of the wind-speed vector with height.

The development of atmospheric convection requires a certain reserve of positive instability energy, which depends on the distribution with height of the air temperature and the wind-speed vector, as these determine the nature of air turbulence. The characteristic measure of turbulence is the Richardson number Ri, which may be found from the equation /47/

$$Ri = \frac{g}{T} \frac{(\gamma_d - \gamma)}{\left(\frac{\partial u}{\partial z}\right)^2}, \tag{1.60}$$

where T is the average air temperature in the layer, $\frac{\partial u}{\partial z}$ is the vector of the change in wind speed with height. The critical Richardson number is unity. At $Ri < 1$ turbulence will arise and intensify at $Ri > 1$ it will weaken. It is evident from (1.60) that the sign of the Richardson number depends on the relationship between the dry adiabatic rate and the actual lapse rate. We have $Ri = 0$ at $\gamma = \gamma_a$, i. e., at neutral equilibrium in free air, $Ri > 0$ at $\gamma < \gamma_a$, i. e., at stable equilibrium relative to the temperature regime. Thus, when the air is stable we may find $Ri \geqslant 1$. Consequently, a necessary condition for the air to be unstable is the inequality

$$\frac{g}{T} \frac{\gamma_d - \gamma}{\left(\frac{\partial u}{\partial z}\right)^2} < 1. \tag{1.61}$$

Hence

$$\gamma_d - \gamma < \frac{T}{g} \left(\frac{\partial u}{\partial z}\right)^2.$$

Finally,

$$\frac{T}{g} \left(\frac{\partial u}{\partial z}\right)^2 + \gamma > \gamma_d. \tag{1.62}$$

According to this inequality, an air mass may become unstable when the lapse rate γ is less than the dry adiabatic rate γ_d, but in combination with the characteristic dynamic factor $\frac{T}{g}\left(\frac{\partial u}{\partial z}\right)^2$ it must exceed γ_d. This means that when the wind changes sharply with height, convection may arise at low γ values, when the thermal stratification is stable if the dynamic factor is ignored. One might say that the variation of wind with height introduces a certain additional thermal gradient, which is added to the lapse rate γ and is therefore called the "thermal equivalent of vertical wind gradient." When the wind changes slowly with height, this factor is small and may be disregarded; but if, say, $\frac{\partial u}{\partial z} = 2$ m/sec per 100 m height, its value is $1.0-1.3°$ per 100 m. If the air contains a significant amount of moisture, it will suffice if the left member of Eq. (1.62) exceeds the wet adiabatic rate γ_w. This increases the importance of the dynamic factor, which causes the total gradient to move even more rapidly to a value sufficient for vertical movement. Dynamic factors may stimulate the development of convection even when there is no possibility of thermal convection as an independent process; conversely, thermal convection may set in under conditions of weak dynamic convection. In many cases these processes reinforce and complement one another, presenting a unified picture of atmospheric instability.

On the basis of his experimental work, Skvortsov /84/ proposed what he calls a multistage model of convection. First, usually in the morning, small-scale turbulence carries water vapor and heat from the ground to a height of 50 – 100 m. At this height vortices (thermals) form on a larger scale and these continue to raise heat and moisture to greater heights.

Recent investigations /17, 18, 46, 72, 73, 90, 172, 173/ have shown that vertical wind shear has a very considerable influence on the development of convection. There is at present no generally accepted view of the role of wind shear in this context, though it is generally agreed that it cannot be considered in isolation from updraft speed.

On the one hand, upon increasing wind shear, the degree of turbulence increases, and there is a higher probability of large "turbulent masses" which may initiate convection. On the other hand, theoretical studies by Turbnikov /19/ have indicated that strong wind shears inhibit the growth of convection. In each specific case, therefore, whether convection will actually ensue depends on the mutual relationship of the different effects of vertical wind shear.

Gandin /24/ states that if the wind direction in a convective layer does not change with height but wind speed does change, there arise two-dimensional cells (Figure 10), shaped like elongated bands of ascending and descending motion lying along the wind direction. But if both the direction and the speed of the wind change sharply with height, it is apparent that this cellular circulation, which, together with gravity-shear waves, is a form of organized medium-scale atmospheric movement, cannot possibly take place.

Vorob'eva and Trubnikov /19, 93/ investigated the structure of cellular convection when the wind vector can be resolved into two components: one independent of height, the other possessing a vertical profile of nonzero curvature. Calculations showed that one then obtains two-dimensional cells lying along the second component of the wind vector.

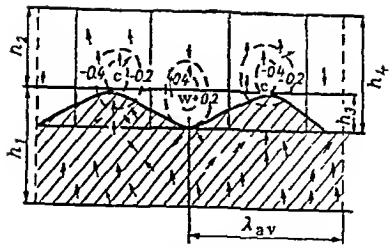

FIGURE 10. Scheme of cellular circulation near upper boundary of stratified cloud (after Zaitsev and Ledokhovich).

h_1) cloud thickness; h_2) thickness of subcloud layer with marked cellular circulation (100—200 m); h_3) thickness of cloud layer with marked cellular circulation (50—100 m); h_4) layer of air showing periodic horizontal fluctuations of temperature (150—300 m); w) warm; c) cold; wavelength $\lambda_{av} \approx 800$ m.

We must also dwell briefly on the effect of wind shear on periodic motion in the air. Periodic motion is one of a number of quite widespread types of medium-scale motion in the air. When unstable, such motion produces vortex formations of various sizes. Some of these, such as cyclones and anticyclones, occupy considerable areas. They are formed upon disintegration of waves whose wavelengths are hundreds and even thousands of kilometers. Small-scale vortices form upon the collapse of waves of a few kilometers wavelength. An example of such short waves in the atmosphere is provided by the gravity-shear waves which form as a result of friction forces and develop thanks to the mechanical potential energy of air parcels.

Information about gravity-shear waves may be found in Laikhtman /54/, Haurwitz /132/, Gandin /22—24/, Naito /153/. Three-dimensional waves have been studied by Sekera /161/, Doi /125/ and others. According to Sekera (and also Brunt /119/ and others), whenever cloud bands were observed lying parallel to the wind, indicating waves just under the inversion layer, the lapse rate γ was found to be higher than the dry adiabatic rate γ_d. This implies the presence of vertical wind shear independent of height.

There are only few studies of waves in clear air, as the lack of visual indications makes their investigation quite difficult. Most of the data are obtained from observations of clouds at wave crests. The material is usually the fruit of airborne observations, though data from meteorological satellites have also been used. Geometrically regular cloud structures were observed in approximately 15% of cases (Vel'tishev), and cloud strips in 13% of cases. Banded (wave) structure was usually a characteristic of cumuliform clouds. The direction of the bands coincided most frequently with that of the wind near the ground, and with increasing height the wind veered relative to the bands. In the 1—2 km layer the angle between wind and bands reached ±10°. When the cloud bands were long, one usually observed lapse rates of 0.7—0.8° per 100 m (almost adiabatic), and the wind speed was higher than when the clouds were randomly distributed. In addition, in most cases the wind direction did not change with height.

Similar data have been cited in work by other authors. For example, on the basis of analysis of radar information about precipitation over Japan, Doi /125/ concluded that well-defined bands of precipitation (and hence also

of clouds) were observed in 84% of cases when there were vertical wind shears of $\frac{\partial u}{\partial z} > 3$ m/sec per 1 km, and in 55% of cases when $\frac{\partial u}{\partial z} \geq 7$ m/sec per 1 km.

Most of the cases in which there were no bands were registered on days when $\frac{\partial u}{\partial z} < 3$ m/sec per 1 km in the cloud zone. The precipitation bands were usually elongated along the wind direction when the wind was slightly veering with height, i. e., changing direction slightly. The experiments also showed that if the vertical shear of wind speed was not large, the cloud strips lay perpendicular to the wind.

It should be noted that according to Vel'tishev the mutual orientation of waves and wind depends on the temperature T, the wind speed u, the lapse rates and wind gradients, the curvature of the vertical profiles and the nature of the change in wind direction with height. He showed that the change of wind speed has less effect on the direction of the waves than the change of wind direction with height. This conclusion is somewhat at variance with the results of Sekera and Doi, according to whom the change in wind speed is decisive for the orientation of the waves.

Shmeter /18, 73, 102, 103, 111/ studied the effect of vertical motion in thick convective clouds on the wind field. To determine how the characteristics of wind disturbance near thick convective clouds depend on updraft speed, wind shear and turbulence, he conducted a numerical experiment. The result was that the magnitude of the disturbance depends primarily on updraft speed and wind shear, turbulence playing only a secondary role.

In 1959—1965, working with a specially equipped TU-104 laboratory airplane, Shmeter made several hundred wind measurements using Doppler apparatus, and measurements of updrafts using equipment to register the vertical speed and acceleration of the plane as well as the angle of pitch. On the basis of these data, he discovered certain regularities in the formation of Cb banks at high wind shears. When the external wind shear was large, the air rose behind the cloud top, and a system of waves formed ahead of the top, similar to that observed when air flows past solid obstructions. At the crests of these waves the updraft speed reached 23 m/sec, and the total thickness of the wave zone was several kilometers.

Shmeter's observations showed that the conditions at the crests of such "cloud waves" are favorable for stormy development of Cu cong., provided the tops of the latter reach the wave zone, so that a whole band of Cu clouds gradually grows in front of the "mother" cloud (cumulonimbus). The new clouds are formed in a chain-like process. The formation of banks of Cb parallel to the wind is also furthered by the induced subsidence of air in the lower regions of the atmosphere, a common occurrence ahead of rapidly moving cumulonimbus clouds.

Pastushkov /72/ used numerical integration of the hydro- and thermodynamic equations of the atmosphere to investigate the effect of (external) wind shear on the development of isolated cumulus clouds. He made three series of computations, including 13 cases which differed both as to initial instability energy E_0 and as to the magnitude of shear. His conclusions from the experiment were as follows:

1. The growth of a cumulus cloud by resolution of atmospheric instability is a nonstationary process, not only during the actual growth of the cloud but also after it has reached maturity. The main factor preventing stationarity

is the conversion of kinetic energy of convective motion into kinetic energy of turbulence.

2. From 80 to 90% of the latent heat of condensation released during convection is consumed to create potential energy of wet air and condensation products. The remaining 10—20% are divided up among the kinetic energy of convective motion and kinetic energy of turbulence. The ratio of the two factors depends on the stage of growth of the cloud. While it is growing, $E_c \geqslant E_{cr}$, while in the mature and dissipation stages $E_{cr} > E_c$.

3. The principal parameters conditioning the growth of the cumulus cloud are the initial reserve E_0 of instability energy, the external wind shear u' and the degree of turbulence.

4. The life cycle of a cumulus cloud may be divided into an active stage, which lasts about 15 min (this figure decreases with increase in E_0, increases with increase in u' and in degree of turbulence), and a dissipating stage, whose length is conditioned largely by the same factors but most significantly by the degree of convective turbulence. The entire life cycle lasts from 30 to 60 min.

5. The terminal result of convection is a new state of the atmosphere, practically free of convective motion.

Thus, almost all of the latent heat of condensation released during convection is consumed in heating the air, increasing the potential energy of moist air and condensation products and the kinetic energy of turbulence.

6. The entire range of wind shear values may be divided into three intervals as regards its influence on the growth of cumulus clouds. Thus the half-plane (u', E_0) is divided into three regions (Figure 11):

a) $|u'| < u'_{1\,cr}$ ·

b) $u'_{1\,cr} \leqslant |u'| \leqslant u'_{2\,cr}$ ·

c) $|u'| > u'_{2\,cr}$

The decisive parameter for $u'_{1\,cr}$ and $u'_{2\,cr}$ is E_0. As the latter increases, the critical shears increase. This is represented by two demarcation curves which divide the (u', E_0) plane into the three shear intervals specified above.

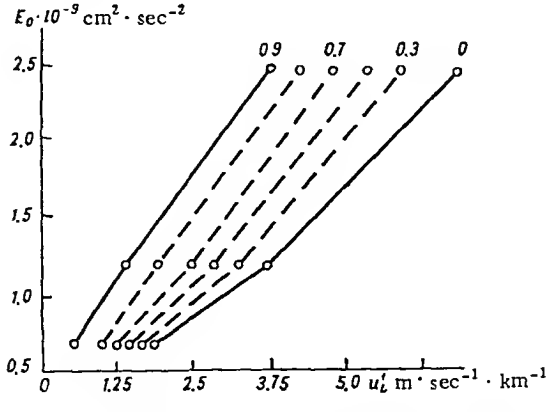

FIGURE 11. Decrease in convection expressed in terms of wind shear u'_L and initial moist-instability energy E_0.

Figures above isolines represent rates of decrease.

When $|u'| < u'_{1\,cr}(E_0)$ the wind shear, which slows down the growth of Cu, has practically no effect on the extremal characteristics of the cloud; at $u'_{1\,cr} \leqslant |u'| \lesssim u'_{2\,cr}$, the slower growth of Cu is accompanied by a decrease in its characteristics; at $|u'| > u'_{2\,cr}$ convection is either entirely suppressed or, having reached the stage of Cu, is dissipated.

It is noteworthy that as the instability energy decreases the transition from one convective regime to the other is sharpened. Pastushkov suggests that this may be one of the reasons for the predominant growth of a few isolated cumuliform clouds from the total cloud mass which remains at the fair-weather stage.

Thus, there are considerable divergences of opinion as to the influence of wind shear on the development of convection.

A. N. Koval'chuk of the High-Altitude Geophysics Institute has studied the effect of vertical wind shear on hail precipitation, as a special case of the above general discussion. This is a highly topical subject in view of the wide range of hail-suppression research being done in the USSR (see Chap. 2). We present some preliminary results of an investigation of the effect of vertical wind shear on the development of atmospheric convection, obtained at the Institute during the combined hail-suppression expedition to the Caucasus.

The results are summarized in Table 4 and Figure 12. Figure 12 shows the distribution profile of vertical wind shear u' for different types of weather. Also shown is the distribution with height of updraft speed w, calculated by Glushkova's method /25/. It should be clear from the data of Figure 12 and Table 4 that in cases of great development of Cb below the maximum speed level, wind shear reaches consider magnitudes, up to 20 m/sec per 1 km. In some cases, higher shear values are observed at 8 – 9 km, from 7 to 25 m/sec per 1 km. On the other hand, when stratification is unstable and negative wind shears are appreciable below the maximum speed level, no development of thick convective clouds was observed. These results are only preliminary.

In order to determine the effect of wind shear on the development of convection, $\frac{\partial u}{\partial z}$ was calculated from data of radiosonde observations made on and around the date of maximum convection, for singular points of the wind. The values of w_m and wind shear values in m/sec per 100 m, calculated for the subcloud layer, were plotted. This layer was selected because the major factor in the development of convection is the layer from the ground to the condensation level. It turned out that when hail fell the value of $\frac{\partial u}{\partial z}$ fluctuated from 1 to 6 m/sec per 100 m. Similar values of $\frac{\partial u}{\partial z}$ were recorded on days characterized by the development of shower-producing clouds.

It is noteworthy that, in cases showing no thermal instability, large wind shear resulted in the formation of cumulus, cumulus cong. and sometimes even cumulonimbus.

Thunderstorm phenomena were recorded at maximum speed 5 m/sec and higher, hailstorms at 15 m/sec and higher. Apparently, an increase in $\frac{\partial u}{\partial z}$ in the layer from the surface to the condensation level stimulates the onset of convection, but if there is no thermal instability above the condensation level thunderstorm and hail clouds will not develop.

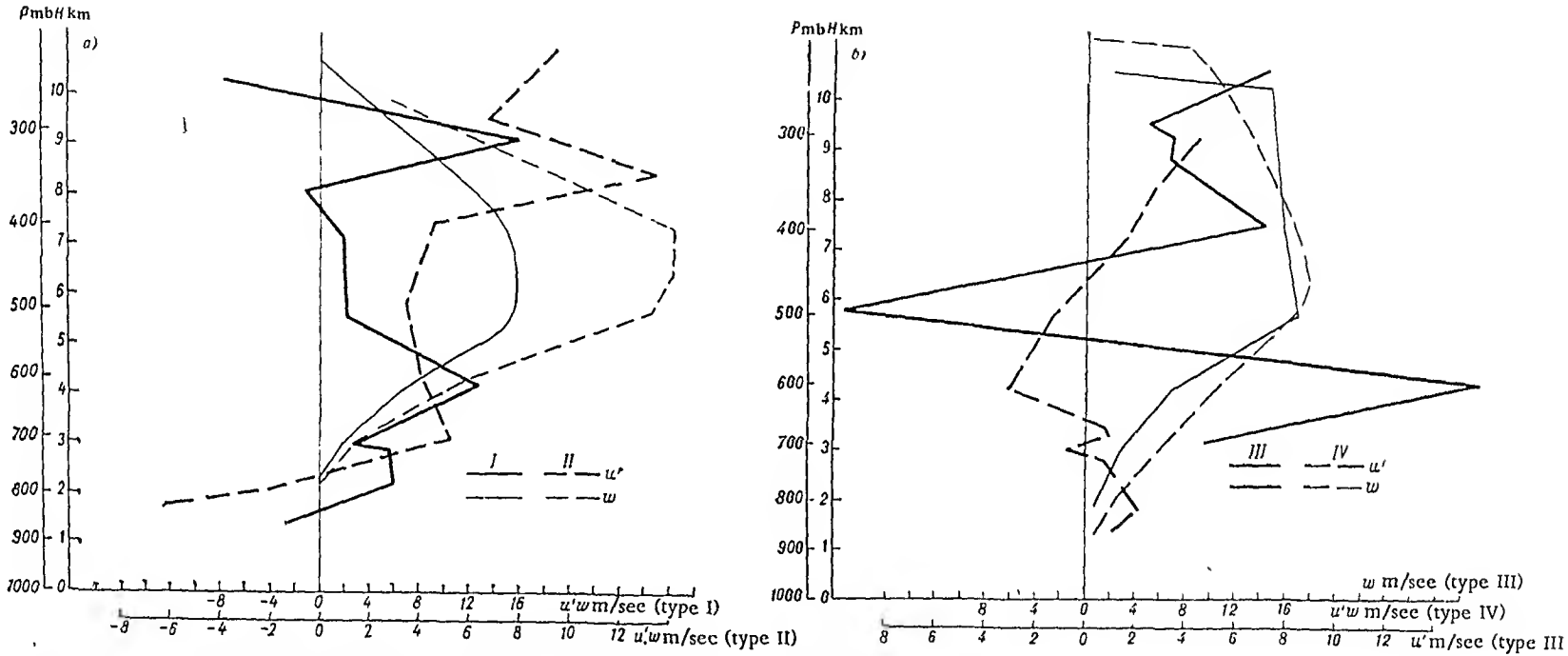

FIGURE 12. Distribution with height of vertical wind shear u' and updraft speed w, for weather types I – IV.

TABLE 4. Calculations of vertical wind shear

H km	w_m m/sec	u m/sec	$\frac{\partial u}{\partial z}$ m/sec per km	H km	w_m m/sec	u' m/sec	$\frac{\partial u}{\partial z}$ m/sec per km
			Kuba-Taba				
			May 10, 1965, 1445 hrs. Development of thick Cb, hail				
14	–	–26	–18	56	154	20	14
195	–	28	56	72	150	19	16
22	–	60	200	82	118	–12	–12
29	14	56	80	92	72	158	15
30	16	26	260	104	18	80	66
42	72	126	100				
			June 18, 1965, 1210 hrs. Development of Cb				
14	10	24	17	565	164	28	20
185	22	42	105	73	168	34	20
285	52	14	14	825	152	54	60
305	58	16	–80	925	132	90	90
33	70	20	66	105	100	26	20
345	76	14	140	110	86	80	160
425	100	60	75				
			Osetiya, Ardon				
			May 26, 1968, 1330 hrs. Development of Cb				
10	—	06	06	60	176	31	38
15	14	09	18	70	160	70	70
20	30	13	26	84	122	58	37
30	62	45	45	94	86	126	126
35	124	32	09	100	—	80	130
40	170	–42	–84	102	—	40	200
475	180	–33	–47	110	-	30	37
525	180	25	50	121	-	98	98
			Khutor Veselyi				
			July 4, 1968, 1050 hrs. Development of Cb, soft hail, 0.2 – 0.3 mm				
15	04	11	07	57	164	82	54
20	02	70	140	73	132	155	90
31	66	40	35	825	104	52	59
425	128	151	140				
			July 7, 1968, 1100 hrs. Development of Cb, hail				
20	–	25	1,2	43	64	–1,1	–55
31	04	21	23	58	150	110	78
35	06	02	06	84	130	–17,3	63
41	22	05	0,7	88	120	35	116
			July 17, 1968, 1100 hrs. Development of Cb, hail				
18	—	–60	–35	58	268	35	24
20	—	–23	–76	75	274	46	27
31	30	50	55	85	192	135	135
32	36	53	106	95	96	70	70
44	118	41	31	11,0	—	96	62

U28 L7

136790

H km	w_m m/sec	u' m/sec	$\frac{\partial u}{\partial z}$ m/sec per km	H km	w_m m/sec	u' m/sec	$\frac{\partial u}{\partial z}$ m/sec per km
July 30, 1968, 0600 hrs. Development of Cb, hail							
2.0	—	−2.9	−1.4	5.8	15.2	1.6	1.1
3.1	4.5	5.3	5.8	7.5	25.7	−5.4	3.2
3.7	4.3	5.3	9.0	8.5	24.1	8.4	8.4
4.1	4.3	4.0	10.0	10.9	–	31.2	13.0
4.4	4.7	5.0	16.0				
August 1, 1968, 1100 hrs. Development of Cb, hail ≤ 1 cm							
2.25	2.8	16.0	7.2	7.3	13.8	7.7	4.5
2.5	3.5	– 3.8	−1.2	7.6	12.1	2.3	7.6
3.0	5.3	−5.1	10.2	8.25	5.5	17.5	25.0
4.25	8.8	3.3	4.2	9.4	—	16.2	13.3
5.6	14.5	2.2	1.5				
Oseriya, Ardon							
August 11, 1968, 1100 hrs. Hail							
0.7	—	4.5	6.3	5.8	23.6	9.0	12.0
1.0	—	1.4	4.6	6.0	22.4	3.0	10.0
1.4	—	−1.2	−3.0	7.0	22.8	5.2	5.2
1.5	—	0.1	1.0	7.4	22.6	3.2	8.0
1.8	—	−1.0	−3.3	8.4	23.2	−3.5	−4.0
2.0	—	1.0	3.3	9.4	8.0	−5.2	5.0
2.2	—	1.0	5.0	10.1	—	12.8	18.0
3.8	10.2	4.8	3.2	11.5	—	3.2	2.2
4.3	13.0	−5.0	8.3	12.1	—	8.8	1.4
5.0	18.6	1.0	1.4				
Khutor Veselyi							
August 17, 1968, 1100 hrs. Hail							
3.2	6.2	6.2	1.9	7.4	17.8	1.3	0.7
3.6	8.8	0.2	0.4	8.4	12.6	8.0	8.0
4.2	10.8	−2.5	−5.0	9.5	—	7.6	7.0
4.4	11.0	0.1	0.3	10.6	—	2.6	2.3
5.8	18.8	3.3	2.4	11.1	—	−2.8	5.6
August 25, 1968, 1100 hrs. Development of thick Cb							
1.5	—	3.3	2.2	5.9	21.4	4.0	3.3
1.8	—	1.4	4.6	7.5	20.4	7.9	4.9
2.4	—	7.0	11.6	8.5	17.4	9.1	9.1
2.9	—	5.6	11.2	9.5	10.8	11.4	11.4
4.4	9.0	12.4	8.2	10.7	2.4	8.0	6.6
4.8	11.6	4.4	14.6				
August 27, 1968, 1030 hrs. Development of Cu cong., no storm or hail							
3.2	3.4	4.8	1.5	8.8	15.2	3.4	2.5
4.4	8.0	15.7	13.0	9.3	15.0	3.5	7.0
5.8	17.0	−9.7	−7.3	9.6	15.0	2.5	8.3
7.5	15.8	7.2	4.0	10.6	—	7.2	7.2

H км	w_m m/sec	u' m/sec	$\frac{\partial u}{\partial z}$ m/sec per km	H km	w_m m/sec	u' m/sec	$\frac{\partial u}{\partial z}$ m/sec per km
August 31, 1968, 1105 hrs. Cb, hail ≤ 1.5 cm							
1.3	4.0	2.0	1.5	4.2	12.2	−1.1	−5.5
1.5	0.0	0.3	1.5	4.3	13.2	−1.1	−11.0
1.6	0.4	1.2	1.2	5.75	22.0	2.6	1.9
2.0	2.0	2.2	5.5	7.4	23.4	8.5	5.0
3.1	6.6	6.4	5.7	8.35	19.0	7.8	8.0
4.0	11.2	−2.7	−3.0	9.4	14.2	−5.7	−5.1

To determine the effect of wind shear on precipitation processes, the change of wind speed vector in the vertical layer 2.5 — 30 km (the accumulation zone /90/) was examined. At wind shears over 2 m/sec per 100 m, no falls of hail were observed. This may be because high wind shear in the accumulation zone prevents the formation of hail, as conjectured previously by Sulakvelidze /90/ and Koval'chuk.

In the future it will be necessary to extend these studies to the effect of wind shear on changes in the thermodynamic state of the atmosphere, and to examine the effect of negative wind shear on the development of convection.

1.6. SIGNIFICANCE FOR CONVECTION OF LATENT HEAT OF PHASE TRANSITIONS

We now consider those forms of atmospheric energy which are converted into kinetic energy of air masses upon the development of convection, and also induce lifting and subsidence of air. It is assumed throughout that the speed of horizontal air currents is zero or, at least, of constant magnitude and direction, while convection is developing.

According to meteorology textbooks, the total energy of an air parcel, assuming no horizontal currents, is defined by the following differential equation:

$$d\Phi = c_v dT + Agdz + d\frac{w^2}{2}, \tag{1.63}$$

where Φ is the total energy per unit mass, T is the temperature, A the thermal equivalent of work, g the acceleration of gravity, z the height, w the speed of displacement of air masses, $c_v dT = dI$ the change of internal energy per unit mass of air, $d\Pi = Agdz$ and $dK = d\frac{w^2}{2}$ the change of potential and kinetic energy, respectively, per unit mass of air.

On the basis of Eq. (1.63) for an adiabatic process, the equation for the total energy per unit mass may be written

$$d\Phi = dI + d\Pi + dK. \tag{1.64}$$

A few remarks are necessary concerning Eqs. (1.63) and (1.64).

First, in order to calculate the total energy of an air mass, it is convenient to use the energy equation for a unit column of air rather than Eq. (1.64), which refers to unit mass, and involves integration with respect to height, a rather difficult task.

Second, not all the quantities entering into the equation for total energy per unit mass depend only on the state of the mass itself. The internal energy I depends on the state of the mass, the potential energy Π on the position of the mass relative to the origin. On the other hand, the kinetic energy depends both on the state of the parcel itself and on the atmospheric stratification.

We should therefore describe Π only as the "total energy per unit mass, given the stratification of the atmosphere," rather than the "total energy per unit mass." Hence it is necessary to find some parameter characterizing the total energy reserves of the parcel, independently of the stratification. This function should reflect all the energy of the parcel (or of the air column), not only the part that can be converted into kinetic energy.

To examine the energy aspect of the processes taking place in the atmosphere, it is convenient to consider those points in time at which the kinetic energy is zero, in other words, to consider the atmosphere before and after the development of convection. When this is done, the kinetic energy must also be assumed to be zero and one must consider all the energy, allowing for the possible release of heat due to condensation of water vapor contained in the unit air column.

Let us calculate the total energy of the air mass in a column of unit cross section extending from the surface z_0 to the 200 mb level, this being the level at which the great majority of convection processes terminate. At this level the water vapor content of the air is so small that condensation cannot significantly affect the energy state of the atmosphere.

Under these conditions, the differential of the total energy is

$$d\Phi = c_v T \rho dz + Agz\rho dz + L \cdot 0.622 \frac{e}{P} \rho dz, \tag{1.65}$$

where e is the partial pressure of water vapor, P the pressure of dry air, which may be assumed equal to the atmospheric pressure, ϱ the density of air, L the latent heat of condensation.

Integrating Eq. (1.65) from P_0 to P_u and from z_0 to z_u (where P_0 is the pressure at the surface z_0 and P_u the pressure at the upper boundary z_u of the troposphere), a few simple manipulations yield

$$\Phi = \frac{c_p}{g}\left[T_0 (P_0 - P_u) + 0.622 \frac{L}{c_p} \int_{P_u}^{P_0} \frac{e}{P} dP \right] - g \int_{z_0}^{z_u} \gamma \rho z dz. \tag{1.66}$$

Equation (1.66) defines the total energy of an air column of unit cross section before the onset of convection, when the kinetic energy of the air mass is zero. The functions $e=f(\varrho)$, $\gamma=f_1(\varrho)$ and $\varrho=f_2(z)$ may be found from the emagram, and Φ may then be calculated.

The energy that may be released in condensation of water vapor is obtained from the second term on the right of Eq. (1.66).

Given the instability energy of the atmosphere, one can determine the maximum updraft speed, the amount of precipitation that can be supported by the updraft, and so on. However, we have not yet considered questions relating to the energy of convection, which is converted (or may be converted) from thermal to kinetic when the instability is resolved.

To simplify the calculations, we replace the integrals in Eq. (1.66) by sums, dividing the intervals $[P_0, P_u]$ and $[z_0, z_u]$ into i layers, in which γ_i remains constant and e_i and ρ_i vary linearly with height. Thus, for the i-th layer:

$$\gamma = \gamma_i; \quad \rho_i = \frac{\rho_{0i} + \rho_{ui}}{2}; \quad e_i = \frac{e_{0i} + e_{ui}}{2},$$

where the subscripts "0" and "u" indicate the appropriate parameter values for the lower and upper boundaries of the layer, respectively. We shall consider the average height of the i-th layer.

Equation (1.66) may now be written

$$\Phi = \frac{c_p}{g}\left[T_0(P_0 - P_u) + 0.622\frac{L}{c_p}\sum_{i=1}^{n} e_i \ln\frac{P_{0i}}{P_{ui}}\right] - g\sum_{i=1}^{n}\rho_i\gamma_i(z_{0i}^2 - z_{ui}^2). \qquad (1.67)$$

A few simple manipulations give

$$\Phi = \frac{c_p}{g}\left[T_0(P_0 - P_u) + 0.622\frac{L}{c_p}\sum_{i=1}^{n} e_i \ln\frac{P_{0i}}{P_{ui}}\right] - 2g\sum_{i=1}^{n}\rho_i\Delta T_i\bar{z}_i, \qquad (1.68)$$

where ΔT is the difference between the temperature of the air at the lower and upper boundaries of the layer, $\bar{z}_i$ is the average height of the i-th layer. Calculation of Φ using (1.68) involves no difficulties.

To estimate the energy of the process, we have to know not only the actual value of Φ but also how it changes during the process. This information may be derived from Eq. (1.68), provided we have at our disposal data of atmospheric stratification before and after the disappearance of instability.

We use one prime to denote parameter values before the onset of the process, double primes to denote values after its termination. Then, for a pseudo-adiabatic process, we have

$$\frac{c_p}{g}\left[(T_0' - T_0'')(P_0 - P_u) + 0.622\frac{L}{c_p}\sum_{i=1}^{n}\left(e_i' \ln\frac{P_{0i}'}{P_{ui}'} - e_i'' \ln\frac{P_{0i}''}{P_{ui}''}\right)\right]$$
$$2g\sum_{i=1}^{n}\left(\rho_i'\Delta T_i - \rho_i''\Delta T_i''\right)\bar{z}_i = \Delta\Phi. \qquad (1.69)$$

The energy of phase transitions is usually embodied in the buoyancy, which, unlike enthalpy or potential energy, depends not on the entire reserve of phase-transition energy but only on the part convertible into kinetic energy under the specific conditions. To compare the thermal energy that may be converted into kinetic energy during convection, when the ascent of air masses is accompanied by phase transitions, with the energy released

upon transition of only potential energy into thermal energy, we consider the maximum updraft speeds for both processes.

As the kinetic energy is proportional to the square of the updraft speed, while the horizontal cross section of convective currents and their lifetime in the absence of phase transitions (clouds) are smaller than when clouds develop, it follows that the ratio of squared velocities of these processes is a good measure of the contribution of the energy released in phase transitions relative to the contribution of the energy produced by change in potential energy during convection.

It is known from numerous observations under field conditions, both in the USSR and elsewhere, that the maximum speed of convection currents in a cloudless atmosphere, w_{cm}, very rarely reaches 3 m/sec. When convective clouds are formed, the maximum updraft speed w_{0m} is frequently more than 30 m/sec.

Thus the ratio of kinetic energy of convection in phase transitions, E_0, to the corresponding energy when there are no phase transitions, E_c, may be expressed by

$$\frac{E_0}{E_c} = \frac{w_{0m}^2}{w_{cm}^2} = \frac{30^2}{3^2} = 100. \tag{1.70}$$

In other words, the energy released in phase transitions and converted into kinetic energy of convection is one hundredfold greater than the potential energy convertible into kinetic energy of convection.

The occurrence of shower-type precipitation, hail, hurricanes and other phenomena is probably due mainly to the release of latent heat of condensation. Evaporation from the surface of wet soil, seas, oceans and other reservoirs leads to the accumulation of considerable quantities of water vapor in the troposphere; this is accompanied by an accumulation of energy which may be set free as latent heat in phase transitions.

Water vapor accumulates in the troposphere, creating large reserves of latent heat of phase transitions, and under suitable conditions this is converted into energy of convection currents. Evaporation may go on for days, weeks, and sometimes even months without any precipitation taking place; the water vapor may then be converted into drops, releasing latent heat, at one location, within a few hours. This apparently explains the large amounts of kinetic energy involved in shower-type precipitation.

It is quite possible that convection in the troposphere accompanying fronta and intra air-mass processes is due mainly to the release of latent heat of phase transitions upon condensation of accumulated water vapor. The heating of the ground during daylight hours, mixing of air masses of different temperatures, and lifting (intrusion) of warmer masses are only the immediate causes of the conditions favorable for release of this latent heat.

It is no accident that hurricanes arise only when the surface temperature of the ocean reaches 28°, for this increases the water vapor content of the lower layers of the atmosphere to 40 g/kg. Hail processes in Transcaucasia and in the North Caucasus have been observed only when the temperature at the condensation level exceeds 6°, which implies a water vapor content of approximately 10 g per kg air. It is thus evident that a certain quantity of water vapor must accumulate in the air, sufficient to provide phase transition energy supporting the process in question. For example, to support hail

processes, the requisite quantity of water vapor in the lower layers is 10 g/kg; the corresponding figure for hurricanes is 40 g/kg.

Changes in enthalpy, occurring in the absence of condensation processes, bring about a vertical redistribution of air masses of different densities; they cannot cause updrafts with a large vertical velocity component. All processes of formation and development of convective clouds are due to the release of latent heat of condensation, which heats the ascending air. This heating causes a significant increase in buoyancy and hence also in velocity of the updrafts in clouds; it is a self-generating process.

The development of convective clouds favorable to synoptic processes depends on the amount of water vapor that the process in question converts into drops or into ice crystals, and on the energy released thereby due to the latent heat of phase transitions.

In the sequel we shall have to make allowance for the approximate proportion of water vapor converted into drops and, on this basis, to calculate the energy that may develop for a given atmospheric stratification.

1.7. ON THE FORMATION OF CUMULONIMBUS

The accepted classification of clouds /2/ specifies two main varieties of cumulonimbus: calvus (Cb calv.) and capillatus (Cb cap.). The latter category includes cumulonimbus incus (Cb inc.). This classification is based on external morphological features of the cloud, thus being dependent on visual observation from the earth and disregarding the dynamics of cloud development. A better basis for the classification of Cb is the delimitation of the stages in the life cycle of these clouds, suggested by Byers and Braham /120/.

Examining the evolution of cumulonimbus clouds, these authors divide the life cycle into three stages: growth, maturity and dissipation. This division depends on the type of distribution of large-scale vertical movements within the cloud. The first stage is characterized by updrafts throughout the cloud. At maturity, the lower part of the cloud includes regions in which downdrafts prevail. Finally, the dissipation stage exhibits prevailing downdrafts throughout the whole cloud.

According to research at the High-Altitude Geophysics Institute, one should divide the life cycle of the cloud into four stages. The first is the formation of individual small clouds with convective ascent of air in isolated thermals; the second lasts from the earliest formation of updrafts to accumulation and dissipation of moisture in the cloud (from 1 to 1.5 hours); the third stage consists of precipitation and parallel accumulation, and the fourth is the disintegration stage. The other classifications combine the first two stages into a single stage; this is unjustifiable, as the time required for the thermals to coalesce into a draft fluctuates between fairly wide limits, while the accumulation time of the moisture necessary for the occurrence of shower-type precipitation is relatively constant.

Studies by Balabuev /2/ of the conditions for formation of cumulus congestus have shown that the period during which the cloud develops from Cu hum. to the Cu cong. stage fluctuates considerably: rapid development

lasts about one hour, whereas cases of very slow development may take up to 4 hours, with Cu med. forms predominating.

The Cu cong. stage may be the last, so that the Cb phase never appears. However, when the cloud does develop into Cb, the process is faster than the preceding slow stage in the Cu cong. phase. The entire process, up to and including formation of Cb inc., usually lasts at most one or two hours, sometimes even less. The instant at which the process speeds up is marked by increased fibrillation of the cloud and appearance of virgas which rapidly reach the ground, so that precipitation begins. The whole is accompanied by various storm phenomena.

Under less favorable conditions, when the early stages produce numbers of smaller clouds rather than a single mass, further development is also typified by masses of more or less limited size. When the processes are rapid and accompanied by shower-type precipitation, thunderstorm phenomena and falls of hail, the cloud masses form via merging of smaller clouds. Several Cu cong. approach to windward, with subsequent growth of cloud towers, ultimately producing Cb calv. and merging with the original cloud. Four or five such stages are observed, at intervals of from 15 to 30 min (only in intra air-mass or weak frontal processes). In the process, the anvils begin to form and grow to leeward of the cloud mass; only after approach of the fourth or fifth cloud do anvils begin to appear to windward as well. The result is a large Cb cloud, accompanied by heavy hail or showers.

The whole formation process of such a cloud (from the onset of rapid growth to full development) rarely lasts more than 2 or 3 hours.

The specific form of the process depends on the complex of all prevailing meteorological conditions, i. e., on the nature of the synoptic process, the atmospheric stratification and the diurnal evolution of the stratification. Thus the phase of cloud development from Cu fr. and Cu hum. to the first stage of Cu cong. occupies a long period, of the order of 4 hours. The updraft speed increases with height until the cloud reaches a level where the lapse rate γ becomes equal to or less than γ_w/26, 90, 98/. When Cu med. reaches the Cb inc. stage, the rate of growth of the cloud gradually falls off. Precipitation and the concomitant downdrafts lead to a "cut-off" of the thermals rising from the underlying surface, so that the "supply" of water vapor to the cloud from below is halted and the vertical motion inside the cloud disappears. The upward growth of the cloud ceases entirely.

According to the conception developed at our Institute /90/, the updraft speed in the cloud increases with height, reaching its maximum w_m in the middle or pre-top region of the cloud, and then decreases toward the top. As a result, a large quantity of water accumulates above the w_m level. Recent theoretical and experimental work /90, 102, 112, 131, 168/ has confirmed the existence of this zone, in which the humidity is several factors higher than the maximum humidity possible for adiabatic ascent of moist air. It is known as the "accumulation zone." The accumulation of such large quantities of water, equal to the critical liquid water content for precipitation to occur, above the maximum speed level requires a certain time, called the "moisture accumulation period." The length of this period depends on what point of time in the development of the cloud is defined as the beginning of the process.

Goral' /27/ proposed a method for determining the accumulation time of water in the accumulation zone as a function of liquid water content q in the lower region of the cloud and the concentration N_0 of giant condensation nuclei. The specified water contents were 1, 2 and 3 g/m^3, and the concentrations of giant condensation nuclei 0.1, 1 and 10 m^{-3}. Fixing these values, Goral' used the most typical values leading to the formation and fall-out of shower-type precipitation. According to his plot of the accumulation time τ_a as a function of liquid water content in the lower region of the cloud and the concentration of giant condensation nuclei, one can determine τ_a from known values of q and N_0 (see Figure 40).

However, these parameters are different in each actual case of shower-type precipitation and are difficult to determine. When solving various problems, therefore, particularly when predicting the amount of precipitation, one should adopt some average figure for the moisture accumulation time. Thus, at moderate values of the water content, $q = 1$ to 1.5 g/m^3, and of the concentration of giant condensation nuclei, $N_0 = 1$ m^{-3}, shower-type precipitation may take place within one hour (see /27/). This agrees with observations of the development of clouds with vertical development /90, 98, 2/. The averaged accumulation time may satisfy the demands of qualitative analysis of precipitation-formation processes, but it should not be used for qualitative evaluation of precipitation. For the latter purpose one should determine the accumulation time of moisture in the high-water-content zone for each specific developing cloud; in other words, one must work out the time during which Cu cong. is converted into Cb, when the updrafts in the cloud die out completely in the upper region of the cloud. Research with this aim is now under way at the High-Altitude Geophysics Institute.

Chapter 2

HAIL PREDICTION

Investigation of the hail-formation process is of considerable value for the national economy, as it should further the development of methods to modify hail phenomena. Government-sponsored insurance against hail damage is an extremely costly business, and so hail prevention would have a significant economizing effect. It has been established that the annual damage to crops in hail-prone regions reaches 30%. In some regions, where large hailstones are common, crops may be completely destroyed. For example, hail damage in Nal'chik on June 9, 1939, destroyed 60,000 ha of wheat and 4,000 ha of other crops. In the Gomel' region during 1950, hail destroyed more than 13,000 ha of crops, a loss of at least 5 million rubles. A detailed account of hailstorms in the USSR and data on the frequency and average number of hail-days in different regions may be found in Pastukh and Sokhrina /109/. The regions of the USSR in which hail is of particularly high frequency are the Caucasus /107/, Ukraine, Moldavia, Middle Asia and the Far East.

Outside the Soviet Union, hail occurs most frequently in Italy, France, Switzerland, USA, China and India /170, 122, 126, 157, 160, 167/. The annual hail damage to crops in the USA is about 300 million dollars.

It should be noted that it is difficult to speak meaningfully of the frequency of hailstorms: hail is a local phenomenon so that stations spaced far apart do not always record significant falls of hail. For example, during the Mushtinskaya Expedition of the High-Altitude Geophysics Institute in 1961, 11 hail incidents were observed over an area of 60,000 ha, whereas the nearby meteorological station of Shadzhatmaz, well within the working area of the expedition, recorded only one. The true incidence of hail must therefore be determined on the basis of Gosstrakh figures for hail damage.

Beckwith /114/ writes that a fourfold increase in the number of stations recording hail yielded a corresponding increase (from 11 to 40) in the number of recorded hail incidents (the observations extended over a period of seven years).

2.1. METHODS OF HAIL PREDICTION

The hail-prediction method most widely used in the USSR is that of Shishkin. It is based on theoretical assumptions originating at the Boeikov Geophysical Observatory: hail will reach the ground without melting provided the average cloud-growth rate exceeds 2 to 3 m/sec /96, 101/.

The potential rate of development of convective clouds as a function of the variation of temperature with altitude is calculated by the layer method /97/. The upper boundary of a mature convective cloud is set at the height at which the updraft speed is zero. The calculation is done on an aerological diagram. Hail prediction makes use of figures for the maximum possible thickness of clouds. The total dew-point deficit at levels of 850, 700 and 500 mb is also taken into consideration.

The reliability of the prediction is measured by the quantity

$$N = \frac{A_h + B - \frac{1}{2}(B_h - B_0) + C_0}{A + B + C} 100\%,$$

where A is the number of days on which the prediction is "hail expected," A_h is the number of days on which hail actually falls, B is the number of days on which the prediction is "possible hail," B_h the number of these days on which hail falls, B_0 the number of days without hail, C the number of days on which the prediction is "hail not expected," and C_0 the number of these days without hail.

Thus, the "possible hail" predictions are considered to be 50% accurate both when hail falls and when it does not. This is clearly due to the fact that the "possibility" of hail falling is inevitably bound up with cloud thickness. When the calculations show that the maximum possible cloud thickness is 7.5 km and the total dew-point deficit at levels 850, 700 and 500 mb reaches 20°, hail will fall with 100% probability. But there are cases when no hail falls despite the cloud thickness reaching as much as 10 km.

A popular hail-prediction method in the USA is that of Fawbush and Miller /126/. They assert that hail grows in the temperature interval $0 - 10°$. Assuming that the growth of hail is possible only if the updraft speed is sufficient to support hailstones, they suggest determining the updraft speed at the $-5°$ isotherm. A shortcoming of this method is that the updraft speed is calculated at a level where the ambient temperature is $-5°$, while it is well known that hail formation depends not only on temperature but also on the liquid water content of the cloud. In some cases of high water content, hail may grow at temperature $-20°$. Consequently, the speed thus determined is not really the maximum updraft speed supporting hail.

Apart from prediction methods, attempts have been made at climatological and synoptic analysis of hail-days. Typical of this approach is the work of Gigineishvili in Eastern Georgia /29/ and of Muller in Switzerland /151/. These authors study the synoptic conditions for the formation of hail phenomena; they determine regions in which these conditions are most favorable and also regions in which the intensity of the hail processes falls sharply. One thus has the possibility of determining favorable conditions for the development of thick convective clouds, but a fully reliable prediction of hail requires determination of its potential formation within a cloud.

2.2. THE MECHANISM OF HAIL FORMATION

Various theories of the mechanism of hail formation have been advanced, both in the Soviet Union and elsewhere. We shall discuss only those based

on physically justifiable assumptions or those which have served as a transitional stage for further research into the physics of convective clouds.

The first theory of hail formation was suggested by 1879 by Reynolds, and later improved by Schumann, who considered the growth of spherical hailstones by acquisition of supercooled cloud drops. Schumann was the first to work out the heat balance equation for hail; this was later made more precise by Ludlam, who experimentally determined the transfer rates of heat and water vapor /139—142/.

The first physically justifiable theory of the formation and growth of hail was proposed by Findeisen in 1938 /127/. It was based on Bergeron's assumption that the main reason for the consolidation of cloud drops is migration of vapor from supercooled drops to ice crystals in the upper mixed region of the cloud /115/.

On this basis, Findeisen postulated the existence of nuclei of crystallization (sublimation) /127/. No drops condense at these nuclei, but once they have been raised by updrafts to a critical temperature they trigger sublimation of ice crystals. According to Findeisen, the average critical temperature over land ranges from —19.4 to —20°, and over sea from —8 to —10°. These figures are characteristic for the most commonly occuring nuclei of crystallization; depending on the type of nucleus, the critical temperature may sometimes be as much as —6°.

Employing Bergeron's theory and his concept of sublimation nuclei, Findeisen developed a theory of the mechanism of precipitation in cumulus clouds. The theory provides for five stages in the development of cumulus.

Stage one is the growth of the cloud up to the critical temperature level (—19, —20°). During this time the cloud consists of only liquid drops, while in its upper region supercooled liquid particles begin to accumulate.

During the second stage, the cloud top rises above the critical temperature level, where, together with supercooled drops, ice crystals begin to form and grow at nuclei of crystallization. The upper region of the cloud takes on a mixed structure. At the beginning of this process, the number of ice crystals is far less than the number of supercooled drops, so that the mixed region is characterized by a rapid growth of crystals due to migration of vapor from supercooled drops to ice particles.

The ice crystals develop as soft hail until they become too large to be supported by the updrafts. Falling into the supercooled region of the cloud, they coalesce with water drops, causing them to freeze and producing small hail and finally hailstones, which subsequently fall to earth as hail or rain, depending on the thickness of the supercooled region of the cloud, the updraft speeds and the altitude of the 0° isotherm.

Findeisen asserted that sublimation growth of hail may take place not only above but also slightly below the 0° isotherm. He called the second cloud-growth stage the hail stage. At this stage the cloud consists of warm water drops (below the 0° isotherm), hail pellets and supercooled drops (from the 0° isotherm to the critical temperature level), small hail and supercooled drops (near the critical temperature level) and soft hail and supercooled drops (above the critical temperature level).

The third stage of development is what Findeisen calls the first rain stage. Ultimately, the second stage produces a substantial reduction in the number of supercooled drops; conditions are no longer suitable for the formation and growth of hail by accretion of supercooled drops, and the soft hail formed above the critical temperature level can grow only to the dimensions of

small hail. As the particles fall into the warm layers of air below the 0° isotherm, they melt and heavy showers result. At this stage, the cloud consists of liquid drops (below the 0° isotherm), supercooled drops and small hail (from the 0° isotherm to the critical temperature level), soft hail and supercooled drops (above the critical temperature level).

At the fourth stage of development, Findeisen's "second rain stage," the number of supercooled droplets has been reduced, the dimensions of the small hail pellets are also small, and moderate rain falls to the surface. The composition of the cloud is now: drops of water (below the 0° isotherm), a thin layer of small hail and supercooled drops (near the 0° isotherm), and soft hail (above the 0° isotherm).

Finally, once the above-described processes have drastically reduced the number of supercooled drops, hollow crystals form in the upper part of the cloud, and in the region of the 0° isotherm these become snow flakes. Slight rain falls. Findeisen called this the residual stage (Figure 13).

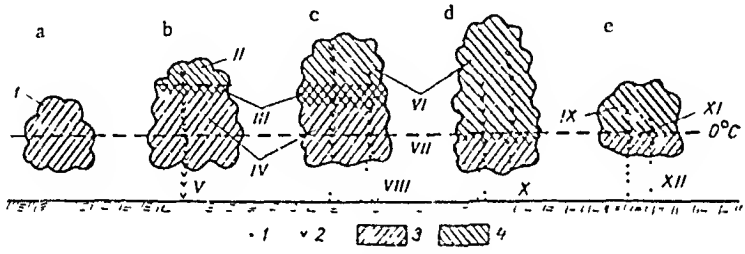

FIGURE 13. Development of shower cloud according to Findeisen.

a) preliminary stage; b) hail stage; c) first rain stage; d) second rain stage; e) residual stage; 1) falling raindrops; 2) falling ice pellets; 3) water-drop clouds; 4) ice-crystal clouds; I, IV) supercooled droplets; II, VI) soft hail; III, VII) small hail; V) hail; VIII) heavy rain; IX) hollow crystals; X) moderate rain; XI) snow flakes; XII) slight rain.

Findeisen's theory was the first attempt to explain precipitation on the basis of the physics of the processes taking place in a cumulus cloud. Many of its basic postulates are still valid: the growth of hail by accretion of supercooled drops, the dependence of hail size and intensity of precipitation on updraft speed, and so on. It is quite clear, however, that these first attempts could not possibly encompass the full range of the processes occurring in a cumulus cloud. First, Findeisen's conception implies that any cloud reaching the second stage of development will necessarily produce hail, which then becomes a heavy shower. Moreover, since the difference in height between the 0° isotherm level and the critical temperature level varies over a relatively small interval, as does the liquid water content in the developing cloud (which is bounded above by the adiabatic water content), it follows that any such cloud would produce hailstones of approximately the same size.

Findeisen ignores the possibility of liquid drops forming anew in the cloud while precipitation is in progress, and there are several other consequences of his theory that have not been confirmed in practical work.

Further investigations of convective clouds have yielded new hail theories. In 1961, Weickmann /172/ proposed a detailed description of the mechanism of formation of cumulus cong., according to which the principal factor in the

formation of such clouds and of hail are updrafts. The updraft speed is determined by the difference between the temperature of the air rising along the wet adiabat from the condensation level and the temperature of the surrounding air at that level.

Weickmann's formula for the updraft speed w in a convective cloud as a function of the difference ΔT between the temperature T of the surroundings and the temperature T_w of the cloud ($\Delta T = T_w - T$):

$$w = c\sqrt{\frac{d\Delta T}{T}}, \tag{2.1}$$

where d is the diameter of the ascending air bubble in meters, c a constant equal to 2 $m^{1/2} \cdot sec^{-1}$ (when ΔT and T are measured in degrees), and w is in units of m/sec. Weickmann postulates that, owing to circulation of air in the ascending bubble, the updraft speed v'_c at the center of the bubble is double the updraft speed v'_t at the top of the bubble:

$$v'_c = 2v'_t. \tag{2.2}$$

In a hail cloud, the convective cells coalesce into a cylindrical jet of rising air which Weickmann calls a tube. The distribution of updraft speed along the axis of this tube is shown in Figure 14.

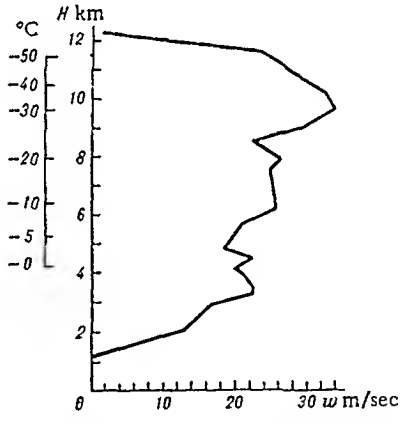

FIGURE 14. Distribution of updraft speed, after Weickmann.

According to Weickmann's data, drops rising in the cloud freeze at the −30° level. Air pollution may raise the crystallization temperature to −15 or −16°.

Weickmann made allowance for the latent heat of condensation and also for the heat of condensation released by additional sublimation of water vapor on ice crystals when the air is rising in the tube. The total heat loss due to these two processes causes, in his opinion, an increase of approximately 1 − 2 km in the height of the cloud.

Analyzing the work of List /137, 138/, Macklin and Ludlam /143/, Weickmann was able to derive a simple formula for the fall speed of a hailstone as a function of its diameter:

$$v = 2.8\sqrt{d}\,, \tag{2.3}$$

where v is the steady fall speed of the hailstone under the sole influence of gravity in m/sec, and d the hailstone diameter in mm. In the derivation, the drag coefficient is taken equal to unity, a clearly exaggerated figure. In addition, no allowance is made for the changes in the density of air with altitude.

Using calculations of Kessler /135/, Weickmann proposed the following formula for the liquid-water content of the cloud:

$$\Delta q = \frac{\Delta T}{T} 348 \varrho_a. \tag{2.4}$$

where Δq is the liquid water content in g/m^3, ϱ_a the density of air. Values calculated from this formula are in good agreement with those obtained from the equation worked out at the High-Altitude Geophysics Institute (see Chap. 3).

Analyzing these data, Weickmann postulates the following four preconditions for a thunderstorm:

1. The buoyancy as determined by the temperature difference between updraft and environment can support all the accumulating water.
2. The accumulating water particles are large, but not so large as to induce a downdraft.
3. The crystallization of cloud particles and condensation of water vapor sets free enough heat to create an equilibrium between the additional air mass entering the upper region of the cloud and the updraft.
4. The downdrafts accompanying the occurrence of precipitation lie outside the main updraft tube.

According to Weickmann, the fourth condition is decisive; in support of this view, he cites a storm which occurred in Calcutta on June 18, 1958, when the height of the radar echo reached 16 km, the top of the cloud being 22—23 m high. The diameter of the cloud anvil was 100 km. The total airflow through the cloud was 12,000 km^3. In Weickmann's opinion, a few minutes after reaching maximum height the cloud disintegrated without any precipitation having occurred, due to downdrafts caused by the action of gravity on the water that had accumulated in its upper regions. The conditions were not suitable for the growth of hail. To determine the conditions for hail formation, Weickmann considers the horizontal movement of the storm cloud, taking into account the velocity and direction of air current in the lower layers of the atmosphere — the principal source of air supply to a storm cloud.

The cloud acts as an obstruction for the horizontal currents, which therefore flow around it and ascend; when the air is unstable, this may create a new hail-formation cell. This focus forms in the rear of the precipitation (relative to the direction in which the cloud is advancing). The changes in the speed of the horizontal currents at high altitudes cause wind shear and drift of the anvil. According to data of Newton and Katz /154/ the thunderstorm cell moves in the direction of the wind at the 750 mb level.

In addition Weickmann considers the formation and growth of new thunderstorm cells, which, according to Newton, lie on the right flank of the advancing cloud.

All these factors cause a visible displacement of the hail cell relative to the surface, toward the right of the wind velocity vector at the 750 mb level (Figure 15).

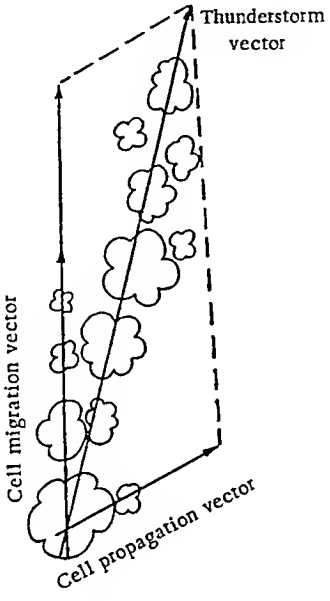

FIGURE 15. Motion of hail cloud (after Weickmann).

Weickmann considers two types of storm.

1. Storm without wind shear. Wind shear is defined as a sharp increase in $\frac{\partial u}{\partial z}$ in the upper region of the cloud, where u is the horizontal component of the air-current speed. If $\frac{\partial u}{\partial z}$ is zero or varies slightly with height, the storm cloud will either remain motionless in space or migrate uniformly due to the wind, while continuing to develop vertically. The anvil is symmetric about the cloud axis (updraft tube). Because of this distribution of horizontal air-current velocities, the moisture accumulated in the cloud suppresses updraft and the thunderstorm cell collapses before large hailstones can grow. This is precisely what happened in the above-mentioned Calcutta storm. If the air remains unstable after disintegration of such a hail focus, a new focus may form, in any direction relative to the old. In Weickmann's opinion, no hail can form unless wind shear is present.

2. Thunderstorm cells whose upper regions extend up to altitudes at which wind shear is observed. This is the case for frontal clouds, gale clouds (Weickmann's terminology) and, apparently, clouds whose tops penetrate jet streams. In this case the cloud top (anvil) must extend in the direction of the wind at high altitudes.

Weickmann remarks, however, that in some cases this tendency is not observed and the hail cell pierces the jet streams, moving together with them and not changing the vertical position of the updraft tube. Using slow-motion photography, Weickmann was able to show that the cloud top is entrained by the jet stream only when the updraft speed is less than the horizontal velocity.

The same conclusion was reached previously by Douglas and Hitschfeld /124/, on the basis of radar investigations of hail cells. Analyzing the results of these observations, Weickmann concludes that even in the presence of wind shear the updraft tube may maintain its original vertical direction. He considers conditions under which the top of a thick cumulus cloud, formed by an updraft in the tube, may be diverted by horizontal currents as a result of wind shear (Figure 16).

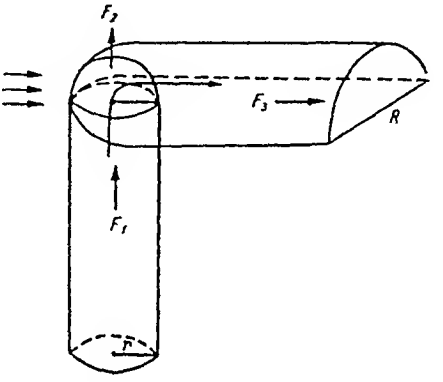

FIGURE 16. Effect of wind shear on shape of hail cloud, after Weickmann.

The law of mass conservation implies a balance of the following three air currents: F_1 — the current throughout the vertical tube, F_2 — the current through the polysphere, and F_3 — the current through the polycylinder.

On this basis, Weickmann finds the relationship between the updraft speed v_1 at the top of the tube, the speed u of the horizontal current, the radius r of the tube and the radius R of the polycylinder of rising cloud air entrained by the horizontal currents. His formula is

$$R = 2r\sqrt{\frac{v_1}{u}}. \qquad (2.5)$$

Since the updraft may drift only when $u > v_1$, Weickmann's equation (2.5) reduces to the inequality

$$R < 2r. \qquad (2.6)$$

Weickmann holds that if $u \leqslant v_1$ the top of the updraft tube does not drift; it remains vertical and the horizontal current flows round it, entraining the cloud mass around the tube.

Weickmann substantiates these ideas by a series of aerosynoptic examples. One consequence of his approach is that the presence of wind shear, which removes accumulated water from the cloud top, increases the lifetime of the thunderstorm cell. Moreover, the horizontal air current acts as a pulverizer, accelerating the divergence of cloud masses at the top of the tube. This leads to an increase in updraft speed within the tube. In addition, the horizontal current flowing round the tube and the precipitation zone creates a head behind the cloud. As we have already stated, when the air is unstable this may create a new hail-formation cell in the rear of the previous one, slowing down the motion of the storm relative to the earth. Zaubner and Gantry believe that these factors explain various incidents of heavy precipitation, such as a storm in Florida in which 400 mm fell in a space of 5 hours. Figure 17 is a model of a thick cumulus cloud, showing its behavior with and without wind shear. On the basis of experimental data, Weickmann assumes that wind shear capable of causing outflow of cloud air from the updraft tube must be located in the tropopause region, where the density of air is approximately a quarter of its density at the condensation level near the base of the tube. He states that in order to preserve the balance between the mass of the air drawn into the tube at the condensation level and the air drawn out at the top of the tube by wind shear, the velocity of the horizontal currents at the top must be four times that of the updraft at the base. Under these conditions the thunderstorm cell will be in equilibrium. New cells form most frequently on the right flank of the original cell.

In Weickmann's opinion, hail forms in the region of maximum updraft speeds, most frequently in the rear of the storm. Growth may take place in a range of temperatures from 0 to −30° in the hail cell. Analyzing the formula and size of the falling hailstones, he concludes that cone-shaped stones may be formed at the initial developmental stage of the cloud. All large hailstones are spheroids. They are opaque, sometimes showing 22 to 23 alternating layers of opaque and spongy ice. According to Weickmann, large hailstones may form due to collisions of smaller stones, which then freeze together; he emphasizes that the formation of a hailstone requires a large quantity of supercooled water. Whether the ice that forms is transparent, porous or opaque depends on the relative proportions of supercooled droplets and ice particles.

Figure 17 shows the different stages in development of a cloud, with and without the presence of wind shear. When there is wind shear, the speeds of the updrafts observed during the first stage depend only on the buoyancy at each level. At this stage, the cloud has still not reached the level at which wind shear is appreciable.

At the second stage, the cloud reaches a level of horizontal air movement with strong wind shear. An anvil is formed, extending along the direction of these movements, and precipitation begins in its forward part. Two types of motion may be observed in the cloud: updraft, accelerated by the pulverization effect, and horizontal drift in the upper region of the cloud.

At the third stage, the upper part of the cloud reaches the crystallization level and the entire anvil crystallizes. Precipitation occurs in the frontal part of the cloud and in the anvil, and a growing cumulus cloud forms below the anvil. Downdrafts arise in the frontal part of the anvil, where precipitation is in progress. At this stage, then, the cloud contains updrafts in the rear of the main thunderstorm cell, updrafts just below the cloud anvil,

horizontal currents in the upper regions and downdrafts in the frontal part of the main cloud. Ice particles falling from the anvil evaporate beneath the cloud. The weight of the moisture accumulating in the cloud cannot suppress the updrafts, as the bulk of the water reaching the upper portion of the tube is carried off by wind shear.

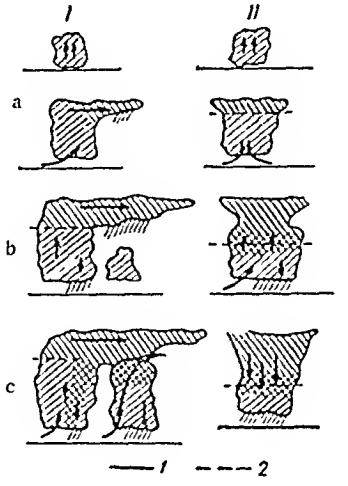

FIGURE 17. Development of a thick cumulus cloud, after Weickmann.

I) strong wind shear; II) no or weak wind shear.
Stages: a) cumulative, b) mature, c) dissipation: 1) flow, jet; 2) glaciation.

At the fourth and last stage, the cumulus cloud formed below the anvil reaches the lower boundary of the latter. Ice particles from the anvil fall into this "forward" cloud, grow by accreting the liquid fraction and, falling in the frontal part of the cloud, produce showers. Weickmann's scheme may thus be summarized as follows. Cloud particles grow in the tube of the main convective cloud while ascending to the level of the anvil, continuing to grow in the anvil and later while falling in the secondary cloud. At surface level, this is expressed first in heavy showers from the secondary cloud, subsequently in weak showers from the frontal part of the main cloud. At this stage one observes updrafts and downdrafts in the main (rear) and secondary clouds, and horizontal flow in the anvil.

This scheme is rather artificial, since it dictates formation of a cloud beneath the anvil as a prerequisite for the occurrence of shower-type precipitation. Radar has not confirmed this type of cloud structure; moreover, studies of updraft in convective clouds have failed to detect the pattern of updrafts and downdrafts suggested by Weickmann. Weickmann holds that this stage in the growth of the cloud is stable, since it does not imply accumulation of water, as would be necessary to suppress the updraft.

When there is no wind shear, the first stage in the development of the thunderstorm cell (Figure 17) is the same as when wind shear is present. At the second stage, the cloud reaches the natural crystallization level, and the young anvil is symmetrically placed with respect to the cloud axis.

The cloud contains only updrafts due to thermal convection (buoyancy, according to Weickmann). The weight of accumulated water in the anvil suppresses the updrafts. During the third stage, ice crystals, grown by water vapor migrating from cloud drops to ice crystals and also by accretion processes, begin to fall (within the cloud). The speed of the updraft is reduced and showery precipitation begins. At this stage, updrafts are observed in the cloud; these introduce an additional contribution of water to the cloud and support it, and downdrafts are triggered by the precipitation. By the fourth stage, the updrafts have disappeared owing to the pressure of the overlying layers of water. Large ice pellets begin to fall from the cloud in showers. The anvil disappears and the cloud itself gradually dissipates, producing relatively weak showers.

This scheme does not explain why, when the air possesses a high degree of instability, the updrafts envisaged at the third stage cannot create a new storm cell. In Weickmann's opinion, the lifetime of a thunderstorm cloud is much shorter in the absence of wind shear than when the cloud grows under the influence of wind shear.

The truth of the matter is that Weickmann's theory explains only the formation and growth of cumulus *congestus, not the mechanism of hail* formation. Above all, Weickmann's assertion that large hailstones cannot form when there is no wind shear is unacceptable. For example, on May 29, 1962, a cloud was reported in North Caucasus whose radar reflection zone remained completely motionless during its entire life cycle. It was produced by thermal convection, the pressure field showing a low gradient. According to radar data, the cloud top reached the −32° isotherm, and the radar reflectivity from the cloud was in agreement with the reflectivity of hail cells. A detailed investigation was made of falling precipitation in the growth region of this cloud. A survey of hail damage in the area established that hail had fallen over an area of approximately 12 km^2; the hailstones were slightly elongated ellipses. In the central part of the region, the layer of hail was as thick as 5—7 cm, while the diameter of the hailstones exceeded 3.5 cm. Such cases of high-altitude calm are comparatively rare, but they serve to demonstrate that hail may also form when there is no wind shear.

Neither can we agree with Weickmann's opinion that hail can grow rapidly at the level of the −30° isotherm. At such low temperatures, only very small drops may remain in the liquid state, and their contribution to the total liquid water content of the cloud is at most 1 g/m^3, while the coefficient of capture for hailstones of radius more than 1 cm is very small. It is readily shown that under such conditions the growth of a hailstone from diameter 0.1 to 1 or 2 cm would require at least 60 to 80 minutes. However, we know from radar data that the time necessary for formation of hail in this way is only a few minutes. Moreover, the maximum dimensions of the hailstones that can form in a cloud are determined primarily by the updraft speed or, in Weickmann's terminology, the buoyancy of the cloud, not by the magnitude of horizontal wind shear.

In 1965, Dessens published a new model of a hail-producing cloud /122/, according to which hail is formed in thick cumulonimbus clouds (Figure 18).

Figure 18 illustrates a model of a thick cumulus cloud, in which small water droplets of 10μ diameter and concentration approximately 500 cm^{-3} are lifted in updraft tubes to the level of natural crystallization. Starting from −12°, isolated ice crystallites appear in the updrafts, in concentration

$1 \cdot 10^{-3}$ cm^{-3}. This concentration does not vary until the −32° isotherm is reached, but above that it increases by about three orders of magnitude. Below −35°, all the drops become crystals, either by sublimation growth of heavy particles and migration of vapor from drops to ice crystals, or as a result of freezing of the remaining drops. This temperature is the lower bound for the existence of supercooled droplets. As a consequence of this process, the anvil of the Cb cloud consists entirely of ice crystals, since it lies above the −35° isotherm; downdrafts appear alongside the updrafts, and carry ice crystals into the middle region of the cloud, between the 0 and −35° isotherms (Figure 18, a). These crystals, re-entering the jet of rising air, induce what Dessens calls a natural seeding process (self-seeding). The concentration of ice crystals in the temperature interval from −12 to −32° rises to 1−10 cm^{-3}.

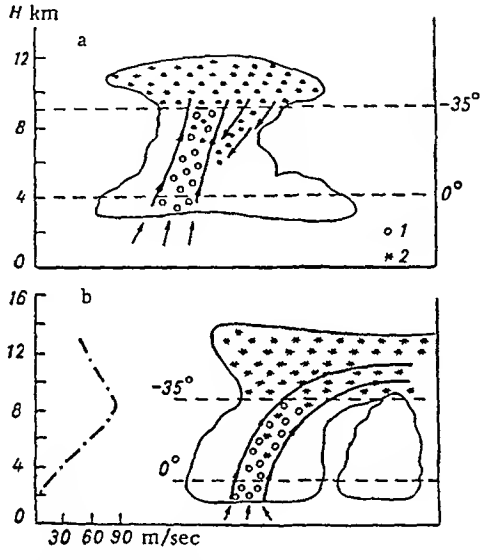

FIGURE 18. Diagram of hail-producing cloud, after Dessens.

a) without wind shear (self-seeding); b) with wind shear;
1) droplets; 2) hail.

At such concentrations, the redistribution of moisture among "competing" ice crystals makes the formation of large hailstones impossible. Consequently, in any convective cloud in the first stage of development hailstones may appear and grow only before the onset of self-seeding. Self-seeding halts the growth of hail.

Dessens asserts that before self-seeding begins hail may fall only for short periods, on the average 1 to 2 minutes and never more than 8 minutes. Hail of this kind cannot cause damage to agriculture. The first stage of hail growth proceeds by sublimation, as in the Bergeron-Findeisen theory, and later by accreting supercooled water droplets. When the liquid water content of the cloud is low, hail grows in a dry regime, implying no danger to agriculture. On the other hand, conditions of high liquid water content produce dense, transparent hailstones, and these may be quite destructive.

According to Dessen's scheme, the main growth of large hailstones takes place in a zone of high liquid water content, and the concentration of the hail embryos must be small. In the absence of wind shear, this process cannot produce large hail.

Large, dangerous hailstones may be formed only when there is wind shear, which transports small ice crystals to the boundary of the main cloud mass so that they no longer participate in the self-seeding process, thus limiting the growth of large stones. Wind shear acts as a filter, removing small ice particles from the cloud and leaving only large ones. In addition, it causes an increase in updraft velocities, via the pulverization effect. A diagram of a hail-producing cloud under these conditions is given in Figure 18, b.

Such are the general lines of Dessens' theory of hail formation. He holds that in all cases an increase in nuclei of crystallization inhibits the growth of hailstones. His scheme does not explain a basic phenomenon — the accumulation of a large mass of supercooled water in the upper region of the cloud. Moreover, it implies that every cumulonimbus cloud that has developed up to the level of the −12° isotherm should (at least initially) produce hail (as implied also by Findeisen's theory). However, this has not been confirmed by observations.

The most detailed account published recently outside the Soviet Union, discussing the distribution of air currents in convective clouds that produce hail, is the paper of Browning and Ludlam /121/. Basing their arguments on radar, visual and synoptic observations, they analyzed the hail-formation conditions in a storm at Wokingham (July 9, 1959). They reached the conclusion that the precipitation from a hailstorm cloud forms a wall athwart the direction of the storm. The width of the wall is about 10 km, its height also 10 km. The lifetime of a single storm may reach 12 hours. Browning and Ludlam reasoned that a thunderstorm may arise only under conditions of characteristic wind shear, the direction of the storm coinciding in magnitude and direction with the wind speed at the middle level of the troposphere. Noting that severe storms arise only at frontal sections, they state that the most widely-held theories of the formation of a simple storm, according to which cool air displaces warm air at low levels, do not provide a satisfactory explanation of the facts observed in actual thunderstorms.

Browning and Ludlam recorded the distribution of airflow most characteristic for thunderstorm processes. Figure 19 shows the distribution of updraft and downdraft in a convective cloud according to their data.

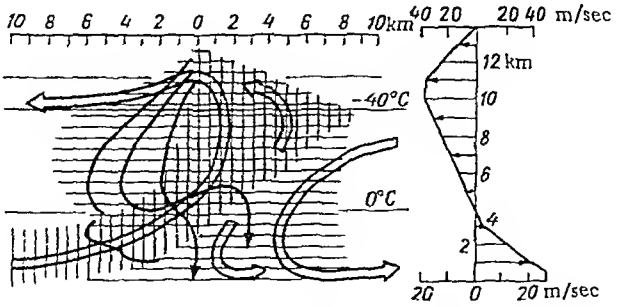

FIGURE 19. Development of hail-producing cloud, after Browning and Ludlam.

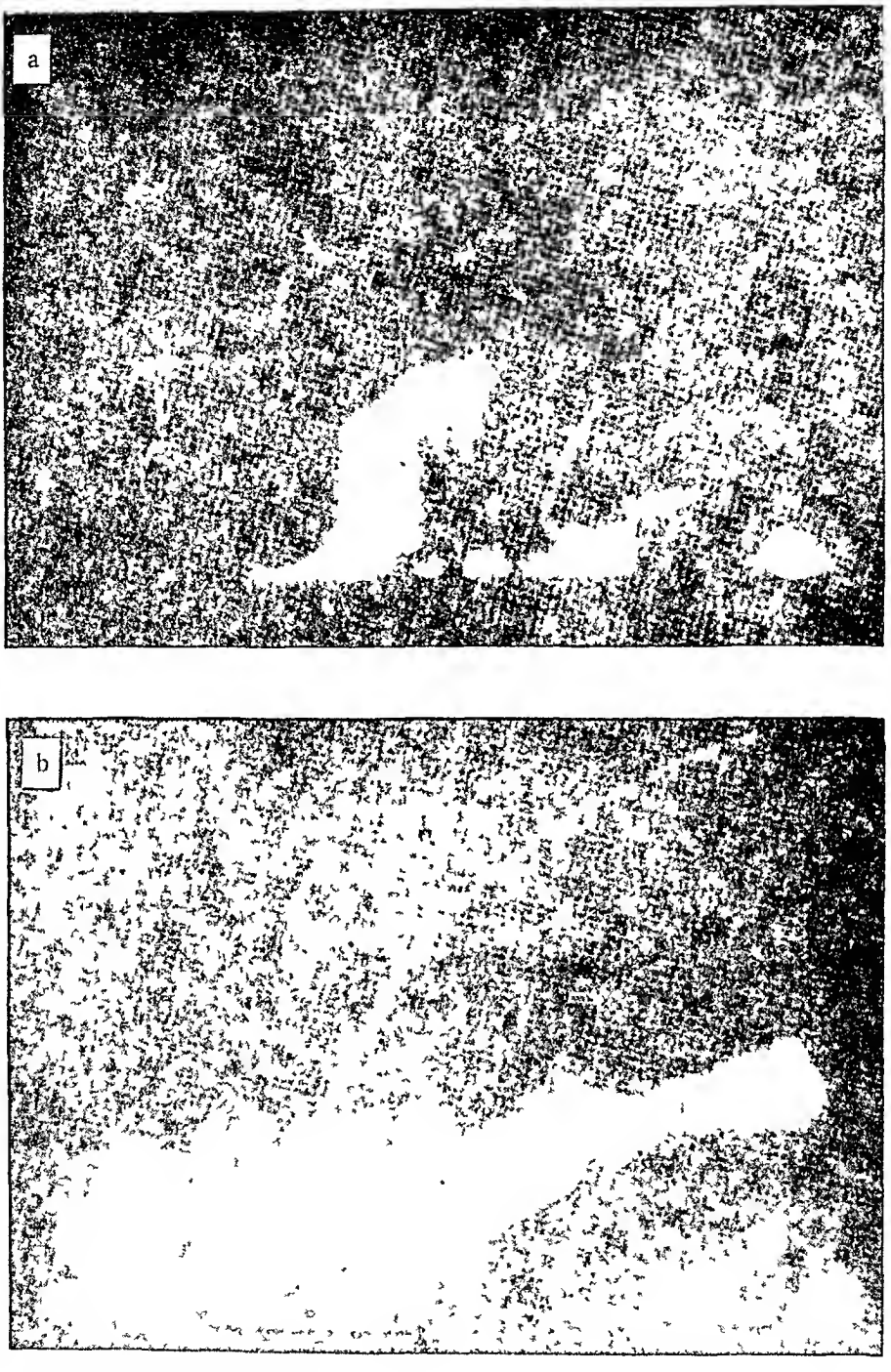

FIGURE 20. Profile of hail zone

a) low wind shear, b) strong wind shear.

Warm masses of air, encountering the precipitation wall, rise and, upon reaching the level of the —40 or —50° isotherm, change direction, creating wind shear. Cold air masses meeting the wall partly move downward, intensifying the precipitation, or flow around the barrier.

According to this conception, then, wind shear is not formed by the variation with height of the horizontal wind component, as proposed by Newton /155/, but as a result of two currents with different wind directions converging near the wall. The airflow generates a circulatory movement of cloud droplets and these, growing to a size sufficient for precipitation, produce showers. In addition, owing to the shift of wind in the direction of the storm, the cloud anvil forms what Atlas and Browning call a forward overhang. This overhang can be detected in radar photographs. According to the data of the Wokingham storm, it extends from 1.5 to 5 km ahead of the thunderstorm cloud, its lower boundary reaching a height of 4 km. In the authors' opinion, the forward overhang formed by wind shear rises slightly near the wall, to form a "vault" whose lower boundary is 5 km high. Newton and Katz state that the precipitation shifts slightly to the right of the direction in which the storm center is advancing. While the storm is advancing, hail falls as a solid swath some hundreds of kilometers long, showing a sharp increase in diameter and intensity at points along the direction of the cloud.

On the basis of detailed analysis of radar reflectivity at different levels of the Wokingham cloud and its time dependence, Browning and Ludlam conjectured that the solid cloud particles participate in a circulatory motion before falling to the surface; the first particles to fall are large hailstones and only then do light hail and showers occur. The wall is slightly inclined to the horizon, and the storm advances in a direction perpendicular to the projection of the frontal plane at the surface, the same as the direction of the front. The most intense radar reflections from the Wokingham storm cloud were observed approximately 6 to 7 km above sea level (—20° ambient temperature), 1 km ahead of the wall; the maximum hailstone diameter was 5 cm. Browning and Ludlam hold that such strong reflections at this height indicate the presence of dry hailstones.

While circulating, the hailstones are carried through zones of differing liquid water content; passage through zones of low water content produce opaque layers of hail, while zones of high water content yield transparent hail, in agreement with List's theory of wet and dry regimes of hail formation.

It should be clear from this superficial account of the Browning-Ludlam theory that their ideas as to the distribution of convective flow and hail formation in thunderstorm clouds to some extent complement the mechanism suggested by Weickmann and by workers at the High-Altitude Geophysics Institute /90/. However, like Weickmann and Dessens, Browning and Ludlam overestimate the importance of wind shear. It does not seem possible that wind shear can cause an appreciable increase in the size of the falling hail or in the intensity of the showers. The very fact that hail has been seen to fall from motionless or almost motionless convective clouds indicates that wind shear is not a prerequisite for hail formation. Moreover, analyzing radar reflectivity data, Browning and Ludlam determined the temperature of the falling hailstones from the ambient temperature, assuming the latter to be equal to the temperature of the environmental air as obtained from radiosonde data. For a hailstone diameter of up to 5 cm, the updraft speed

in the cloud should be about 50 m/sec. The corresponding difference in the temperatures of the environment and of the cloud may reach from 13 to 15°. Thus, at the level of free-air temperature —20°, where peak radar reflectivity was observed, the temperature of the cloud was probably at least —5 to —7°. At such temperatures wet growth of hail is quite possible, especially as the hailstone diameter reaches 5 cm.

The research of Browning and others has considerably enriched our conceptions of the circulation of airflow in thunderstorm clouds, though their data as to the length of the overhang (only 5 km ahead of the precipitation wall) is clearly too low. In the North Caucasus, the present authors have frequently seen such overhangs, nicknamed "elephant trunks," extending 10 to 12 km, sometimes as much as 20 km ahead of the precipitation zone (Figure 20).

In 1964, Moore et al. published a paper /150/, based on data from experiments performed in the region of the Grand Bahama Islands, in which they concluded that the main forces governing the formation of hail and shower-type precipitation are electrical: cloud particles accrete and grow rapidly as a result of lightning charges. They conjectured that lightning produces a large quantity of positive ions. These ions charge the cloud particles, and this accelerates accretion processes. In regard to this theory, it should be noted that accretion of cloud particles due to electrostatic forces can enlarge cloud particles only as long as their diameters are not in excess of 15 μ. This local phenomenon is apparently due to acoustic accretion. However, the fact that in most cases precipitation is not accompanied by thunderstorms shows that the latter are not necessary for accretive growth of particles and showery precipitation.

A recent Soviet theory of the formation of hail has been published by Kartsivadze et al. /44/. These authors hold that there are several levels of maximum updraft speed in a convective cloud. Over each such level there forms a "large-drop" zone (accumulation zone). Hail particles forming in the upper part of the cloud grow by accretion and begin to fall inside the cloud, traversing layers of alternating high and low liquid water content. Where the water content is low, growth proceeds in the dry regime, so that an opaque layer is formed in the hailstone. In an accumulation zone, the hailstone grows in the "wet" regime, forming a transparent layer. As we shall see below, this conjecture is a development of the theories worked out at the High-Altitude Geophysics Institute in 1958—1959 concerning the growth of hail in the accumulation zone, according to which the latter is the result of a decrease in updraft speed with increasing altitude.

It seems improbable, however, that there should be several accumulation zones at different altitudes in the same cloud while in the developmental stage. At any rate, fairly detailed radar studies by workers at the Institute have failed to detect this, although the distribution of precipitation in the cloud is indeed nonuniform. A vertical radar section of the precipitation zone reveals 5 or 6 regions of elevated liquid water content, alternating with low-content regions. In addition, the originators of the conjecture hold that hail pellets can gather speed while falling in the upper layers of the cloud and by inertia "pierce" levels at which the updraft speed is larger than the steady speed of free fall. This does not seem plausible.

There are many other theories of hail formation, but they will not be considered here, as the underlying factual material has not been corroborated by recent investigations.

In /98/, Shishkin conjectured that the development of convective clouds is a pulsating process; this idea was based on pulsations observed in the tops of convective clouds (such observations were recently made by G. Eidinova under the supervision of A. G. Balabuev, in the Alazani valley). We might mention, however, that pulsations have been observed only at the initial stage of development. Once the cloud has reached the shower-precipitation stage, the growth pulsations fall off.

Shishkin holds that the cloud particles grow via gravitational coagulation. At the top, or in the pre-top region of the trajectory, they freeze, forming hail embryos. Subsequently, as they fall in the supercooled part of the cloud, these embryos grow to the size of large hailstones by accreting supercooled cloud drops. Hail may also fall even in cases where the updraft speed is as low as 2 m/sec.

However, no hail has ever been observed falling at such velocities. Elementary calculations prove that hail of diameter 1—2 cm cannot fall unless the updraft speed is at least 15—20 m/sec. In addition, it is hard to imagine a thick convective cloud in which the updraft speed is no more than 2 m/sec.

On the other hand, Shishkin's theory dictates that for formation of large hailstones the supercooled region of the cloud should be at least 10—12 km. It follows that in summer months, when the zero isotherm lies 4—5 km above sea level, the top of a hail-producing cloud should reach an altitude of 14—17 km above sea level. Not infrequently, however, large hailstones will fall from a cloud whose top is only 9—10 km above sea level.

Some years ago, Gordon suggested that the ascent of cloud air in clouds in which hail is observed to grow takes place in toroidal-shaped regions with a vertical axis. However, clouds consisting of multilayer "toroids" have not been observed by investigators other than Gordon; moreover, even if they do exist, they must be extremely rare, so that they cannot significantly affect hail-formation processes. We shall therefore not discuss Gordon's views here.

The work of Karalp /133/ on the origin of hail is worthy of mention. He presents the results of 10 years of observations of cumulonimbus in South-East France. In 17-day studies of storms, including stereophotogrammetric measurements, covering cumulonimbus clouds of maximum heights ranging from 5.3 to 14.5 km, the most destructive hail was observed when the maximum height of the cloud exceeded 12.5 km. It was shown that destructive hail falls when the wind at high altitudes was very strong. The 38 days on which hail was particularly destructive were correlated with maximum velocities of very strong winds between the surface and the tropopause. These maximum velocities were generally observed between 7 and 11 km, sometimes at altitudes of 11—13 km; they usually ranged from 90 to 320 km/hr. Conversely, on days when hail was slight the speed of the upper wind was rarely more than 90 km/hr. Karalp notes that the existence of high-altitude winds is necessary to support the updraft zone ("tube") which in turn is a prerequisite for hail formation. The updraft zone may be supported by

1) an unstable layer of air near the surface, due to local superheating;
2) condensation processes;
3) freezing of drops;
4) kinetic energy of upper currents, which forces the "tube" into a horizontal position in its uppermost part (Figure 21).

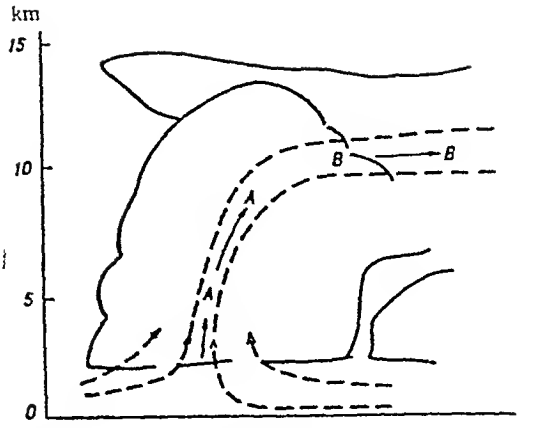

FIGURE 21. Vertical development of hail-producing cloud and wind speed at high altitudes.

A) updraft zone; B) strong-wind zone.

Karalp remarks that if there are no upper currents only short-lived "tubes" will develop, producing heavy but brief showers. When there are upper currents, the updraft zone formed near the surface becomes a true generator of large hailstones.

2.3. THE THEORY OF HAIL FORMATION DEVELOPED AT THE HIGH-ALTITUDE GEOPHYSICS INSTITUTE

In 1958, a survey was made of the various theories of shower and hail formation at the High-Altitude Geophysics Institute, and the details of the process were subsequently worked out more precisely. During that time, no significant changes were introduced in the basic ideas. The theory was the result of processing data from an all-round investigation of precipitation processes, based on experimental laboratory and theoretical research initiated in 1956.

The results concerning the formation of precipitation and new theories as to the mechanism of these processes were reported at the anniversary session of the Geophysics Institute of the Academy of Sciences of the Georgian SSR in 1958, and at a meeting of the Faculty of Physics of the Atmosphere at Leningrad University in the same year. These ideas were repeatedly discussed at all-union and international conferences, and published in a series of papers /8—11, 87, 89, 90/. The basis of the theory is that, at the first stage in the development of a cumulus cloud, the air masses ascend within the cloud in separate bubbles of warm air; with further development, these bubbles merge with one another and form a jet of rising air. The updraft speed increases from the cloud base to the level z_m at which it attains its maximum value $w_m(z_m)$. With further ascent, the updraft speed decreases toward the cloud top (convection level). At each level, the updraft speed is determined by the buoyancy of the air, or, in other words, by the temperature difference between the rising and

surrounding air. This behavior of the updraft speed creates conditions for the accumulation of large quantities of water in the liquid or solid state, above the maximum updraft speed level z_m. If the maximum speed $w_m(z_m)$ exceeds the velocity at which drops of diameter 5 —6 mm are pulverized, and the z_m level lies below the level of natural crystallization of large drops (—18, —20°), the main source of accumulated water in the upper region of the cloud are large drops formed at giant nuclei of condensation in the lower region of the cloud.

Large drops may also be produced by collisions of small drops with one another. A necessary condition for the precipitation process to be maintained is that for every 10^8 to 10^9 droplets at concentration $1 \cdot 10^3\,cm^{-1}$ there be 10 collisions per second. Large drops, rising with the updraft, grow by accreting the droplet fraction and exceed the maximum speed level, reaching a height at which their steady free fall speed becomes equal to the updraft velocity. At this level the large drops slow down and continue to grow by accreting the droplet fraction arriving from below with the updraft Growing to critical size ($R \approx 0.2$ to 0 3 cm), the large drops are atomized and a Langmuir chain reaction sets in

The growth of the large-drop fraction proceeds mainly via droplet accretion and arrival of new large drops in the accumulation zone with the updraft, forming on giant nuclei of condensation, or in some other way in the lower region of the cloud. The coefficient of capture, adiabatic liquid water content and number of giant condensation nuclei create conditions for the accumulation of critical water content within 30 to 60 minutes after formation of updraft in the cloud. One thus has an accumulation of large cloud particles in the upper region of the cloud, above the level of maximum updraft speeds. Workers at the Institute have coined the term "large-drop zone" or "accumulation zone" for this region.

The process described may occur when $w_m(z_m) > v_c$. The phase state of precipitation from the cloud depends to a significant degree on the temperature interval within which the large-drop fraction accumulates in the cloud. If the upper boundary of the accumulation zone lies at the level of the —18° isotherm, then, whatever the temperature at the lower boundary, the drops in the accumulation zone will not freeze and the cloud water gathers in the form of large, possibly supercooled drops.* When the weight of the accumulated water exceeds the byoyant force created by updrafts, the drops collapse and liquid precipitation occurs as showers. The process of accumulation and renewal of moisture content continues as long as the atmosphere is unstably stratified

Hail is destructive only when the accumulation zone lies between the 0 and —25° isotherms. Under these conditions, the large drops in the upper region of the accumulation zone freeze, forming hail embryos, which grow by accreting the droplet fraction, moreover, in the central (supercooled) part of the accumulation zone, the hail grows rapidly by accreting supercooled large drops.

Radar studies all over the world have shown that growth of hailstones of diameter 0.1 to 2 or 3 cm takes 4 or 5 minutes. At the same time, calculations of the rate of growth by accretion with the droplet fraction show that the time necessary for such growth is at least 50 minutes. One must

* We are speaking of the temperature of the cloud environment, not of the surrounding air.

therefore assume that the main part of hail growth takes place in the accumulation zone, by hail embryos accreting supercooled large drops. The liquid water content of the large-drop fraction must be at least 20 g/m^3.

According to Ludlam's data, the accumulation zone contains on the average from 1 to 3 hail embryos per 1 m^{-3}. Studies of radar reflectivity from clouds, combined with data on the spectrum and size of hail falling to the surface, have shown that the average concentration of hail in the cloud is $7-8$ m^{-3}. In some cases the hail concentration fluctuates over a wide range, from 0.05 to 50 m^{-3}, increase of hail concentration in the cloud leading almost inevitably to a decrease in hail size.

The factor exerting most influence on the development of hail processes is wind shear. When the vertical gradient of the horizontal wind speed attains high values, hail is either not observed to fall, or is seen to fall sparsely, the few scattered hailstones being incapable of inflicting much damage to agriculture. When wind shear is significant, there are several possibilities.

1. The altitude at which wind shear sets in lies below the peaks of the trajectories of the cloud particles. In that case wind shear has little effect on the development of the cloud, and hail formation depends on thermal convection.

2. The altitude at which wind shear begins lies below the maximum speed level. According to Newton, Dessens, et al., in that case the updraft speed rises slightly and the upper part of the cloud slopes forward in the direction of the horizontal flow; in all other respects the formation of hail follows the scheme described above.

3. The altitude at which wind shear begins lies between the peaks of the trajectories of the cloud particles and the maximum updraft-speed level. In this case, hail formation depends on two factors:

a) rotation of the direction of horizontal air currents in the lower and upper regions of the cloud;

b) magnitude of wind shear.

Both these factors determine whether cloud particles are carried away from the accumulation zone and hence whether the hail-formation processes will weaken or break off.

Koval'chuk has determined how cloud particles are removed by wind shear (Figure 22). The vertical updraft speed above the maximum speed level may be expressed as

$$w(z) = w_m\left(1 - \frac{z}{z_p}\right). \tag{2.7}$$

The differential equation of horizontal motion of a cloud particle is

$$\frac{dx}{dt} = v_0 + a(z - z_1), \tag{2.8}$$

where x is the horizontal displacement of the particle, v the horizontal velocity of air currents at the level where wind shear begins (z_1), and a the acceleration of the horizontal current as a function of height. The relaxation time is taken to be zero.

Integrating this equation from z_1 to the peak of the trajectory z_{pm}, we obtain the horizontal displacement of the particle during its ascent from level z_1 (the initial time t_0 is put equal to zero) to the apex z_{pm} of the trajectory. During this time, the lower region of the cloud advances horizontally for a distance $v_0 t$, where t is the length of the relevant time interval. It is assumed that the horizontal component of the cloud's motion below z_1 coincides with the corresponding component of the motion of the cloud particle. In other words, v_0 remains constant throughout the closed interval from z_1 to z_1, where z_1 is the lower boundary of the cloud.

Since the ascent speed of a particle of radius R depends on its radius, which increases as a result of gravitational coagulation along the rising branch of the trajectory, and on the updraft speed, it follows that Eq. (2.8) should be solved together with the equations for the maximum hail diameter and the critical liquid water content in the accumulation zone. Solution of these equations yield the following value for x:

$$x = [v_0 \mp a_1 (z_{pm} - z_1)]t + \left(\frac{R_m}{R_1}\right)^{A_3} \frac{e^{-A_2 A_3 t} - 1}{A_2 A_3} - \\ - \frac{A_1 R_1}{A_3} (e^{A_3 t} - 1) + A_1 R_1 \left(\frac{R_m}{R_1}\right)^{A_3+1} \frac{1 - e^{-(A_2+1)t}}{A_2 + 1}, \qquad (2.9)$$

where

$$A_1 = \frac{4\rho_p \beta t_p}{-4\rho_p w_m \mp 3qEz_p}; \quad A_2 = \frac{4\rho_p w_m}{qE\beta z_p}; \\ A_3 = \frac{Eq\beta}{4\rho_p}.$$

Thus, during time t, the cloud particle advances horizontally for a distance x as defined by Eq. (2.9), and the cloud (provided the directions of motion coincide) for a distance x_1. The falling time of a particle from height z_p to the maximum speed level is usually about 2 to 3 times longer than the ascent time, and so the probability of the particle re-entering the cloud in which it grew is reduced. Let us calculate x_1 approximately as a function of $\frac{dv}{dz}$, assuming, say, that $z_p - z_m = 3$ km. Then x is equal to 7.5 km, while x_1 will be only 900 m. While the particle is falling to level z_m, it advances at least 7.5 km, and is thus distant about 12 to 13 km from the center of the cloud and does not reach it, at least not in the accumulation zone. Even if low-level horizontal currents pull the particle back into the cloud, its dimensions upon reaching the ground will still be smaller than in the absence of wind shear, since the updraft speeds at the periphery of the cloud, where the particle re-enters the cloud, are smaller than at the center.

A typical instance of wind shear inhibiting the formation of hail as just described was observed on May 11, 1966, when a jet stream axis passed over the region in which the Caucasus expedition was working. The atmospheric cross section at the time is shown in Figure 23.

As is evident from the figure, at 9 km above sea level the velocity of the horizontal current reached 40 m/sec. Up to 4 km the velocity was negligible, but then it suddenly increased to 17 m/sec. The change in the velocity of the horizontal current with altitude was $0.6 \cdot 10^{-2}$ sec^{-1}.

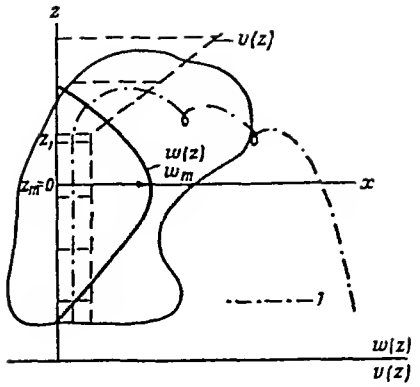

FIGURE 22. Transport of cloud particles under the influence of wind shear.

1) trajectory of cloud particle.

Under these conditions, particles from the center of the cloud were carried to a distance of about 12 km, taking into account the speed of the advancing cloud. The particles regained the periphery of the cloud, but since the updraft speeds there were small there was little hail, and the precipitation reached the ground as rain.

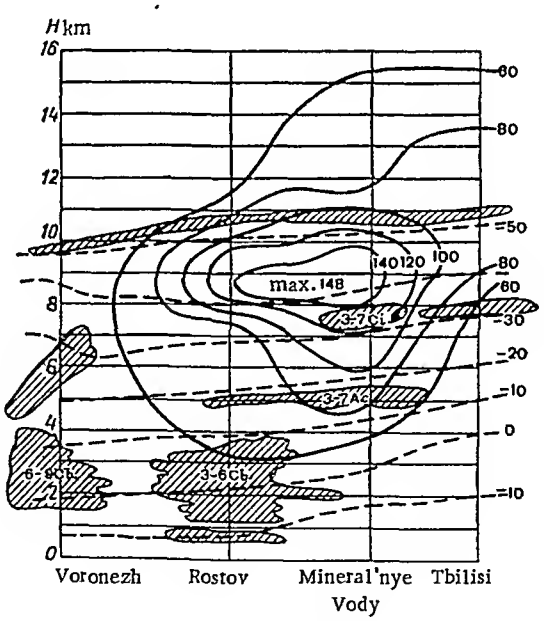

FIGURE 23. Distribution of horizontal currents, May 11, 1966.

The scheme of development of a hail-producing cloud as worked out at the High-Altitude Geophysics Institute is illustrated in Figure 24. When updraft speeds are small and the horizontal motion of the cloud significant, the growth of hail in the accumulation zone lags behind the motion of the cloud, and hail falls to the surface as isolated pellets along the path of the cloud. If the horizontal velocity of the cloud is comparatively small (15 – 20 km/hr),

the hail usually grows to a considerable size while the cloud is advancing and precipitation reaches the surface in the form of a long, solid swath of hail, sometimes hundreds of kilometers in length.

Analysis of data concerning the effect of wind shear on hail formation in North Caucasus has led to the following conclusions:

a) in some cases wind shear suppresses hail, but it cannot cause an increase in the hailstone diameter;

b) wind shear is the principal factor determining the direction of advance of the hail-formation process, and together with the motion of the cloud under the influence of the steering current it determines the direction in which a hail-producing cloud will move relative to the surface;

c) weak wind shear leads to the formation of an "elephant-trunk" hail cloud.

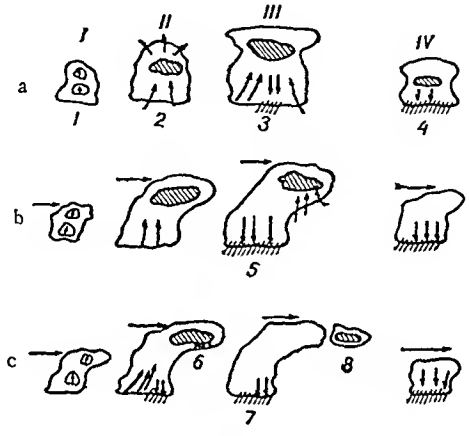

FIGURE 24. Scheme of development of hail-producing cloud.

Stages: I) initial; II) accumulation; III) showers; IV) dissipation; a) no wind shear; b) weak wind shear; c) strong wind shear; 1) isolated bubbles; 2) water collecting in accumulation zone; 3) precipitation; 4) precipitation and dissipation of cloud; 5) intensive precipitation; 6) weak precipitation; 7) heavy shower-type precipitation; 8) detachment of accumulation zone.

2.4. THERMODYNAMIC CONDITIONS OF HAIL GROWTH: METHODS OF PREDICTION

Hail grows because of an influx of ice crystals and frozen drops into the supercooled region of a cloud. Thus, in order to ascertain the mechanism of hail processes, it is important to determine the reasons for appearance of the solid phase in a cloud.

Findeisen postulates the existence of nuclei of crystallization (sublimation) in the air. At a suitable temperature, ice crystals grow at these nuclei and water converts directly from vapor to the solid state, without passing through the liquid phase.

There is no condensation growth of water drops at crystallization nuclei, so that if such nuclei ascend in the cloud their activity becomes evident only at considerable altitudes and suitable temperatures.

According to Findeisen, the temperature at which ice crystals form on crystallization nuclei depends on the properties of the nuclei and of the air mass, and may vary within wide limits (from about −6 to −30°).

Dessens holds that isolated nuclei of crystallization cause the first appearance of ice crystals in the cloud at $t \leqslant -12°$; in the temperature interval from −25 to −32° the number of crystals increases sharply, and at temperatures between −32 and −35° all particles in the cloud are in the solid phase.

Much work has been done recently, mainly in the USA and in Australia, concerning the nature of these nuclei of crystallization. Analysis of the results leads to conflicting conclusions. The Australians believe that natural nuclei of crystallization enter the troposphere from the stratosphere and are of cosmic origin, while the US investigators believe that they are of terrestrial origin.

There are still many open questions in connection with nuclei of natural crystallization. Most investigators agree that the temperature threshold of natural crystallization is low. The temperature at which there appear considerable numbers of crystals on natural nuclei of sublimation is usually less than −25°.

Analysis of data from recent studies gives grounds for the conjecture that hail embryos first appear in convective clouds at lower temperatures (−18 to −22°) than do crystals at sublimation nuclei (−25 to −32°). It seems that hail embryos are the result of freezing of large drops in the upper part of the accumulation zone.

Ludlam /139 − 142/ has shown that during the growth of a solid spherical particle by collisions with cloud particles, the rate at which latent heat is released into the environmental air may be insufficient, and then not all drops will freeze upon collision with the particle. Thus, the particle will be coated with liquid water even when the temperature of the environment is much lower than 0°, and large drops may break off its surface. These drops may grow by accretion and even set off a chain reaction. The accreting particle will give off heat to the environment, mainly due to conduction and surface evaporation of water. The heat balance equation of a hailstone is

$$\theta_1 + \theta_2 = \theta_3. \tag{2.10}$$

Here θ_1 is the heat loss from the hailstone by heat exchange, which is $-4\pi\alpha r^2(T_1 - T_2)$, where α is the coefficient of heat exchange, r the radius of the hailstone, T_1 and T_2 the temperature of its surface and of the surrounding air, respectively; θ_2 is the heat loss by evaporation: $4\pi\beta r^2 L\Delta\sigma$, where β is the coefficient of mass exchange, L the latent heat of evaporation, $\Delta\sigma$ the difference in water-vapor concentration far from the hailstone and at its surface. α and β are determined from the equations

$$Nu = 0.6Pr^{\frac{1}{3}} Re^{\frac{1}{2}}; \tag{2.11}$$

$$Nu' = 0.6Sc^{\frac{1}{3}} Re^{\frac{1}{2}}, \tag{2.12}$$

where $Nu = \frac{2r_2}{\lambda}$ is the Nusselt number, $Nu' = \frac{2r_2}{D}$ is an analog of the Nusselt number, $Pr = 0.71$ is the Prandtl number, $Sc = 0.61$ is the Schmidt number, λ the thermal conductivity, D the coefficient of diffusion of water vapor in air; Θ_3 is the addition of heat to the hailstone due to acquisition and freezing of cloud particles:

$$E\pi r^2 q w \bar{c} (t_1 - t_2),$$

where q is the quantity of deposited water, w the fall speed of the hailstone relative to the cloud particles, $\bar{c}$ the average specific heat of water.

Assuming that all the water captured by the hailstone is frozen, equating the values $\Theta_1 + \Theta_2 = \Theta_3$ for a single particle, Ludlam solved the equation for q and obtained the critical liquid water content at which the heat lost to the environment is equal to the heat released when the captured drops freeze:

$$q = \frac{1.2\sqrt{Re}}{Ewz} \frac{LD\Delta\rho - kT_1}{80 + T_1}. \qquad (2.13)$$

Figure 25 plots the critical values of q for different-sized particles at air temperatures from 0 to −30° in the cloud, assuming a temperature of 10° and pressure 900 mb at the cloud base. The dashed line represents the change in liquid water content with height, corresponding to adiabatic lifting of air without allowance for mixing with environmental air. If the actual liquid water content exceeds the critical value for the appropriate particle size, a film of water will be deposited on the particle as it captures cloud drops. Such hailstones have a high density (0.9 g/cm^3) and are known as "wet hail"; they are said to grow in the wet regime. If the actual liquid water content is less than critical, all drops captured by the particle will freeze and a coat of completely frozen opaque ice will form on the hailstone. This is known as the dry regime of growth; the density of such hailstones is about 0.3 g/cm^3.

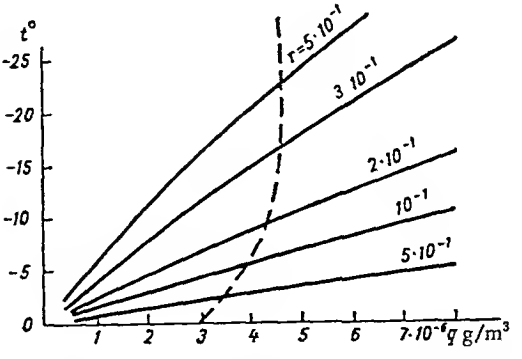

FIGURE 25. Critical liquid water content in accretion growth of particles in a cloud.

Much experimental and theoretical work has been devoted to studying the freezing point of water drops as a function of their diameter. It has been shown that the state of a supercooled water drop is metastable and the probability that it will freeze at a given temperature ($T_s < 0°$) is proportional to its volume. Various impurities (dissolved and otherwise) affect the freezing point. But even data on the freezing point of chemically pure water fluctuate, depending on the conditions prevailing at the time of freezing; this may be seen from the plot of T_s (log d) in Figure 26. Utilizing data from different authors, Mason constructed a general curve, according to which the freezing point of a drop of diameter 1 is —41°. This is in good agreement with theoretical calculations by Kachurin /45/ and Mason /149/.

Curves of T_s(log d) proposed by Bigg /118/, Dorsch and Hacker are almost parallel (Figure 26). They thus represent the same probability of freezing as a function of temperature. A special feature of Bigg's curve is that the freezing point of micron drops behaves differently. The data at these points approach Mason's curve.

An examination of the techniques used by these various authors confirm these distinctions. In fact, the results summarized in Mason's general curve were obtained either for drops of diameter a few microns, which are apparently poor captors of foreign nuclei capable of triggering freezing, or for volumes of water contained in glass or ceramic tubes, and thus shielded from nuclei by the tube walls.

The set-up of the experiments of Bigg, Dorsch and Hacker was quite different. They placed water probes in an environment containing foreign nuclei, which were somehow capable of penetrating the drops.

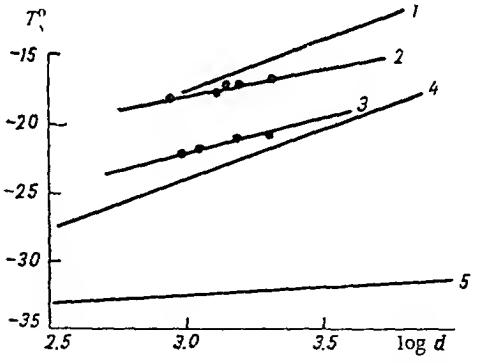

FIGURE 26. Plot of T_s (log d) according to different authors.

1) Dorsch and Hacker, after material of Ivanov (High-Altitude Geophysics Institute); 2) castor oil-CCl_4 vapor and chloroform-castor oil vapor; 3) CCl_4 and watch oil; 4) Bigg; 5) Mason.

Thus, Mason's curve for T_s(log d) describes a process of spontaneous freezing, while the curves of Bigg, Dorsch and Hacker represent the result of heterogeneous freezing. It is clear, therefore, that the property of heterogeneous nuclei, introduced by Mason:

$$n = n_0 e^{kT_s}, \qquad (2.14)$$

where n is the concentration of nuclei with ice-forming temperature T_s, is indispensable for an interpretation of experimental results.

Instead of this property, it is more convenient to consider the ability of the drop surface, whose sorption properties are known, to collect nuclei.

This idea was checked by a modification of Bigg's method. A refrigerating plant was devised to achieve optimum regulation of cooling rate (Figure 27). The plant consists of a heat exchanger, with a special cavity in which a container with drops is placed. Vapor from liquid nitrogen in a Dewar vessel is introduced into the cavity. The rate of cooling is regulated by varying the intensity with which the liquid nitrogen is boiling. The device kept the cooling rate of the drops constant to within 3% of the rated value of 0.5°/min. As in Bigg's experiments, a drop of twice distilled water was placed at the interface between two immiscible liquids insoluble in water. As liquids heavier than water, CCl_4 and chloroform were used, while the light components were castor and watch oil.

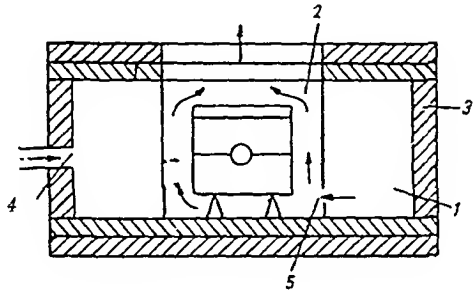

FIGURE 27. Heat chamber used in experiment to determine T_s (log d).

1) metal heat exchanger; 2) air cavity for container with drops; 3) thermally insulated jacket of Plexiglas; 4) fitting for supply of coolant; 5) opening for injection of nitrogen vapor into cavity.

According to Bigg, the frequency of values obtained for the freezing point of a drop of standard diameter is symmetric about the maximum value and approximates a normal distribution. Thus, temperatures (in this experiment) equidistant from the T_s value representing the most frequent freezing point should occur equally often and their average is T_s. Hence there is no need to study a large number of drops of the same diameter. The range of temperatures (on both sides of T_s) corresponding to an e-fold change of frequency is about 2° (for drops 1 mm in diameter). Consequently, even if an insufficient number of drops is used, the error in T_s for drops of 1 mm diameter should not exceed ±1.0°.

The optimum number of drops needed to obtain each freezing point figure was taken to be 10 − 15. The temperatures were measured as usual by a thermocouple. A microscope was used to determine the drop size and to follow the freezing process. Of the above-mentioned four liquids, three pairs were studied (chloroform and castor oil, CCl_4 and castor oil, CCl_4 and watch oil). For the first two pairs, the T_s(log d) curves obtained coincided but gave exaggerated values for the freezing point in comparison with Bigg's figures. When castor oil was replaced by the less viscous watch oil,

the T_s (log d) curve came nearer to Bigg's curve (Figure 26). Thus the freezing point curve was found to depend on the selected pair of supporting liquids.

This cannot be explained by measurement errors. The absolute calibration error of the thermocouple was ±0.5°, and so the maximum possible error in temperature determination, allowing for errors due to insufficient experiments, should not exceed ±1.5°. The error in determination of the drop diameter may be ignored, as it is relatively small. The minimum temperature difference read off from the T_s (log d) curves for different pairs of liquids was 3.8°.

It was conjectured that the mechanical properties of the supporting liquids somehow affect the motion of heterogeneous nuclei within the drop. To verify this, particles of AgI were added to watch oil. This led to a sharp increase in the freezing point of the drops, without changing the shapes of the curves. Figure 28 shows two curves of this type, obtained at different concentrations of AgI particles. They are hardly useful for quantitative analysis, owing to the indeterminateness of the AgI concentration. It may seem strange that these curves of T_s (log d), plotted with addition of AgI, do not reflect the familiar threshold properties of this reagent. This may be due to partial deactivation of the reagent, which cannot be identified with any interaction of supercooled drops and reagent particles in the air or in oil.

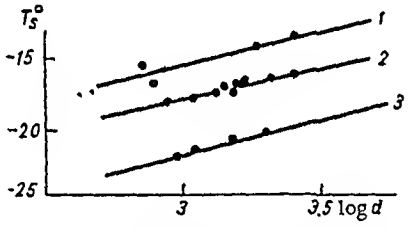

FIGURE 28. Effect of increasing the concentration of ice-forming nuclei in the upper component of the pair of supporting liquids.

1) watch oil with AgI and CCl_4; 2) transformer oil with AgI and CCl_4; 3) watch oil and CCl_4.

The experiment involving addition of AgI aerosols clearly illustrate our previous assertion concerning the triggering of freezing in the experiments of Bigg, Dorsch and Hacker by heterogeneous nuclei captured by the drop surface. It follows that the freezing of large drops in a cloud should be described in accordance with the experiments of Dorsch and Hacker, as these were carried out with drops freezing in air.

These results show that hail nuclei are formed by the freezing of large drops in the accumulation zone. Analysis of the available data, both those available in the literature and those obtained in experimental work at our Institute, indicate that the natural freezing point of large cloud drops ranges from −15 to −22°, depending on the radius of the drop.

Another process of importance for hail suppression that can be studied under laboratory conditions is the growth of hail particles. Experiments to this end are comparatively recent.

List /137, 138/, on the basis of careful experiments, reached the conclusion that hail does not grow as suggested by Schumann and Ludlam (as much water is deposited on the hailstone as can freeze); he showed that their ideas were at variance with experimental data.

List examined the growth of hailstones in a closed wind tunnel. The growing hailstone was allowed to rotate freely about a fixed axis in the tunnel. The purpose of List's experiments was to study the liquid water content of the hailstone as a function of water content, velocity of motion and thermodynamic parameters of the air.

These experiments determined the conditions for formation of what List called "spongy" ice — a mixture of water and ice. Namely, the addition of heat (due to freezing of captured water, condensation or evaporation) must exceed the convective loss of heat from the surface of the growing hailstone. If the added heat exceeds the loss, the water deposited on the hailstone surface does not freeze completely. Some of it, not blown off from the surface by air currents, forms liquid inclusions which freeze slowly. As a result, the density of a layer of transparent ice in a hailstone may exceed the density of pure ice (0.92 g/cm^3), depending on the water content and thermodynamic parameters of the air.

If the addition of heat is less than the convective loss, the density of the hailstone will be less than or equal to the density of pure ice. At the same time, the actual density is again dependent on the water content, hailstone diameter and the thermodynamic parameters of the air. According to List, these are precisely the conditions under which a hailstone of smaller diameter has a higher probability of growing.

List performed 100 experiments with spheres of diameters up to 2.5 cm, air speeds of up to 30 m/sec, and water content of up to 20 g/cm^3; in none of these experiments did he observe any escape of excess water from the particles to the air. He then used the results to solve the heat balance equation for a hailstone. The percentage water content of a hailstone is given by

$$q_m = 100\left(1 - \frac{\Theta_4}{\Theta_3}\right). \tag{2.15}$$

Here Θ_4 is the amount of heat released upon freezing of water deposited on the hailstone: $E\pi r^2 qLI$ (L is the latent heat of fusion), Θ_3 is the heat which would be released if all the deposited water were frozen.

Substituting the values of Θ_3 and Θ_4 and performing some simple manipulations, one obtains the following condition for wet growth of hail:

$$I = \frac{-1.68kt_1 - c_1 D_w T_1^{-1}(e_{sn} - e_{sv})}{0.785 L_f E q w^{\frac{1}{2}} \nu^{\frac{1}{2}} d^{\frac{1}{2}}} - \frac{\bar{c}\, t_1}{L_f}, \tag{2.16}$$

where d is the hailstone diameter, L_f the latent heat of fusion at temperature t_2, $c_1 = 207$ kcal · g^{-1} · m^{-3} · mb for the water-vapor phase transition, t_1 is the ambient temperature, ν the kinematic viscosity, D_w the diffusion coefficient, T_1 the absolute temperature of the environment, e_{sn} and e_{sv} the elasticity of saturated vapor over water and ice, E the coefficient of capture, q the liquid water content, w the fall speed of the hailstone, $\bar{c}$ the specific heat of the water deposited on the hailstone, $\Theta^{-1}E = 0.675$. If $t_2 < 0°$, $I = 1$; if $t_2 = 0°$, $I \leqslant 1$.

Thus, if $I < 1$, the deposit on the hailstone consists of a mixture of water and ice. Using Eq. (2.16), List found boundary conditions for wet growth of hail as a function of water content in the growth zone and of the ambient temperature, for freely falling particles of different diameters. The results are shown in Figure 29. It is evident from the figure that wet growth requires a water content double that postulated by Ludlam. This is because Ludlam, solving the heat balance equation, assumed that all the water deposited on the hailstone is frozen, disregarding the necessary addition of heat to the hailstone due to its composition as a mixture of water and ice.

The structure of falling hail shows that in order to cause crop damage, hail must be "wet" – a water-ice mixture. It is thus clear that the conditions in the cloud should be such as to guarantee wet growth of hail as defined by Eq. (2.16). It is known that the zone of supercooled water necessary for the growth of hail lies above the maximum speed level, but at the same time the conditions for hail formation depend on the liquid water content and on the ambient temperature. The critical water content for wet growth of hail is calculated from Eq. (2.16). To this end one must determine the actual water content taking part in the process, compare it with the critical value, and then determine the unique solution of the water-content equation for hail in the cloud.

The maximum accumulated water content per unit volume may be calculated as a function of the buoyant force from the equation

$$q_m = \rho_m \frac{w_m^2}{2gh_{a.z}},$$

where $h_{a.z}$ is the thickness of the accumulation zone (on the average 1500 m).

The calculated values are compared with the critical water content and ambient temperature necessary for wet growth of hail, as obtained by List for initial hailstone radius 0.25 cm (Figure 29). The results of calculation of the boundary conditions for wet and dry growth for different maximum updraft speeds are as follows:

w_m (m/sec)	....	12	15	20	25
q_m (g/m^3)	....	3.4	5.3	9.3	14.8
T_m	....	−9.0	− 12.0	−20.0	−29.0

The results were then plotted on a graph (Figure 30) on which the boundary curve ab, representing growth of hail under thermal equilibrium conditions, divides the plane into two zones: zone I – formation of hail (wet growth), zone II – formation of graupel and snow (dry growth).

Above the −30° level, hail cannot grow in the wet regime, as the concentration of supercooled drops becomes negligently small compared with the concentration of ice particles, while data of Bigg, Kiryukhin and others imply that drops 200 to 300 μ in diameter freeze at temperature −30°. Hence, even at high velocities, the dry regime prevails above the −30° level /118/. If the calculated maximum speed w_m and temperature at that level fall into zone I, this means that there may be wet growth of hail in the cloud; if it falls in zone II, one has dry growth, with formation of spongy hail of low density, which melts completely as it falls through the warm layers of the atmosphere /142, 143/. On the other hand, if the maximum speed level is in a positive-temperature zone, conditions in the cloud are not suitable for hail formation.

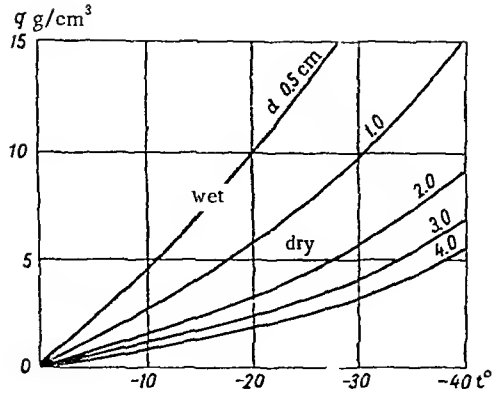

FIGURE 29. Conditions for growth of hail as a function of water content and temperature of environment, for freely falling particles of different diameters.

The calculations thus yield the phase state of the precipitation as a function of the maximum updraft speed and of the temperature at the maximum speed level.

Whether hail will actually fall to earth depends on the size of the hail at the level of the zero isotherm. The maximum hail radius may be defined from the equation

$$g\rho_h V = \pi r^2 \frac{1}{2} C_D \rho' w^2. \qquad (2.17)$$

The terminal fall speed of the hailstone (relative to the air) is equal in magnitude to the updraft velocity of the air in the supercooled region of the cloud, πr^2 is the area of its cross section, g the acceleration of gravity, ρ_h the density of hail, V the volume of the hailstone, r its radius, C_D the drag coefficient, w the fall speed.

Substituting $V = \frac{4}{3}\pi r^3$ into Eq. (2.17), we obtain

$$w = \sqrt{\frac{8g\rho_h}{3C_D\rho'} r} \qquad (2.18)$$

It is clear from (2.18) that the terminal fall speed depends on the drag coefficient C_D and on the hail radius. The coefficient C_D in turn depends on the Reynolds number Re. For $10^2 < Re < 10^5$, C_D lies between 0.4 and 0.5. When Re reaches the vicinity of $3 \cdot 10^5$, C_D falls sharply to 0.1 (experiments of Bilham and Relf). The critical Reynolds number, and consequently the drag coefficient at a given hailstone diameter, vary as functions of the roughness of the solid surface and the turbulence of the air.

On the basis of the experiments of Prandtl and Eiffel, we can assume $C_D = 0.5$ for spherical hailstones. As the hailstone becomes more oblate the drag coefficient increases, approaching unity. On the basis of experimental data, List /137, 138/ concluded that hailstone should not be treated as smooth, but as rough balls. The air is then turbulent at lower Reynolds numbers and higher drag coefficients. List measured the drag coefficients of various hailstones as functions of the Reynolds number.

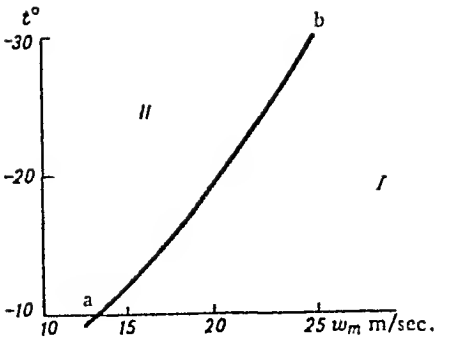

FIGURE 30. Phase state of precipitation in cloud as a function of maximum updraft speed and temperature at maximum speed level.

It turned out that smooth spherical hailstones fall most rapidly. Depending on the shape of the surface, the terminal speed is usually lower.

In our calculations we assume that the hailstone is falling at the optimal speed, so that C_D='0.5 (smooth spherical surface). Therefore, substituting C_D into (2.18), we obtain the following formula for a hailstone of density ϱ= 0.9 g/cm^3:

$$w = \gamma \sqrt{r}\,. \tag{2.19}$$

where $\gamma = 2.63 \cdot 10^3$ cm$^{-1} \cdot$ sec.

The downward motion of the hail creates downdrafts; the hailstones fall rapidly from the cloud, so that their size is determined chiefly by the growth conditions in the accumulation zone. Hail begins to fall when its fall speed exceeds w_m. We present a partial table of hail size as a function of maximum updraft speed:

w_m (m/sec)	12	15	20	25	30	35
r (cm)	0.21	0.34	0.60	0.93	1.34	1.82

It has been shown that hailstones of diameter greater than 3 cm are affected only slightly while falling through the warm part of the atmosphere, so that for maximum speeds above 30 m/sec the hail radius may be calculated directly from Eq. (2.19).

Smaller hailstones are melted to a significant degree when they fall below the zero isotherm. The effect of melting for such hailstones has been determined using a result obtained by Ivanov /40/ of the High-Altitude Geophysics Institute. Using the graph of Figure 31 and the above data, the terminal hail radius R_t was determined as a function of the height of the zero isotherm above the surface at different maximum speeds. The results are shown in Table 5 and plotted in Figure 32. The ordinate of the plant (w_m, H_0) in Figure 32 is equal to the terminal radius R_t of the hail reaching the surface.

Summarizing, we see that determination of the maximum updraft speed is indispensable both in predicting the potential formation of hail and in determining its terminal radius. Hail prediction should thus involve the following steps:

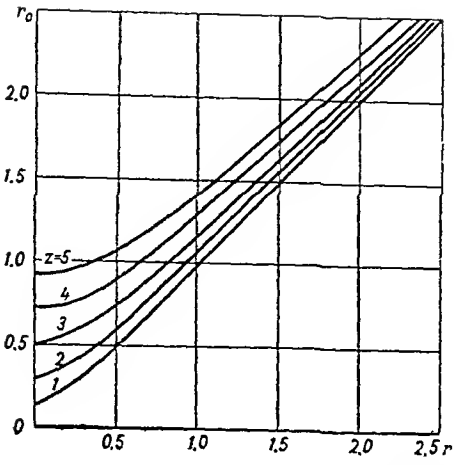

FIGURE 31. Terminal radius of hailstone as a function of height of zero isotherm and original radius.

γ=0.7°/100 m, P_0=600 mb.

1) Calculate and plot prognostic stratification curves of temperature and humidity.

2) Calculate the maximum updraft speed and determine the temperature of the rising air at the corresponding level.

3) Using Figure 30, determine whether the conditions in the cloud are suitable for formation of hail.

4) Using Figure 32, calculate the terminal size of the hail reaching the ground.

TABLE 5. Terminal hail radius as function of height of zero isotherm at different speeds w_m

H_0, km	w_m m/sec					
	12	15	20	25	30	35
0	0.21	0 34	0 60	0.93	1.34	1 82
1	0.16	0 31	0 57	0 93	1 34	1 81
2	—	0 14	0 48	0 81	1 27	1.74
3	—	—	0 29	0 72	1 19	1 68
4	—	—	—	0.56	1.07	1.59
5	—	—	—	0 16	0 96	1 49

Field investigations carried out by the Caucasus hail-suppression expedition produced data of atmospheric stratification up to the time of maximum development of convection. These data were utilized to calculate the possible convection level according to the aerological diagram.

Using radar of wavelength λ=3.2 cm with a vertical scanning antenna, the development of the cloud was observed. First the radar echo from the cloud rose to 6 —7 km, and then, within a few minutes, to 8 —9 km. This increase of the radar echo continued until the cloud had attained maximum development, and thereafter began to decrease. Data of the echo tops at

the time of maximum cloud development were used for the analysis. As the error in measuring the echo top increases with increasing distance, the results used for the analysis pertained to clouds developing at most 40 km from the station. Calculations have shown /90/ that the maximum error in determining the upper boundary of the radar echo is at most 0.5 – 1.0 km, the mean error being from 300 to 400 m.

Table 6 presents the results of a comparison of convection levels calculated from the aerological diagram with measurements of the echo tops. It is evident from the table that the echo tops for the hail clouds are on the average 1500 m higher than the calculated convection level; the echo tops for rain clouds are 1300 m lower. The maximum difference between these figures for hail clouds is +3400m, the minimum figure +500 m; the maximum and minimum differences for rain clouds are –5200 and +200 m, respectively. Only in two cases was the echo top from a rain cloud higher than the calculated convection level, by 100 and 200 m.

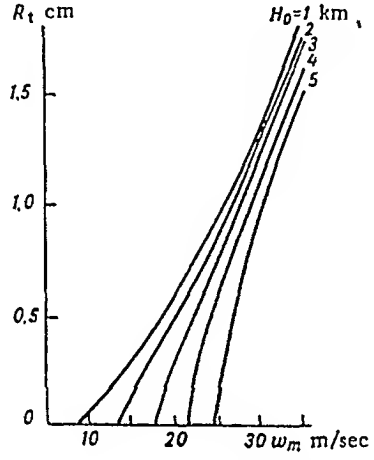

FIGURE 32. Terminal radius of hailstone as a function of updraft speed, for different heights H_0 of zero isotherm.

The stratification curve from which the convection-level data were extracted was corrected by the use of radiosonde observations made directly before the beginning of the hail process. Hence the change in the height of the convection level cannot be attributed to readjustment of atmospheric stratification during the soundings and the development of the cloud.

The data of Table 6 were plotted, yielding the graph of Figure 33, showing the calculated and actual convection levels.

The dependence observed here between the actual and calculated altitudes of the cloud and the nature of the precipitation may be explained as follows. Calculation of the convection level from the aerological diagram ignores the heat released when the supercooled water freezes. If we assume that hail grows by accretion of accumulated water and that all the supercooled water freezes completely, the calculation must take this additional heat into consideration. The released latent heat of fusion is

$$\Delta\theta = L\Delta q, \qquad (2.20)$$

TABLE 6. Comparison of calculated convection levels H_{cal} with measured radar echo tops H_{act}

Date	H_{cal}, m	H_{act}, m	ΔH, m	Type of precipitation
9/V 1965	10 000	13 400	3400	Hail
10/V	9 400	11 000	1600	"
12/VI	12 200	13 800	1600	"
16/VI	10 600	8 200	—2400	Rain
1/VII	10 200	13 200	3000	Hail
3/VII	11 000	12 400	1400	"
7/VII	12 200	13 900	1700	"
7/VII	12 200	13 600	1400	"
7/VII	12 200	13 000	800	"
30/VIII	11 000	13 100	2100	"
30/VIII	11 000	13 000	2000	"
22/V 1966	10 300	13 600	3300	"
9/VI	11 500	13 700	2200	"
20/VI	8 000	9 000	1000	"
11/VIII	13 000	14 000	1000	"
18/VIII	10 000	10 000	0,0	Rain
24/V 1967	10 200	11 700	1500	Hail
25/V	10 700	10 300	—400	Rain
26/V	11 500	10 100	—1400	"
26/V	11 500	12 200	700	Hail
26/V	11 500	11 200	—300	Rain
26/V	11 500	12 200	700	Hail
26/V	11 500	8 600	—2900	Rain
28/V	9 500	7 700	—1800	"
28/V	9 500	8 600	—900	"
28 V	9 500	9 200	—300	"
29/V	8 000	6 700	—1300	"
29/V	8 000	8 100	100	"
29/V	8 000	9 700	1700	Hail
31, V	10 700	5 500	—5200	Rain
3/VI	10 700	6 200	—4500	"
3/VI	10 700	10 000	—700	"
13/VI	11 500	10 900	—600	"
13/VI	11 500	12 000	500	Hail
13/VI	11 500	12 000	500	"
13/VI	11 500	12 000	500	"
14/VI	12 200	14 000	1900	"
14 VI	12 200	11 700	—500	Rain
14/VI	12 200	10 700	—1500	"
15, VI	12 000	9 000	—3000	"
15/VI	12 000	10 700	—1300	"
15/VI	12 000	10 200	—1800	"
15/VI	12 000	11 200	—800	"
15/VI	12 000	14 000	2000	Hail
19/VI	9 600	11 000	1400	"
19/VI	9 600	6 900	—2700	Rain
19/VI	9 600	6 000	—3600	"
22/VI	10 500	8 400	—2100	"
22/VI	10 500	10 200	—300	"
22/VI	10 500	10 600	100	"

TABLE 6 (Contd.)

Date	H_{cal}, m	H_{act}, m	ΔH, m	Type of precipitation
22/VI	10 500	12 200	1700	Hail
22/VI	10 500	10 700	200	Rain
23/VI	10 000	10 000	0.0	"
	10 000	12 000	2000	Hail
23/VI	10 000	9 400	−600	Rain
26/VI	10 500	10 500	0.0	"
	10 500	8 900	−1600	"
	10 500	9 100	−1400	"
26/VII	10 300	9 800	−500	"
	10 300	12 200	1900	Hail
	10 300	10 000	−300	Rain
31/VII	9 400	10 700	1300	Hail
		7 600	−1800	Rain
		9 800	400	Hail
9/VIII	10 500	10 200	−300	Rain
		9 100	−1400	"
		13 500	2000	Hail

$\Delta\bar{H}_{hail} = 1570$ m; $\Delta\bar{H}_{rain} = -1350$ m

where L is the latent heat of fusion of 1 g water (80 cal/g), Δq the quantity of water frozen. As a result, the temperature of the cloud air is increased by ΔT, say. Under conditions of constant pressure, the addition of heat per unit volume of air is determined by

$$\Delta\theta = \bar{\rho} c_p \Delta T. \tag{2.21}$$

where c_p is the specific heat of air at constant pressure, $\bar{\rho}$ the mean density of air in the accumulation zone.

The quantity of accumulated water may be calculated from Eq. (2.12). Using this equation and also Eqs. (2.20), (2.21), with $\rho_m \approx \rho$, we obtain

$$\Delta T = \frac{L w_m^2}{2 c_p g (z_w - z_m)}. \tag{2.22}$$

Using Eq. (2.22), ΔT was calculated as a function of w_m. The rise in temperature due to hail formation may reach 10 − 15°. The calculated value of ΔT was added to the maximum deviation of the curve of state from the stratification curve on the aerological diagram, which represents the maximum amount of heat released in condensation of water vapor; the result was then used to calculate the possible convection level, for the case that all the supercooled accumulated water was frozen and hail had formed.

TABLE 7. Comparison of calculated H_{cal} and measured H_{act} radar echo tops from hail clouds

Date	H_{cal}, m	H_{act}, m	ΔH, m	Type of precipitation
7/VII 1965	14 000	13 600	100	Hail
30/VIII	13 000	13 000	0.0	"
30/VIII	13 000	13 100	100	"
22/V 1966	13 500	13 600	100	"
9/VI	14 000	13 700	300	"
20/VI	9 200	9 000	—200	"
11/VIII	14 500	14 000	500	"
24/V 1967	11 500	11 700	200	"
26/V	12 500	12 200	—300	"
26/V	12 500	12 200	—300	"
29/V	9 800	9 700	100	"
13/VI	12 000	12 000	0.0	"
13/VI	12 000	12 000	0 0	"
13/VI	12 000	12 000	0.0	"
14/VI	11 000	11 000	0.0	"
15/VI	14 000	11 000	0.0	"
19/VI	11 000	11 000	0.0	"
22/VI	12 000	12 200	200	"
26/VII	12 000	12 200	200	"
9/VIII	13 500	13 500	0.0	"

$\Delta\bar{H} = +112$ m

The results of the calculated and measured radar echo tops from hail clouds are shown in Table 7.

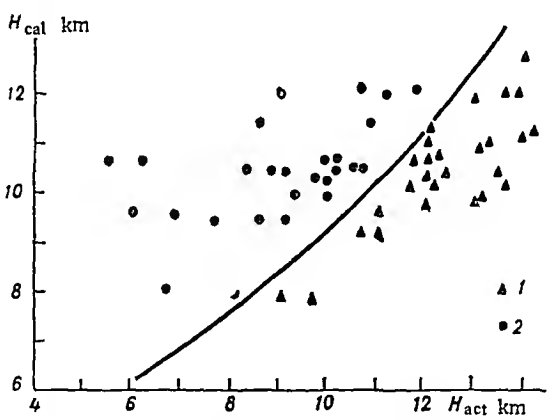

FIGURE 33. Comparison of calculated convection levels with measured heights of echo tops.

1) hail; 2) rain.

The data of Table 6 are more readily visualized from the graph of Figure 34, on which the calculated convection levels (with allowance for the latent heat) are plotted against the measured echo tops. It is clear

from the figure that the agreement of calculated and measured values is good. According to the data of Table 7, the difference between the measured echo tops and the calculated convection level fluctuates between 500 and −300 m, the average being +112 m. In other words, the difference between the altitude of the cloud as calculated from Eq. (2.22) and as determined by radar remains within the bounds of the measurement error.

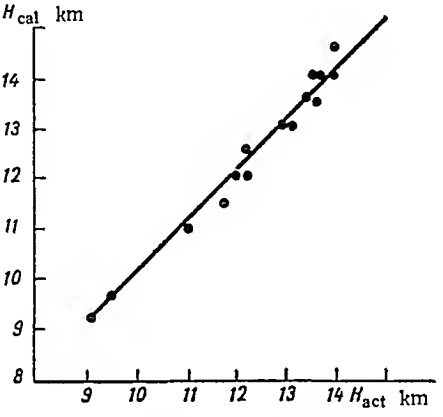

FIGURE 34. Comparison of calculated and measured radar echo tops from hail clouds

The conclusions drawn from this work at the Institute were as follows.

1. If hail is forming in a cloud, the echo top at the time of maximum development exceeds the convection level calculated from atmospheric stratification data via the aerological diagram.

2. Wet growth of hail proceeds by hail seeds accreting the large-drop supercooled fraction in the accumulation zone, when the water content of the latter is at least 15 −25%.

3. The growth of hail occupies a short time interval (from 4 to 10 minutes); otherwise the echo tops would not show such "surges," insofar as the released heat would be distributed uniformly over the entire cloud.

4. An altitude increase in the radio echo, 0.5 −2.5 km compared with the convection level as calculated from the aerological diagram, may serve as a reliable indication of the formation of hail in a cloud, thus yielding a method for the identification of hail clouds.

In view of the results described in this section, there are good prospects for the use of combined radar and infra-red techniques for a more detailed study of conditions for hail formation.

Chapter 3

CALCULATION OF AMOUNT OF SHOWER-TYPE PRECIPITATION

Heavy showers constitute a dangerous weather phenomenon. They inflict considerable damage on agriculture and as a result many investigators, both in the Soviet Union and elsewhere, have devoted attention to their prediction. Despite these efforts, the complexity of the problem is such that a reliable prediction method has yet to be found.

At the turn of this century, many well-known Russian meteorologists were studying showers and storms. The first physical analysis of the process of convection and the formation of cumulus and cumulonimbus is due to Kasatkin /41 – 43/, who utilized visual and kite observations. He stated two basic factors determining the intensity of vertical development of cumulus clouds: the location of the condensation level ("dew surface") and of the convection level ("spreading surface"). He determined the intensity of advection of warm air in the upper layers necessary for inversion to occur in free air, showing how inversion affects the vertical development of clouds and consequently the height of the convection level. As early as 1905 he had constructed a model of a convective cell, comprising the following elements:

1) lower layer – intake layer, in which heated air reaches the vicinity of an updraft;

2) rising layer, in which the temperature difference between the heated air and the environment cause the former to rise;

3) spreading layer, in which the raised air spreads sideways over the equilibrium surface (convection level).

This model (see Figure 35) is still of value today. Kasatkin observed that the convection process involves the ascent not only of the lower, heated air layers but also of air parcels "pulled in" from the sides; this is the process now known as entrainment.

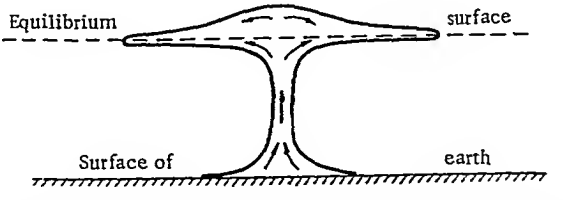

FIGURE 35. Diagram of cumulonimbus cloud, according to Kasatkin.

New prospects for the prediction of convective precipitation appeared when the concept of wet instability energy was introduced and graphical techniques worked out for its determination. Several papers established the relationship between instability energy and the occurrence of precipitation was established /12, 28, 62/.

Investigations of Muchnik /62/ and Orlova /66–70/ showed that positive instability energy, established by morning radiosonde observations, does not necessarily imply the occurrence of shower-type precipitation. Cases were found in which the calculated instability energy was negative and precipitation nevertheless occurred, or, conversely, in which the instability energy was positive and no precipitation was forthcoming. Such contradictory situations could be due to underestimates of possible changes in stratification at the onset of convection, which weakened the correlation between the initial instability energy and the subsequent weather phenomena. It was assumed at the time that the stratification and humidity in a homogeneous air mass remain more or less constant over 24 hours. For this reason the instability energy was calculated from the morning emagram and compared with precipitation occurring in any part of the day.

Orlova showed, however, that temperature stratification and air humidity may vary in the course of one day, for various reasons, such as advection, vertical motion, heating of lower layers of air, and so on. Thus, only by determining the stratification of temperature and humidity at the onset of convection can one establish whether showers may or may not occur.

A technique for identifying and predicting showers, based on variations in temperature and air-humidity stratification at the onset of convection, was developed at the Central Forecasting Institute (TsIP) in 1944–1953, on the basis of work by Lebedeva /57/ and Orlova /66–68/.

Since then, this stratification-based technique, incorporating some additional shower-producing factors, has found wide applications and has been considered the definitive method for shower prediction /4/.

The great shortcoming of the method, however, is that all it predicts is the fact – the occurrence of showers. To develop a method which will also predict the amount of precipitation is extremely difficult, as the occurrence and evolution of precipitation involves a complex of factors, all of which must be taken into consideration. Attempts by various investigators to work out such a method on the basis of correlations between the amount of precipitation and updraft velocities alone have met with little success.

Positive updraft velocities constitute a necessary but not sufficient condition for the formation of clouds and the occurrence of precipitation. To understand the physics of precipitation, one must call on a considerable complex of factors which are decisive for the occurrence and evolution of precipitation.

3.1. THE BASIC SHOWER-PRODUCING FACTORS

The study of aerological characteristics of the atmosphere has been given considerable impetus by the need to determine the factors that condition the occurrence of precipitation. These data have made it possible to compare the behavior of meteorological elements on days with and without precipitation.

The distribution of temperature and humidity in the troposphere has been investigated by Orlova /66—70/, Petrenko /65/, Pavlovskaya /71/, Cherkasskaya /106/, Nakorenko /64/, Khrgian /104, 105/, Bogatyr and Romov /13/, Drozdov /30, 33, 34/, Rossi /158/, Bordovskaya /14/, and others.

Selezneva /82/, studying the distribution of temperature and humidity on days with slightly developed cumulus clouds, analyzed data from a series of aircraft soundings carried out over Leningrad for 24 days in 1946.

Cherkasskaya /106/, studying the specific features of thunderstoms under various synoptic situations, gave examples of the range of variation of temperature and humidity at the surface and at the levels of the principal isobaric surfaces in dry weather, on the one hand, and in rainy and stormy weather, on the other.

A series of observations of specific humidity up to 4 km, carried out by Khrgian over Moscow /104, 105/, yielded average figures for the specific humidity in different months and at different altitudes; on this basis, an interpolated equation was devised, expressing specific humidity as a function of height. The distribution of specific humidity is closely related to the processes of evaporation and condensation in the atmosphere.

Muchnik /62/, Selezneva /80—83/, Tkachenko /92/ and Cherkasskaya /106/ established that, both at the lowest atmospheric level and in the free air, the humidity of the air on stormy and showery days exceeded that obtaining when there are either no clouds or only weakly developed clouds.

The most significant factor in the development of cumulus clouds and precipitation is the stratification and humidity of air masses. Bogatyr' and Romov /13/, Pavlovskaya /71/ and Selezneva /82, 83/ showed that small lapse rates were indicative of good weather, high ones of thunderstorms and showers. In addition, certain regular features were observed in the variation of lapse rates from layer to layer.

Thus, Pavlovskaya /71/ found that over flat country the behavior of lapse rates on stormy and showery days displayed the following features:

a) Lapse rates increased from the surface to the 850 mb level on stormy and showery days, and to the 800 mb level on days with cumulus, the peak rate being observed at 0400 hours.

b) Lapse rates increased in the 600—450 mb layer in all observation periods.

c) Lapse rates decreased from the surface to the 600 mb level at 1300 hours.

d) Lapse rates were smallest in the 700—600 mb layer.

Bordovskaya /14/ described some aerological characteristics of the state of the atmosphere over mountainous regions on days with intra air-mass showers. The most characteristic feature of atmospheric stratification in such cases is unstable behavior of the lapse rate as a function of altitude, represented by rather jagged stratification curves.

Characteristically, on stormy days the stratification curves were quite steep, indicating high lapse rates during the morning. Analyzing the changes in lapse rate from layer to layer as obtained from morning and afternoon soundings, Bordovskaya discerned the following features:

1) The lapse rate decreased from the surface to the 800 mb level, according to data of soundings taken at 0900 and 1500 hours.

2) Lapse rates increased from the 600 mb level during all observation periods.

In mountainous regions, on days with cumuliform clouds, the average lapse rate reached its maximum in the layer extending from the earth's surface to the 850 mb level, though some cases showed superadiabatic lapse rates near the surface at 1500 hours. High lapse rates constitute a necessary condition for the development of thick cumulonimbus and occurrence of showers.

Bordovskaya /14/, Gritsenko and Dyubyuk /28/ and Muchnik /62/ established that large reserves of instability energy are a major factor in the formation and fall-out of shower-type precipitation. It was shown, however, that showers do not necessarily occur at the same value of instability energy.

Orlova /66, 70/ was able to correlate the absolute humidity in the lowest atmospheric levels with the intensity and amount of convective precipitation.

Considering data from mountainous regions, Muchnik /62/ and Bordovskaya /14/ traced a connection between the probability of precipitation, on the one hand, and the relative humidity of the air in the 2—5 km level and the instability energy, on the other. They found that in many cases, when positive energy reserves are available and the humidity aloft is less than 50% (Figure 36), no precipitation was observed, whereas precipitation occurred when the instability energy was low but the humidity in the sub-5 km layer high.

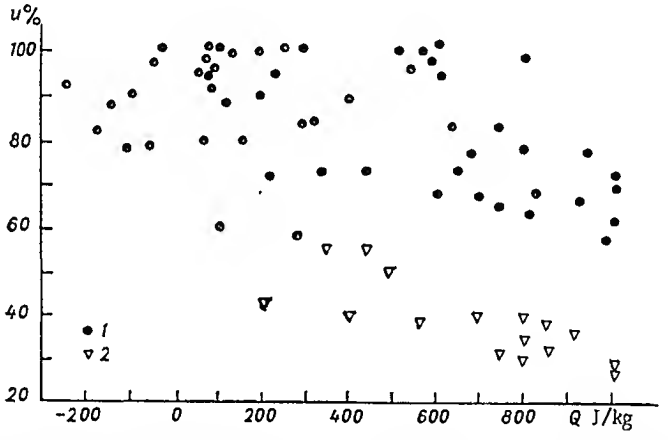

FIGURE 36. Precipitation as a function of relative humidity u and instability energy Q in 850—500 mb layer.

1 — Showers; 2 — clear weather.

That water content of the air and relative humidity in the precipitation-producing mass largely condition the amount of precipitation actually falling has been pointed out by Grigor'ev and Drozdov /30/ and Budilova and Shishkin /15/. They made the very important observation that allowance for relative humidity considerably improves the accuracy of forecasts of the amount of precipitation. Drozdov /33, 34/, making this remark, also states that the absolute humidity largely determines the intensity of precipitation, which also has some influence on the probability of precipitation because of the low wet adiabatic lapse rate obtaining at high water contents.

Relative humidity is one of the most significant parameters of condensation processes. Employing data from seven stations in the South-European territory of the USSR for April—October, 1946—1948, relative humidity at

altitudes 1.5 and 3.0 km was compared with precipitation, revealing that the probability of precipitation increases together with the relative humidity. At each station, the amount of precipitation falling from 0700 to 1900 hours was compared with the relative humidity at 0700 hours. The probability of precipitation showed a particularly marked correlation with the previous relative humidity at altitude 1.5 km, since at 3.0 km the humidity may fall sharply toward evening, regardless of precipitation occurring subsequently.

Drozdov remarked that the connection between relative humidity at 1.5 km during the night and subsequent precipitation during the day cannot be due entirely to the effect of updrafts on the relative humidity, since in that case the correlation should have been stronger at 3.0 km than at 1.5 km. In actual fact the reverse is true; this is evident when the probability of precipitation is calculated and even more so when semidiurnal rainfall figures are compared with relative humidity. Drozdov offers a possible explanation: at altitudes around 3.0 km, downdrafts are not infrequently observed during night hours.

Thus, allowance for high-altitude relative humidity is a prerequisite for predicting not only intra air-mass precipitation but also precipitation from diffuse fronts, when it is doubtful whether passage of the front will indeed cause precipitation.

Summarizing, we can draw up a list of the basic shower-producing factors, based on the above-mentioned investigations, all of which should be taken into account for a reliable forecast of convective precipitation. The necessary conditions for the development of convection and, in particular, of showers are as follows:

1. A high degree of convective instability, representing by a mean deviation of 2 to 3 degrees or more of the curve of state from the stratification curve (from the condensation level to the 500 mb level).
2. High relative humidity of the lower atmospheric levels (up to 3 km) during morning hours (at least 60%). Conditions are even more favorable if the relative humidity is higher, from 70 to 80%.
3. Heating of the lowest layers during the day — this is especially important for the development of thermal convection.
4. Correlation of high specific humidities at the surface with other shower-producing factors and with atmospheric stratification.

This complex of factors enables one to predict the occurrence of precipitation, but it is inadequate for quantitative prediction. A quantitative estimate of precipitation requires a thorough understanding of the physical nature of the phenomenon: construction of a model of the shower-producing cloud; only then can one gain satisfactory results upon comparison of the figures calculated from the model with the actual rainfall.

In field work at the High-Altitude Geophysics Institute, an attempt was made to obtain quantitative criteria for the principal meteorological elements (lapse rate, specific humidity, wind speed, air temperature at the surface, etc.) that produce showers of various types. The relationship between rainfall figures and cloud parameters was also studied. It is possible that the results are valid only for the South Caucasus, requiring significant modification if they are to be applicable to other physico-geographical regions.

The difference between the present work and earlier attempts is that the relevant elements have been compared at different times on days with

different weather. In order to establish the critical values of the various elements implying different weather types, the previous work employed radiosonde data pertaining only to the time of day at which the development of convection was maximum or near-maximum.

The basis for the new project was actual radiosonde data for the period of May—August, 1965—1967. 182 cases were analyzed, 44 of them with no precipitation, 18 with continuous precipitation, and 120 with showers. Of the total, 114 cases were associated with the passage of frontal interfaces and 68 with air-mass phenomena. The data were recorded at the Mineralnye Vody station and by the Kuba-Taba detachment of the Combined Caucasian Hail-Suppression Expedition. The time of the observation was close to the maximum development of convection. The observations extended over a radius of 100—150 km from the sounding point and were based on data from meteorological stations and posts spread over this territory, also on a network of self-recording raingauges in the Kuba-Taba Autonomous SSR.

According to Drozdov /33, 34/, the principal factors causing precipitation are vertical currents in the air and sufficient reserves of water vapor. Since the creation of large reserves of instability energy is determined largely by the height of the condensation level, it is important to consider not only the absolute (specific) water content of the air but also the relative humidity of the air, which is a significant factor in determining the height of the condensation level; another important factor is the moisture loss from clouds due to diffusion of vapor into the environment. The maximal temperature at the surface is an indication of the potential accumulation of sufficient instability energy in the air. An attempt was therefore made to ascertain the specific values of these atmospheric parameters corresponding to weather with and without precipitation (continuous rain or showers).

It was found that precipitation occurred mainly at $u > 55\%$ and $t > 21°$. When the relative humidity in the layer extending from the surface to the 500 mb level was average ($u = (u_{938} + u_{850} + u_{700} + u_{500})/4$) and the maximum temperature at the surface $t > 21°$, precipitation occurred in 90% of cases. A similar pattern held true for intra air-mass processes. At $u > 55\%$ and $t > 21°$, precipitation occurred in about 85% of cases. A study of the effect of specific humidity on precipitation revealed that in frontal processes, when $q > 4$ g/kg ($q = (q_{938} + q_{850} + q_{700} + q_{500})/4$)precipitation occurred in about 88% of cases at any temperatures above 17°. In intra air-mass processes, when $q > 4$ g/kg and $t > 19°$, precipitation occurred in 85% of cases since in these processes thermal convection is the decisive factor in the formation and fall-out of precipitation, whereas the major factor in frontal precipitation is dynamic convection. Therefore, even if the heating of the underlying surface is insufficient for thermal convection, precipitation may occur thanks to additional energy produced by dynamic causes. In such cases, however, the intensity of precipitation was usually low.

Analysis of these cases showed that the probability of precipitation falls if the temperature at the surface is significantly elevated (to 26° or higher). Such high surface temperatures of air are observed in the months of July and August, the relatively "dry" summer months. In all probability, this is because high surface temperatures reduce relative humidity, so that the condensation level is elevated and the probability of precipitation reaching the surface is lessened.

Recent publications on the dynamics of cumulus clouds show a tendency to use the distribution of wind with respect to altitude as a criterion for the development of convection. It has been found that vertical wind structure has a strong influence on the formation of precipitation, but intensive wind shear reduces the probability of fall-out /46, 90, 172, 173/. Considerable precipitation may be observed even when winds are weak. As the wind speed increases there is a marked tendency to less precipitation. Analysis of the influence of wind speed v in the 500—250 mb layer and of updraft speed w_m on the formation of precipitation showed that precipitation is produced in only 25% of observed cases with $w_m<10$ m/sec, whatever the value of v; in all occurrences of precipitation at $w_m>10$ m/sec, the wind speed in the 500—250 layer was in the range 5 to 27 m/sec. At $v<5$m/sec the probability of precipitation was extremely low; the same was true when $v>27$ to 30 m/sec. This may be due to the fact that at low wind speeds atmospheric instability dissipates quite quickly, so that stability is achieved before sufficient moisture has collected in the accumulation zone. Very high wind speeds also inhibit the formation of precipitation, due to rapid dissipation of the upper part of the cloud, above the w_m level, where there is rapid growth and accumulation of precipitation particles.

In intra air-mass processes, precipitation occurred at $v=5$ to 30 m/sec and $w_m>5$ m/sec. If $w_m<5$ m/sec there was usually no precipitation, whatever the wind speed in the 500—250 mb layer.

An important precondition for the onset of convection is that there be no intercepting layer in the lower region of the atmosphere (from the condensation level down); the thickness of this layer is one of the major parameters determining the difference between the actual air temperature at the condensation level and the air temperature at the point where the surface isogram intersects the dry adiabat through the maximum surface temperature. This difference ΔT indicates to what degree the temperature at the condensation level must be lowered or the moisture at the surface increased, in order to eliminate the intercepting layer. Unless these conditions hold, the rising air is either not condensed at all or condensed at a greater altitude, and this means respectively that either no cloud develops or the lower boundary of the cloud will lie very high. Hence the great importance of studying the effect of this temperature difference on precipitation.

Analysis of the influence of ΔT in combination with specific humidity showed that precipitation occurred at $q_{surf} > 7$ g/kg with ΔT values up to 4.5°. Heavy falls of various types of precipitation (continuous and shower-type) were observed when $\Delta T=0$ and $q_{surf} >8$ g/kg, in other words, when the intersection point of the surface moisture isogram and the dry adiabat through the maximum surface temperature coincided with the stratification curve. These conditions are the most favorable for convection and considerable fall-out may then occur. In frontal processes, the value of ΔT is unimportant, and so precipitation may occur at $0<\Delta T<4.5°$. The reason is that frontal processes are associated both with advection of moisture and with advection of heat or cold, corresponding to a drop in the condensation level and creation of favorable conditions for the onset of convection. In intra air-mass processes, precipitation occurred at $q>6$ g/kg and $\Delta T<2°$. At these parameter values precipitation was observed in 70% of cases. If $\Delta T>2°$, the weather was fair even at large values of q_{surf}, for in such processes conditions are not suitable for dynamic convection.

Another important criterion for the onset of convection is the lapse rate γ. Its influence on precipitation-formation processes has therefore been studied by many investigators.

An attempt has been made to find some correlation between the lapse rate and precipitation of various types. It has been found that precipitation occurs at $q>7$ g/kg and $\gamma>0.55°/100$ m. Of all cases observed with such values of q_{surf} and $\gamma_{850-700}$, precipitation occurred in 87%. When $\gamma_{850-700}<0.55$ and $q_{surf}>7$ g/kg, 92% of cases showed fair weather or continuous precipitation.

In intra air-mass processes, precipitation occurred mainly at $q_{surf}>8$ g/kg and $\gamma_{850-700}>0.6°/100$ m (89%). At $q_{surf}<8$ g/kg but $\gamma_{850-700}>0.6°/100$ m, and also at $q_{surf}>8$ g/kg and $\gamma_{850-700}<0.6°/100$ m, the weather was mainly without precipitation (86 and 100%, respectively).

Similar results were obtained for the effect of the mean lapse rate in the 850—500 mb layer on precipitation: a) frontal processes — 80% of probability of precipitation at $q_{surf}>7$ g/kg and $\gamma_{850-500}>0.6°/100$, 90% probability (steady rain and otherwise) at $q_{surf}>7$ g/kg and $\gamma_{850-500}<0.6°/100$ m; b) intra air-mass processes — 80% probability of precipitation at $q_{surf}>8$ g/kg and $\gamma_{850-500}>0.6°/100$ m, high probability of precipitation at $q_{surf}<8$ g/kg and $\gamma_{850-500}>0.6°/100$ m, no precipitation or continuous precipitation at $q_{surf}>>8$ g/kg and $\gamma_{850-500}<0.6°/100$ m. Analysis of the effect of $\gamma_{850-500}$ and $\gamma_{800-700}$ showed that even when only the humidity of the air near the surface is high but the lapse rate is low, showers will not fall. A high value of q at the surface, about 7 to 8 g/kg, is apparently a sufficient condition for steady rain, since this type of precipitation does not require strong vertical currents.

We know at present of only a few publications concerning the effect of maximum updraft speed on the amount of precipitation /56—58, 90, 98, 144/. This may be due to the fact that till recently there was no reliable technique to calculate w_m, the basic cloud parameter conditioning the nature and intensity of the process. The development of cumulus and cumulonimbus, thunderstorms, squalls, showers, etc. all involve powerful updrafts in unstably stratified air.

Sulakvelidze et al. /87/ also described a correlation between w_m and Q, but the data presented there were so sparse as to make the conclusions hardly reliable. An attempt was therefore made to determine the relationship using Glushkova's technique to calculate w_m. The calculation was based on actual radiosonde data for a time near the onset of precipitation, when there were considerable air movements aloft and a sharply changing pressure field at the surface.

For intra air-mass processes, the data used were from soundings taken at morning hours, since when one is concerned with a homogeneous air mass these data are representative of the entire day. The actual amounts of precipitation were provided by a network of self-recording raingauges, meteorological stations and posts. It turned out that an increase in w_m implied an increase in Q, but the relationship was more complicated than supposed in /87, 98/. Moreover, several cases were recorded in which precipitation occurred when $w_m=0$, or when $Q=0$ but $w_m\neq0$. This was probably due to faults in the calculation technique used for w_m, or to the impossibility of accurately recording precipitation.

Calculations showed that 90% of precipitation incidents occurred at $w_m \leqslant 30$ m/sec. The updraft speed w_m may have considerably varying values for rainfalls > 30 mm. The reason is that w_m cannot provide an unambiguous answer to the question of whether a definite amount of precipitation may fall. The same may be said of intra air-mass precipitation.

It was noted in /87/ that the amount of precipitation is independent of the size of the cloud. In order to verify this statement calculations were made of the vertical thickness of the lower part of the cloud, from the condensation level to the maximum updraft-speed level ($H_m - H_c$), and of the upper part of the cloud, from the maximum speed level to the convection level ($H_v - H_m$); Q was then plotted aginst the thickness of the lower part and the quotient $\frac{(H_v - H_m)}{(H_m - H_c)}$ for frontal and intra air-mass processes. Why specifically these cloud parameters? The thickness of the lower part characterizes the maximum energy reserves in the active layer which guarantee a specific amount of precipitation. Conversion of potential into kinetic energy in the active layer and "resolution" of this energy in the penetrative convection layer may take place in different ways, depending on the specific synoptic and aerological conditions /16/. Thus, in anticyclonic weather types, considerable instability energy must be used up in the penetrative convection layer; hence the vertical thickness of these layers is less than that of the penetrative convection layer in frontal processes. Considering only cases of precipitation, an increase or decrease in the ratio of the upper part of the cloud to the lower part will imply a decrease or increase, respectively, in the lower part of the cloud (inasmuch as under summer conditions the thickness of the convection layer varies only slightly), implying a decrease or increase in w_m, whose importance in determining the amount of precipitation Q has already been mentioned. This explains the choice of the above parameters. It was found that 80% of cases of precipitation up to 30 mm occur in the thickness interval $H_m - H_c = 3.0$ to 6.5 km. Moreover, a thickness $H_m - H_c$ of from 3.0 to 4.0 km was found to be an indication that the amount of precipitation would reach 30 mm. When $H_m - H_c = 4.0$ to 6.5 km, precipitation could reach and even exceed 30 mm. In frontal processes, precipitation of less than 30 mm was found to be uncorrelated with the value of the quotient $\frac{(H_v - H_m)}{(H_m - H_c)}$. Only when it exceeded 30 mm was an inverse relationship discerned: a decrease in this ratio implied an increase in the amount of precipitation. In intra air-mass processes there was a direct relationship between $(H_m - H_c)$ and Q, an inverse relationship between $\frac{(H_v - H_m)}{(H_m - H_c)}$ and Q.

These results may be explained in terms of the physical conditions governing the formation and fall-out of precipitation. We must note that these correlations were less evident in frontal processes. This was probably because the radiosonde data employed for the altitudes of the clouds observed at the front were not adequately representative. The correlation that has been found for frontal precipitation exceeding 30 mm may therefore be accidental.

We can now summarize the criteria for shower-type precipitation in North Caucasus following from the above analysis of 182 cases of radiosonde observations.

1. The relative humidity should be at least 55%, for both intra air-mass and frontal processes.

2. The maximum surface temperature should be higher than 19°.

3. The specific humidity in the earth — 500 mb layer, for all types of precipitation, should exceed 4 g/kg; the specific humidity at the surface should exceed 7 g/kg for frontal processes, 8 g /kg for intra air-mass processes.

4. The difference between the actual temperature and the temperature at the point where the surface isogram intersects the dry adiabat through the maximum surface temperature should be less than 2° for intra air-mass processes, at most 4.5° for frontal processes.

5. The average lapse rate in the 850—700 mb layer should be higher than 0.6°/100 m for intra air-mass processes, higher than 0.55/100 m for frontal processes. The lapse rate in the 850—500 mb layer should be 0.6°/100 m in either case.

6. Precipitation occurs in the 500—250 mb layer (all types) when the velocities of horizontal airflow are in the range from 5 to 30 m/sec.

7. Higher updraft speed implies increased precipitation.

8. If the thickness of the lower part of the cloud is 3—4 km, the amount of precipitation is at most 30 mm.

An increase in the thickness of the lower part of the cloud implies an increase in the amount of precipitation. An inverse relationship exists between $\frac{H_v - H_m}{H_m - H_c}$ and Q: an increase in this ratio implies a decrease in Q. Examination of cases of continuous precipitation showed that, in comparison with other meteorological elements, moisture, both at the surface and aloft, is the most significant factor. Even when the lapse rate in the lower troposphere is low, so that there are only sparse reserves of positive instability energy, a sufficient supply of moisture will produce continuous precipitation.

Cases have been recorded of no precipitation occurring even when all the above indices show values different from those necessary for the production of showery and continuous precipitation.

The above conclusions are in full agreement with present-day theories of the mechanism of precipitation. Nevertheless, they are not exhaustive and need further refinement.

3.2. CALCULATION OF AMOUNT OF SHOWER-TYPE PRECIPITATION BY TECHNIQUES OF LEBEDEVA, SHISHKIN AND ORLOVA

At present, three techniques are available to calculate the amount of shower-type precipitation: the techniques of Lebedeva, Shishkin and Orlova.

The principal aim of Lebedeva's work /56—59/ was to set up a model of convection, to describe the formation of convective intra air-mass clouds and precipitation, and in addition to determine the main shower-producing factors. Lebedeva proposed a scheme for calculating the amount of shower-type precipitation, which is also applicable in quantitative investigations of the development of intra air-mass thermal convection under various synoptic conditions.

Lebedeva's technique is based on her "convection model" and on calculation of shower-type precipitation, using prognostic stratification curves for temperature and humidity to allow for the transformation of the air mass at the onset of convection. Once a model has been constructed for given convective conditions and its basic parameters determined (thickness and upper boundary of convectively unstable layer; average condensation level; average convection level, defining the altitude of the dissipation level; critical temperatures at beginning and end of effective convection; duration of convection process), one proceeds to calculate the amount of condensed moisture (Figure 37).

The idea is as follows. Given the model, it is easy to determine the amount of moisture condensing in one ascent of the entire convectively unstable layer to the convection level, provided the thickness of the layer and the distribution of moisture with respect to height are known:

$$Q_{con} = \bar{q}_{con}\, m_{con}, \qquad (3.1)$$

where Q_{con} denotes the moisture reserves in a unit column of the convectively unstable layer (convergence layer), $\bar{q}_{con}$ the average specific humidity of the layer, m_{con} the mass of air per unit column of the layer.

The moisture reserves in the dissipation layer are found by determining the saturation specific humidity for the average altitude of the convection level, assuming that the masses of converging and dissipating air are equal:

$$Q_{dis} = \bar{q}_{dis}\, m_{con}. \qquad (3.2)$$

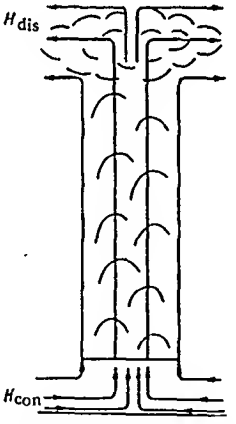

FIGURE 37. Model of convection, after Lebedeva.

H_{dis} : dissipation layer, H_{con} : convergence layer

The difference between the quantities of moisture in the two layers gives the amount of moisture condensed during ascent of one column:

$$\Delta Q = Q_{con} - Q_{dis}. \qquad (3.3)$$

The time necessary for unit ascent is found by dividing the average ascent height by the vertical convective speed averaged over altitude and time; the duration of the convection process is assumed known. With these data at hand one can determine the number of ascents during the entire effective convection cycle. The total quantity of condensed moisture is the product of the number of unit ascents by the quantity of moisture condensed in each:

$$Q = n\Delta Q, \tag{3.4}$$

where n is the number of unit ascents.

Introducing a correction for loss of condensed moisture (in elevating the humidity of the surrounding air and forming clouds), one can determine the amount of moisture falling as precipitation.

In many synoptic situations, this technique is capable of producing estimates even before the actual calculation; this is true in various sharply defined situations, for example: in cases of heavy precipitation (10–30 mm and more), or when neither showers nor even convective clouds are formed.

In the first case one has the most favorable combination of Lebedeva's basic shower-producing factors:

a) The convectively unstable layer is very deep (80–150 mb), because of the low specific humidity gradient up to 1.5 km and the high lapse rate ($\gamma > \gamma_w$) in the 850–700 mb layer.

b) The reserves of instability energy per unit mass of the layer are sufficient, and the specific humidity of the layer at the time of maximum heating has its average value.

c) Effective convection lasts a sufficiently long time (60 min. or more).

d) The relative humidity in the entire air column from the condensation level to the convection level is high (60 – 70% or more), and this prevents significant evaporation of condensed moisture into the surrounding air.

The combination of all these conditions implies a large quantity of convection-condensed moisture and a large quantity of precipitation.

An advantage of Lebedeva's method is the simplicity of the calculations needed for routine forecasting. Also important is the forecast of temperature and humidity stratification. However, the method has serious shortcomings. For example, the treatment of updraft speed as a function of height and time is oversimplified, and this may cause considerable error in the calculated rainfall. The duration of effective convection is underestimated, since convection does not break off at the moment the surface temperature reaches its maximum. The assumption that it does is unwarranted, particularly in cases of forced convection.

Lebedeva's calculation encompasses the entire adiabatic liquid water content, extending throughout the cloud. However, research at the High-Altitude Geophysics Institute /90/ has shown that showery precipitation draws only on that part of the water content pertaining to the accumulation zone, in other words, to its large-drop fraction. Moisture evaporating at the top of the cloud plays no part in the formation of showers. Hence the quantity of evaporation obtained by Lebedeva's method is exaggerated.

The difference between the entire adiabatic water content and the quantity of accumulated water depends on the shape of the updraft curve, the temperature stratification and the relative humidity of the air; it is therefore difficult to establish an unequivocal relationship between evaporated moisture and these parameters.

Lenshin, Osipova and Shishkin /60/ and Shishkin /5, 94, 96, 98/ proposed a method for predicting the amount of intra air-mass shower-type precipitation, based on the slice method.

The first paper /60/ is based on the fact that the amount of showery precipitation depends on the updraft speeds within developing convective clouds and on their thickness. Both these parameters may be obtained from aerological sounding data with the help of the slice method /98/.

Lenshin showed that the calculated average updraft speed is an almost linear function of cloud thickness. The correlation equation is

$$w = 0.94H - 0.5, \tag{3.5}$$

where H is the cloud thickness in kilometers and w the updraft speed in m/sec. The correlation coefficient is 0.89, with probable error $E = 0.02$.

In /60, 99/ the amount of precipitation from convective clouds is expressed as a function of their vertical development rate, assuming that the latter is uniform.

The amount of precipitation was plotted against the calculated cloud thickness, using the linearity of the latter with respect to average cloud-development rate (Figure 38). Once the average and maximum vertical thickness of a convective cloud has been calculated, the plot may be used to predict the average and maximum amount of precipitation, using the equation

$$Q_{\text{pred}} = kQ_{\text{cal}}, \tag{3.6}$$

where Q_{cal} is the precipitation as determined from the graph, Q_{pred} the predicted precipitation and k a correction factor.

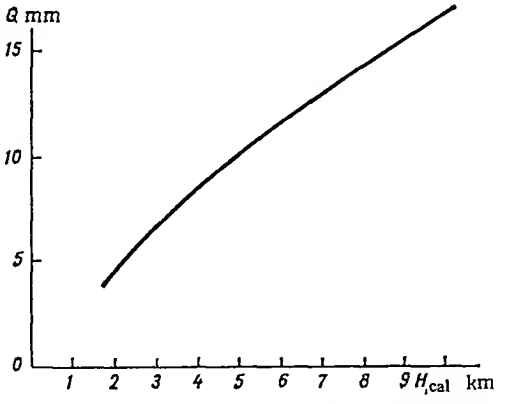

FIGURE 38. Amount Q of shower-type precipitation vs. calculated vertical thickness H_{cal} of convective clouds, after Shishkin.

The correction factor is determined graphically. Shishkin's technique /98, 99/ is very simple; provided prognostic graphs are plotted to determine the correction factor, it may therefore be recommended for use in various physico-geographical regions.

However, tests of the calculations of shower-type precipitation based on Shishkin's method have shown that the resultant accuracy of shower forecasting is lower than in the method of /78/. The reason is apparently that in the latter method the prognostic curves for temperature and humidity stratification are plotted for the layer from the surface up to 5—7 km, whereas Shishkin does not require prediction of stratification (with the exception of the boundary layer), using instead the actual stratification as determined from observations made during the night. Plotting of prognostic temperature and humidity stratification curves /79/ considerably improves the accuracy of the technique. Nevertheless, the basic underlying assumptions of the method, particularly the assumption that updrafts break off once precipitation has begun, leave their mark on the results. It may well be true that in intra air-mass processes the updrafts cease once precipitation has begun. In frontal processes, over flat country, or in orographic precipitation (when the air mass extending over a mountain ridge rises steadily), updrafts are present even after the onset of precipitation, and in such cases Shishkin's technique will not yield satisfactory results. To summarize: Shishkin's technique, coupled with the use of prognostic plots to determine the correction factor, seems reliable in calculating precipitation from intra air-mass clouds, when updrafts may indeed break off once precipitation has begun.

The scheme proposed by Orlova /70/ involves calculating the temperature and humidity stratification, determining convective velocities and duration of showers, and finally calculating the amount of precipitation. The calculation of stratification is described in /78/. To calculate the convective velocity of air in a cumulonimbus cloud, one uses the empirical formula

$$w = \frac{m w_c H_1 \varkappa}{m_1}, \tag{3.7}$$

where m is the mass of the air in the convectively unstable layer (c. u. l.), m_1 the mass of air in the 1000—100 mb layer (taken equal to 10^3 g in the examples), $H_1 = \frac{h}{H}$ (h is the thickness of the convection layer as determined by the parcel method, H the thickness of the atmospheric layer in which convection develops, approximately 12—14 km or 900 mb in summer), $\varkappa$ a coefficient representing the density of the warm rising jets in cumulonimbus clouds ($\varkappa = 0.7$ in the examples), w_c the velocity of vertical convective currents (warm jets) determined at the middle of the c. u. l. If the stratification shows several c. u. l. at the onset of convection, the average convective velocity in Cb should be determined as an average:

$$\overline{w} = \frac{\sum_1^n (m w_c H_1 \varkappa)_n}{m_1}, \tag{3.8}$$

where n is the number of c. u. l. , and w_c is a solution of the equation

$$\frac{dw_c}{dt} = g \frac{(T' - T)}{T}, \tag{3.9}$$

where the w_c values are averaged over the different convection thicknesses and c. u. l. thicknesses and halved to allow for internal friction.

The difference $T'—T$ should be determined from the calculated stratifications. Knowing the updraft speed in the atmospheric column where the Cb is developing, one can define the amount of precipitation from the formula

$$Q = \frac{1}{g}\int_0^t\int_{P_c}^{P}\frac{dq}{dt}dPdt. \tag{3.10}$$

Integration yields a working formula for the intensity of shower-type precipitation:

$$I = 0.01\,(P_0 - P_1)\,\frac{1}{n}\sum_1^n \delta q_i, \tag{3.11}$$

where I is the rainfall per unit time (mm/hr), P the pressure (mb), δq_i the individual changes in specific humidity (g/kg) per unit time for ascent of air from the appropriate surfaces.

For the 1000—100 mb layer, Eq. (3.11) may be given the form

$$I = 1.5\Delta q_{850} + 1.8\Delta q_{700} + 2.0\Delta q_{500} + 1.5\Delta q_{300} + \\ + \Delta q_{200} + 0.5\Delta q_{100} \approx 1.5\Delta q_{850} + 3.0\Delta q_{700}, \tag{3.12}$$

where I is the intensity of showers (mm/hr), Δq, the individual changes in specific humidity per hour in ascent of air from the levels of the isobaric surfaces at 850, 700, 500, 300, 200 and 100 mb. If the duration t of showers in a 12-hour period is known, the overall amount of showers is

$$Q = It.$$

Determination of the duration of showers is one of the most complex problems in precipitation calculations. Orlova has suggested an approximate solution. If d is the diameter of the base of a cumulonimbus cloud (approximately 30 km on the average), the number of cells N_{ce} and the number of cumulonimbus clouds N in the region of the point at which rainfall is being measured may be found from the following approximate formulas:

$$N_{ce} = \frac{\bar{S}_{1000-850}}{d} \qquad N = \frac{\bar{S}_{1000-850}}{2d},$$

where $\bar{S}_{1000-850}$ is the length of a 12-hour trajectory in the 100-850 mb layer.

As shown by Shmeter and Riehl /110, 111/, cumulonimbus clouds often travel at the velocity of the air currents at the middle level of the troposphere. If this velocity is defined in terms of wind data in the 700—500 mb layer, one can define the time needed for one Cb to pass over the point as $t' = \frac{d}{v}$. Clearly, a weather condition characterized by the development of convection (Cb clouds and gaps between them) will be observed in the region for a time $t_1 = \frac{\bar{S}_{1000-850}}{v}$, and the duration of the shower will be

$$t = \frac{0.7dN}{v} = \frac{0.35S_{1000-850}}{v}, \tag{3.13}$$

where v is the velocity. In accordance with observations of showery precipitation and convective currents, which have shown that most of the precipitation originates in the central part of the Cb cloud, a factor of 0.7 has been introduced into Eq. (3.13). Calculations have shown that application of this scheme for the duration and amount of shower-type precipitation yields good results, the calculated precipitation being as a rule close to the maximum observed over an area of radius 100 km.

However, Orlova's scheme is rather artificial. Referring to Eq. (3.8), one notices that the physical principle underlying the averaging of convective velocity is not clear, and the validity of the equation is open to doubt. Indeed, the ratio m/m_1 is proportional to $H_1=h/H$, so that one gets the impression that the same parameters are utilized twice. In addition, the factor $\varkappa$, representing the so-called density of thermal air jets, is taken equal to 0.7, whereas according to Shmeter's data /102/ it should vary in the range 0.3–0.5. It thus follows that the airflow velocities calculated from Eq. (3.8) and implying high rainfall values are unrealistically small.

According to Orlova's calculations, an airflow velocity of 3.5 m/sec implies precipitation of 46.4 mm. If the precipitation occurs as showers, it is not clear why the airflow velocity is so small. According to experimental data of Bibilashvili /8/, Byers and Braham /120/, and Shmeter /102/, updraft speeds reach 20 m/sec and more even in Cu cong.; and work carried out at our Institute /90/ implies that showers are associated with updraft speeds exceeding 10 m/sec. Another shortcoming of Orlova's technique is the rather inaccurate calculation of the duration of the shower, which leaves its mark on the calculation results.

As the above methods are all based on simplified conceptions of the structure of updrafts in convective clouds, they can only provide a schematic picture of the accumulation of moisture in a cloud and its precipitation as rain. The complexity of this process, the complicated structure of a cumulonimbus cloud and the distribution in time and space of vertical air currents all imply that, in order to devise a satisfactory practical method, one has somehow to incorporate in greater detail the host of interacting factors that produce and maintain the process.

We now present an attempt to develop a method for calculating the maximum amount of shower-type precipitation, based on the theories developed recently at the High-Altitude Geophysics Institute. We make essential use of the fact that, given a certain stratification of temperature and humidity in the atmosphere, the accumulation of moisture may proceed in several recurring stages, so that the rainfall may well exceed by a considerable factor the liquid water content of the cloud at any particular time. This is taken into account by a newly defined concept — the resolution time of atmospheric instability, to which the next section is devoted.

3.3. RESOLUTION TIME OF ATMOSPHERIC INSTABILITY — BASIC ASSUMPTIONS UNDERLYING THE DEFINITION

According to present-day theories /90/, the updraft speeds in a growing cumulus cloud increase with altitude, reaching a maximum in the middle part of the cloud and then decreasing toward the cloud top. Results of actual

studies of updrafts in the atmosphere provide the basis for a new hypothesis as to the formation of shower-type precipitation, whose salient point is the idea of a zone of accumulation and its release as showers.

The most widespread types of atmospheric convection are the following.

1. The time elapsing from the onset of convection till the termination of updrafts is too short for the accumulation of sufficient moisture to produce showers. In this case the air becomes stable before enough water collects in the accumulation zone, so that this type of stratification does not produce showers.

2. The above-mentioned time interval is just long enough. Showers fall from the cloud and the cloud dissipates.

3. More time elapses from the onset of convection than is necessary for sufficient moisture to collect in the accumulation zone. Here the processes of moisture accumulation and showery precipitation may recur.

The third case occurs most frequently in frontal processes, producing heavy showers over a large area. In intra air-mass convective processes, the most frequently observed cases are the first and second, though the third sometimes occurs. In other words, in intra air-mass processes instability is generally resolved as a local shower, owing to the lack of conditions to maintain it. As the third case is that most conducive to the formation of showers, we shall consider it in the greatest detail.

The convection process may be described as follows. The temperature and pressure are assumed to be horizontally uniform at the outset. A layer of air displaced by some vertical impulse will move under the action of the buoyant force. If the acceleration imparted by buoyancy is in the same direction as the "triggering" impulse, the layer is said to be unstable. If the acceleration opposes the original force, the air is stably stratified. Clearly, if an air mass is lifted, the surrounding air will subside and there will be some mixing of updrafts and downdrafts, tending to reduce the temperature contrasts and vertical accelerations. If the rising air reaches the condensation level, a cumulus cloud begins to form; further ascent will involve the release of latent heat of condensation. Thanks to the change of updraft velocity with altitude and time, a large quantity of drops will accumulate above the maximum speed level, and these will grow by coalescence with the upcoming droplets. When the quantity of water in a unit column of the accumulation zone can no longer be supported by the buoyant force of the updrafts, precipitation begins, usually at the rear of the cloud. At the same time, there may be further accumulation of moisture in the frontal part of the cloud, if the conditions obtaining in the air can maintain updrafts. These are precisely the conditions under which the overall rainfall will exceed the liquid water content of the cloud by several factors.

If the cloud is motionless and the stratification of a type that promotes regeneration of the cloud, moisture may accumulate several times, implying recurring showers from the cloud. In other words, the mass of water in the cloud may be "renewed" several times. In moving clouds (the case most frequently observed in nature) the process is as follows. At any one point, there may be precipitation from different "mature" clouds passing over the point. In each of these clouds, fallout from the rear part may be accompanied by re-accumulation of moisture in the frontal part, provided that stratification conditions are suitable.

Thus, precipitation may occur several times over one point, depending on the above-mentioned factors and particularly on the time that elapses until instability is resolved. The resolution time of atmospheric instability is defined as the interval from the time water begins to accumulate to the time at which the updrafts terminate (all with reference to a particular point). The resolution time is calculated using the slice method /50, 52, 53/.

To derive an equation for the resolution time, the entire layer from the earth's surface to the convection level is divided into two layers: the lower extends from the surface H_0 to the maximum updraft speed level H_m (active cloud-formation layer), the upper from H_m to the convection level H_{conv} (Figure 39). The convection level is defined as usual, as the point at which the stratification curve intersects the curve of state through the condensation level. The upper boundary of the lower layer is determined by the level at which the temperature difference between the rising and surrounding air is a maximum, $\Delta T = (T_w - T)$. The depth of the second layer indicates the vertical extension of the air over which the updraft dies out. The process of convection depends on the instability energy of the active layer. It is assumed that the upper boundary of the cloud lies at the convection level; this has been corroborated by *Selezneva et al.*

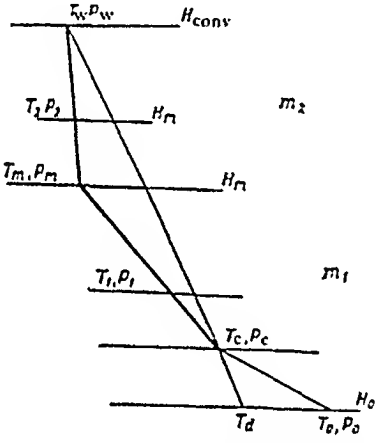

FIGURE 39. Illustrating calculation of instability resolution time.

We stipulate that the air becomes stable when, as a result of mixing of rising and falling masses of air, the lapse rate γ at the time of maximum convection becomes equal to a certain rate γ^* at which the updrafts die out. The time during which γ falls by $\gamma - \gamma^*$ is defined as the decay time τ_2 of convection. The time elapsing from the onset of convection to its maximum development is assumed equal to the time τ_1 necessary for sufficient moisture to collect in the accumulation zone so that showers will be produced.

It is assumed that maximum development of convection is reached when the accumulation zone contains the maximum quantity of the large-drop fraction, as given by Eq. (1.21); we stipulate that this is when precipitation begins. The decay time of instability when moisture is accumulating steadily in the frontal part of the cloud and precipitation occurring in its rear is given by the interval elapsing from the onset of precipitation till the increase

in precipitation intensity falls off, i. e., till the updrafts in the cloud die out (over the reference point). If the precipitation rate shows several "surges," separated by periods of lessened rate and even cessation of precipitation, the resolution time of instability is taken to be the sum of the intervals during which the precipitation rate is increasing.

Summarizing, we can represent the resolution time as

$$\tau = \tau_1 + \tau_2. \tag{3.14}$$

According to data of Shishkin /98/, the material presented in Chapter 1, and calculations of Goral' /27/, a cumulus cloud may develop to its maximum height within 30 — 90 minutes.

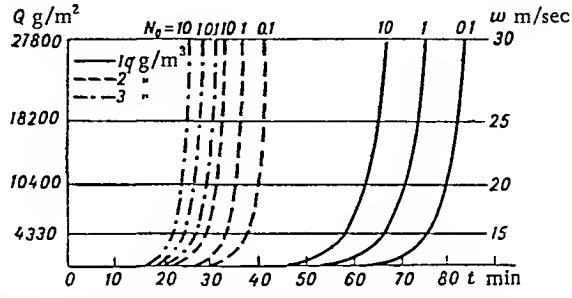

FIGURE 40. Accumulation time of water in accumulation time vs. liquid water content q and concentration N_0 of giant nuclei.

It is evident from Figure 40 that the accumulation time of moisture in the accumulation zone is strongly dependent on the liquid water content in the lower part of the cloud and on the concentration N_0 of giant nuclei. At average water contents $q = 1.0$ to 1.5 g/m^3 and giant nucleus concentration $N_0 = 1\,\text{m}^{-3}$, the accumulation zone may dissipate within one hour. Calculations performed by the present authors to determine the accumulation time in a cloud corroborate this figure.

The reader should note that the above scheme of resolution of atmospheric instability does not claim to be exhaustive, but it nevertheless covers the most typical cases of formation and release of intensive shower-type precipitation.

3.4. EQUATION FOR RESOLUTION TIME OF ATMOSPHERIC INSTABILITY

The decay time of convection is determined by calculating heat exchange between the upper and lower layers /50, 52/. We consider a layer of unit cross-sectional area.

The heat content of the lower and upper layers at the outset (counting from the time of maximum development of convection) may be expressed as follows:

$$\theta_1 = c_p m_1 T_1; \tag{3.15}$$

$$\theta_2 = c_p m_2 T_2, \tag{3.16}$$

where m_1 and m_2 are the masses of the layers per unit cross section, c_p the specific heat of air at constant pressure, T_1 and T_2 the initial average air temperatures in the layers.

As a result of mixing, the lower layer receives additional heat $c_p \Delta m(t) T_{21}$ from falling air, and the upper layer receives additional heat $c_p \Delta m(t) T_{12}$ from rising air. At a certain time, the heat contents of the two layers will be equal:

$$c_p T_1'(t)\, m_1 = c_p m_1 T_1 - c_p \Delta m\,(t)\, T_1 + c_p \Delta m\,(t)\, T_{21}; \tag{3.17}$$

$$c_p T_2'(t)\, m_2 = c_p m_2 T_2 - c_p \Delta m\,(t)\, T_2 + c_p \Delta m\,(t)\, T_{12}, \tag{3.18}$$

where T_1' and T_2' are the average air temperatures at the time in question, T_{21} the temperature of air falling from level z_2 when it reaches level z_1 (z_2 and z_1 denote the altitudes of the centers of gravity of the layers), T_{12} the temperature of air rising from level z_1 when it reaches level z_2:

$$T_{21} = T_2 + \gamma_d (z_2 - z_1); \tag{3.19}$$

$$T_{12} = T_1 - \gamma_w (z_2 - z_1) \tag{3.20}$$

where γ_w and γ_d are respectively the wet and dry adiabatic lapse rates; $\Delta m(t)$ is the mass of air transported by rising or falling.

If the amount of clouds passing over the reference point is S_m, the total mass transported at the end of the instability-resolution process will be

$$\Delta m\,(\tau_2) = \rho_m S_m w_m \tau_2 = \rho_m' (1 - S_m)\, w_m' \tau_2. \tag{3.21}$$

where w_m and w_m' are the maximum updraft and downdraft speeds, ρ_m and ρ_m' the density of wet and dry air at the maximum updraft speed level.

Eqs. (3.17) and (3.18), valid for layers of considerable depth, are derived from the analogous equations for elementary layers (over each of which the process is assumed to take place at constant pressure) by summing over height and time.

The validity of our argument is dependent on the following laws being true:

$$\sum_{z=z_0}^{z_m} \sum_i c_p \rho_i \Delta z_i T_i + \sum_{z=z_m}^{z_v} \sum_i c_p \rho_j \Delta z_j T_j = \text{const};$$

$$\sum_{z=z_0}^{z_m} \sum_i \Delta m_i = \sum_{z=z_m}^{z_v} \sum_i \Delta m_j,$$

where z_0, z_m, z_v are the absolute altitudes of the earth's surface, the maximum speed level and the convection level, respectively; the indices i, j indicate elementary layers in the lower and upper layers.

In view of (3.19) and (3.20), we can write Eqs. (3.17) and (3.18) thus:

$$T_1'(t) = T_1 + \frac{(\gamma_d - \gamma)(z_2 - z_1)}{m_1} \Delta m(t); \tag{3.22}$$

$$T_2'(t) = T_2 + \frac{(\gamma - \gamma_w)(z_2 - z_1)}{m_2} \Delta m(t). \tag{3.23}$$

A necessary condition for the air to be stably stratified is that the temperature distribution satisfy the following relation:

$$T_{II} = T_I - \gamma^*(z_2' - z_1'), \tag{3.24}$$

where T_I and T_{II} are the average temperatures of the layers at the end of the instability-resolution process, z_1' and z_2' the altitudes of the centers of gravity of the layers at that time.

We shall assume that

$$z_2' - z_1' = z_2 - z_1. \tag{3.25}$$

Then, rewriting Eqs. (3.22) and (3.23) for the time τ_2 and inserting the results into (3.24), with due attention to (3.21) and (3.25), a few manipulations yield the following expression for τ_2:

$$\tau_2 = \frac{(\gamma - \gamma^*) m_1 m_2}{\rho_m S_m w_m [m_1(\gamma - \gamma_w) - m_2(\gamma_d - \gamma)]}. \tag{3.26}$$

Simplifying the denominator, we obtain

$$\tau_2 = \frac{(\gamma - \gamma^*) m_1 m_2}{(m_1 + m_2)\left\{\gamma - \left[\gamma_w - (\gamma_d - \gamma_w)\frac{m_2}{m_1 + m_2}\right]\right\}\rho_m S_m w_m}, \tag{3.27}$$

The resolution time of atmospheric instability may be determined from the formula

$$\tau = \tau_1 + \frac{(\gamma - \gamma^*) m_1 m_2}{(m_1 + m_2)\left\{\gamma - \left[\gamma_w + (\gamma_d - \gamma_w)\frac{m_2}{m_1 + m_2}\right]\right\}\rho_m S_m w_m}. \tag{3.28}$$

On the assumption that in the stable state γ is equal to the wet adiabatic lapse rate γ_w, we find after similar arguments that

$$\tau = \tau_1 + \frac{(\gamma - \gamma_w) m_1 m_2}{(m_1 + m_2)\rho_m S_m w_m \left\{\gamma - \left[\gamma_w + (\gamma_d - \gamma_w)\frac{m_2}{m_1 + m_2}\right]\right\}}. \tag{3.29}$$

We now return to Eq. (3.25), and prove that it represents a plausible assumption.

a) Let us assume first that the heat released in condensation of water vapor in ascending air masses has uniformly heated the entire layer from the earth's surface to the convection level. Then, with the temperatures T_I and T_{II} defined as before, we can write

$$T_{\mathrm{I}} = T_1 + \Delta T_1; \tag{A}$$

$$T_{\mathrm{II}} = T_2 + \Delta T_2, \tag{B}$$

where ΔT is the change in the temperature of the layers due to condensation processes. By assumption, $\Delta T_1 = \Delta T_2$. It follows from (A) and (B) that

$$T_{\mathrm{I}} - T_{\mathrm{II}} = T_1 - T_2,$$

or

$$T_1 - T_{\mathrm{II}} = \gamma(z_2 - z_1). \tag{C}$$

where γ is the average lapse rate over the entire layer.

On the other hand,

$$T_{\mathrm{II}} - T_1 = \gamma^*(z_2' - z_1'). \tag{3.30}$$

Hence

$$T_1 - T_{\mathrm{II}} = \gamma^*(z_2' - z_1') \tag{3.31}$$

From (C) and (3.31) we obtain

$$\frac{z_2' - z_1'}{z_2 - z_1} = \frac{\gamma}{\gamma^*} \tag{3.32}$$

In practice, the ratio γ/γ^* does not exceed unity, although $\gamma - \gamma^* > 0$.

This is evident from Table 8, from whose data one sees that the error incurred by assuming Eq. (3.25) is on the average 15% (with fluctuations from 1 to 31%). To calculate γ^*, one uses Eq. (1.12) (see Chapter 1).

b) Now let $\Delta T_1 \neq \Delta T_2$, or, more precisely, $\Delta T_2 > \Delta T_1$. Under this condition unstable air will ultimately become stable. One can then show as above that

$$\frac{z_2' - z_1'}{z_2 - z_1} = \frac{\gamma}{\gamma^*} - \frac{\Delta T_2 - \Delta T_1}{\gamma^*(z_2 - z_1)}. \tag{3.33}$$

Here ΔT_1 and ΔT_2 are calculated on the basis of the data in /128/. According to Table 8, the average error in this case is 18.5%, and so the assumption of (3.25) is admissible.

Summarizing, we can state that no significant errors are introduced if one assumes that the differences in altitude at the end of the instability-resolution process and at the time of maximum development of convection are equal.

Now that we have Eq. (3.29) for the resolution time of atmospheric instability, we can derive certain criteria for stability or instability of the air. The results were shown in Chapter 1. Calculations with Eq. (3.29) involve working with lapse rates, which is rather tedious. It is therefore preferable to use Eq. (3.28) with some modifications. An analysis of this equation shows that it can be brought to the form

TABLE 8. Time dependence of z_2-z_1, according to radiosonde data from Kuba-Taba (K.-T.) and Mineral'nye Vody (M.V.)

Date	Point	Time of day	Altitude: surface z_0 km	surface P_0 mb	w_m level z_m km	w_m level P_m mb	convection level z_v km	convection level P_v mb	T_{0m} °K	T_m °K	T_v °K	γ	γ^*	A	B	$\frac{1-A}{A}$ %	$\frac{1-B}{B}$ %
31/V 1965	K.-T.	07 00	0.67	930	7.90	370	11.72	210	299	243.5	217	0.740	0.75	0.990	0.94	1.0	6 4
1/VI	"	06 20	0.67	940	4.60	580	10.95	250	295.5	264.8	224	0.695	0.83	0.837	0.90	19.1	26.0
5/VI	M.V.	15 00	0.30	980	7.40	400	10.38	260	303.5	247	225	0.779	0.76	1.022	0.97	2.0	3.1
6/VI	K.-T.	07 00	0.67	930	6.60	450	11.40	225	298	253.5	222	0.707	0.89	0.855	0.81	17.6	23.4
9/VI	M.V.	15 00	0.30	980	9.30	300	10.94	260	297	228.5	228	0.648	0.84	0.782	0.74	28.1	35.1
16/VI	"	09 00	0.30	980	5.70	500	10.40	260	296	255.8	224	0.712	0.81	0.880	0.83	13.6	20.5
18/VI	"	15 00	0.30	980	7.30	400	10.60	250	296	246.8	226	0.679	0.76	0.890	0.54	12.4	19.0
20/VI	"	09 00	0.30	980	8.40	350	11.22	235	298	239	225.5	0.663	0.87	0.762	0.72	31.5	38.8
20/VI	K.-T.	06 15	0.67	936	7.40	400	10.60	250	295	245.5	220	0.755	0.77	0.980	0.93	2,0	7.5
25/VI	"	14 50	0.67	936	5.80	500	9.84	280	296	259.5	230	0.828	0.87	0.952	0.90	5.2	1.1
29/VI	"	06 15	0.67	930	3.65	650	8.80	280	295	270	230	0.713	0.85	0.839	0.79	19.1	26.5
1/VII	"	06 10	0.67	936	7.50	400	11.15	235	298	250.5	229.5	0.654	0.77	0.845	0.80	18.9	25.0
2/VII	M.V.	15 00	0.30	980	8.45	350	11.25	235	301	243	229	0.712	0.86	0.824	0.78	21.8	28.2
5/VII	"	15 00	0.30	980	7.40	400	10.90	255	301	240.6	231	0.660	0.72	0.915	0.86	8.7	16.3
11/VII	"	03 00	0.30	980	7.40	400	10.35	265	299	248	232	0.665	0.72	0.924	0.87	8.6	14.9
20/VII	"	03 00	0.30	980	6.04	480	10.10	275	300	257	235	0.663	0.74	0.895	0.85	12.3	17.7
25/VII	K.-T.	06 20	0.67	940	6.50	400	9.50	300	298	250	235	0.714	0.72	0.990	0.93	1.0	7.5
27/VII	"	06 18	0.67	940	5.80	500	8.84	330	300	262.2	245	0.671	0.70	0.956	0.91	4.2	8.8
24/VIII	M.V.	03 00	0.30	980	9.05	315	12.20	200	299	235.5	219	0.671	0.88	0.763	0.72	31.4	38.8
30/VIII	K.-T.	06 20	0.67	930	7.10	480	12.50	185	300	253	215	0.718	0.78	0.920	0.88	8.7	13.6
																15.0	18.5

N o t e: The lapse rates γ and γ^* are calculated for the entire layer with positive instability energy, to justify the assumption (3.25). In estimates of instability, however γ and γ^* are calculated for the layer from the surface to the w_m level, as this is the active layer.

$$A=\frac{\gamma}{\gamma^*};\quad B=\frac{\gamma}{\gamma^*}-\frac{\Delta T_2-\Delta T_1}{\gamma^*(z_2-z_1)}.$$

$$\tau = \tau_1 + \frac{m_1 m_2}{\rho_m S_m w_m (m_1 + m_2)}. \tag{3.34}$$

This equation involves the still unknown masses of the layers, m_1 and m_2. They may be found from the formulas

$$m_1 = \int_0^{z_m} \rho dz; \tag{3.35}$$

$$m_2 = \int_{z_m}^{z_v} \rho dz, \tag{3.36}$$

where z_m and z_v are the maximum speed and convection levels, respectively. Utilizing standard equations of statics and rearranging, we obtain formulas for m_1 and m_2:

$$m_1 = \frac{P_0 - P_m}{g}; \quad m_2 = \frac{P_m - P_v}{g}.$$

Inserting these formulas into Eq. (3.34), we finally have

$$\tau = 1 + \frac{(P_0 - P_m)(P_m - P_v)}{\rho_m S_m w_m g (P_0 - P_v)}. \tag{3.37}$$

3.5. EFFECT OF CHANGES IN MAXIMUM UPDRAFT SPEED WITH TIME AND WITH DISTANCE FROM CLOUD CENTER ON CALCULATION OF RESOLUTION TIME

As stated, the instability resolution time is the time elapsing from the onset of convection to its termination, when γ becomes equal to the critical lapse rate. The use of Eq. (3.37) to determine τ yields the resolution time on the assumption that the updraft speed w_m is constant in time and across the cloud cross section. This is the minimum resolution time. In reality, the maximum updraft time varies both with time and across the cloud. As shown in Chapter 1, this must be taken into consideration, since clouds passing over a given region will be at different stages of their development. Assuming τ calculated for the center of the cloud, a more accurate description of the process must treat the maximum updraft speed w_m as a function of time, as well as of the distance from the cloud center if we are interested in finding τ when the peripheral parts of the cloud are passing over the observation point.

To calculate the resolution time for a given point, over which an amount S_m of clouds are passing at various stages of development, we must average the updraft speed over time and over the cloud cross section and insert the result in Eq. (3.37).

To determine the average updraft speed, we use the mean-value theorem, which may be expressed analytically as follows:

$$\bar{y} = \frac{\int_{x_1}^{x_2} y\,dx}{\int_{x_1}^{x_2} dx}, \tag{3.38}$$

where x_1 and x_2 are the endpoints of the interval over which the function y varies.

By Eq. (3.38), the time average of the updraft speed is

$$\bar{w}_t = \frac{2}{3} w_m, \tag{3.39}$$

if the updraft speed is given by Eq. (1.16).

Similarly, the average of the updraft speed over the cloud cross section is given by

$$\bar{w}_x = \frac{3.14}{4} w_m; \tag{3.40}$$

$$\bar{w}_r = \frac{w_m}{2\sqrt{\ln \frac{w_m}{v_d}}} \sum_{n=0}^{\infty} (-1)^n \frac{2\left(\sqrt{\ln \frac{w_m}{v_d}}\right)^{2n+1}}{n!(2n+1)}; \tag{3.41}$$

$$\bar{w}_x = \frac{2}{3} w_m. \tag{3.42}$$

Of the above equations, Eq. (3.40) for $\bar{w}_x$ is determined on the basis of Vul'fson's data of the distribution of vertical velocity over the cross section of the cloud (Eq. (1.17)), and Eqs. (3.41), (3.42) are derived by analysis of results of Pinus and of U. S. investigators, respectively (Eqs. (1.18), (1.19)).

Note that when integrating over the cloud cross section, the updraft speed is assumed to remain with the interval

$$0 \leqslant w \leqslant w_m.$$

An exception to this rule is the derivation of Eq. (3.41), in which

$$v_d < w \leqslant w_m,$$

where v_d is the fall speed of a drop of radius 2.5—3.0 mm, since here one is integrating an exponential function.

Equations (3.40)—(3.42) yield the average updraft speed over the cross section of a cloud. Replacing w_m in these equations by the time average $\bar{w}_t$ from Eq. (3.39), we obtain the required average updraft speed.

We can now write down the equation for the instability-resolution time allowing for the changes in updraft speed with time and over the cloud cross section:

$$\tau = 1 + \frac{(P_0 - P_m)(P_m - P_v)}{\rho_m S_m \bar{w}_{t.x} g (P_0 - P_v)}. \tag{3.43}$$

As a final remark, we note that this derivation of the time-averaged updraft speed utilizes data of Shishkin. Determination of the average over the cloud cross section utilizes only data of Byers and Braham, since their solution for the velocity distribution is in better agreement with the facts.

Vul'fson's data for velocity were obtained in studies of relatively shallow cumulus clouds, and Pinus' data, on which the corresponding velocity distribution was based, refer to the upper parts of deep cumulus clouds, whereas Byers and Braham treat the middle sections.

Summarizing the above formulas, we find that the updraft speed averaged over time and over cloud cross section is

$$\overline{w}_{t.x} = \frac{4}{9} w_m. \tag{3.44}$$

3.6. COMPUTATION OF AMOUNT OF CONVECTIVE CLOUDS BY THE SLICE METHOD: COMPARISON WITH ACTUAL DATA

Equation (3.43) for the instability-resolution time involves as a factor the amount of clouds at the maximum updraft speed level. This parameter is extremely important for the computation results.

Considerable attention has recently been devoted to the connections between atmospheric stratification before the appearance of clouds and the nature of the subsequent cloudiness. A correlation certainly exists, as convective clouds are formed as a result of updrafts, which in turn are caused by stratification. Experimental research of Bibilashvili /8/, Vul'fson /20, 21/, and Shishkin /98/ concerning updrafts has shown that direct measurements of updraft speed yield results which show considerable discrepancies from the calculated values.

In calculating the ascent of air masses by the slice method /63/, one obtains the following formula for the solenoidal term, which is responsible for the development of convection:

$$\frac{\partial E}{\partial t} = c_p \frac{M_w}{M_d} [M_d(\gamma - \gamma_w) - M_w(\gamma_d - \gamma)] w, \tag{3.45}$$

where $\frac{\partial E}{\partial t}$ is the rate of change of energy with time in a certain layer containing clouds and cloudless intervals; M_w and M_d are the masses of wet and dry air, respectively.

Using Eq. (3.45), we can calculate the amount of convective clouds, $S = \frac{M_w}{M_w + M_d}$, corresponding to the maximum release of kinetic energy. This calculation is done for the case in which convection may develop. After simple manipulations, one finds the following formula for S /98/:

$$S = 1 - \sqrt{\frac{(\gamma_d - \gamma)}{(\gamma_d - \gamma_w)}}. \tag{3.46}$$

If convective clouds penetrate several atmospheric levels with different lapse rates, one must sum a number of expressions of this form, obtaining

$$S_{w_m} = 1 - \sqrt{\frac{\sum_i (T_i - T_d)}{\sum_i (T_{w_i} - T_d)}}, \tag{3.47}$$

or

$$S_{w_m} = 1 - \sqrt{\frac{\sum_i (T_i - T_d)}{\sum_i (T_{w_i} - T_d)}}. \tag{3.48}$$

Calculations show that

$$\sum_{i=1}^{n} (T_i - T_d) \cong T_{w_m} - T_{d_m};$$

$$\sum_{i=1}^{n} (T_{w_i} - T) = \bar{T}_{w_m} - T_m. \tag{3.49}$$

Thus, in order to simplify the computation of cloudiness at the w_m level, one uses not Eq. (3.48) but

$$S_{w_m} = 1 - \sqrt{\frac{T_m - T_{d_m}}{\bar{T}_{w_m} - T_{d_m}}}. \tag{3.50}$$

Workers at the Main Geophysical Observatory /1/ and A. Abramova of the High-Altitude Geophysics Institute have studied the altitude variations of the total radar echo areas at the time of maximum development of convection over an area of radius 100 km.

Comparing figures for cloudiness calculated from Eq. (3.50) with observational data, they showed that the actual value of S_{w_m} is less than the calculated value. An empirical coefficient was worked out defining the relationship between the actual and calculated values. If the atmospheric stratification is such that $w_m \leqslant 20$ m/sec, this factor is $K = \frac{S_{act}}{S_{cal}} \approx 1$; but at $w_m > 20$ m/sec one has $K = \frac{S_{act}}{S_{cal}} \approx 0.65$. Thus, the equations for cloudiness at the w_m level are as follows:

$$w_m \leqslant 20 \text{ m/sec}: \; S_{w_m} = 1 - \sqrt{\frac{T_m - T_{d_m}}{\bar{T}_{w_m} - T_{d_m}}}; \tag{3.50'}$$

$$w_m > 20 \text{ m/sec}: \; S_{w_m} = 0.65\left(1 - \sqrt{\frac{T_m - T_{d_m}}{\bar{T}_{w_m} - T_{d_m}}}\right). \tag{3.50''}$$

3.7. CALCULATION OF AVERAGE AND MAXIMUM RAINFALL

Previously, we obtained an equation for the maximum amount of condensed moisture in the accumulation zone:

$$\theta'_m \leqslant \rho_m \frac{w_m^2}{2g}. \qquad (3.51)$$

It is clear from this equation that the amount of moisture accumulating in the cloud depends on the updraft speed and therefore determines the maximum quantity of water that can fall from the cloud, provided one disregards the evaporation of drops as they fall. But since Eq. (35.1) determines the large-drop fraction, which is responsible for the bulk of showery precipitation, evaporation may be ignored. At the same time, one must bear in mind that this equation is useful in calculating rainfall figures only for a single cloud (over the reference point) at its maximum development stage, which is moreover motionless and dissipates immediately after releasing precipitation. In nature, however, this is an extremely rare situation. Growing clouds move over the sky, so that any one point may receive precipitation from several clouds or from clouds which do not scatter after the initial occurrence of precipitation but continue to develop due to further accumulation of moisture in their frontal parts while precipitation is falling from their rear parts. In such cases Eq. (3.51) is useless in precipitation calculations.

The dense raingauge network over the Kabardino-Balkarian Autonomous SSR provided the means to estimate the relationship between actual precipitation and the amount of accumulated moisture /35/. This was done as follows. The average liquid water content in the accumulation zone was calculated using Eq. (1.21) with w_m averaged over time and over the horizontal cross section of the cloud. The dimensions of the accumulation zone were then determined from radar observations, and it was thus possible to find the average water reserves in the accumulation zone. For this purpose the accumulation zone was taken to be a cylinder whose base was the horizontal cross section of the zone and whose height was its vertical extension. The amount of moisture thus calculated was compared with the actual precipitation from the cloud.

The results, pertaining to days on which sizable showers occurred, are shown in Table 9. It is evident from the table that the average amount of condensed moisture in shower-producing clouds is usually considerably less than the average precipitation per unit area. This confirmed a previous conclusion of certain authors (Mamina and Fedorova /61/ for steady precipitation, Muchnik /62/ for showers) that if stratification conditions are suitable a cumulonimbus cloud will produce precipitation considerably exceeding its water content at any given time during its existence. We may thus conclude that in such clouds the entire mass of water is reconstituted again and again during the process of precipitation.

As mentioned, Eq. (3.51) gives the maximum precipitation from convective clouds per unit area, assuming that water accumulates only once. To determine the average precipitation from a cloud due to one accumulation of water, we must substitute into this equation the average updraft speed as given by Eqs. (3.39)–(3.42). This gives

$$Q_{av} \leqslant \rho_m \frac{\overline{w}_{i,s}^2}{2g}. \qquad (3.52)$$

TABLE 9. Comparison of actual average rainfall with calculated water content of a convective cloud

Date	Period of precipitation	w_m, m/sec	Calculated water content, $t/km^3 \cdot 10^3$	Cross-sectional area of zone, km^2	Depth of zone, km	Volume of zone, $km^3 \cdot 10^6$	Calculated water reserves of zone, $t \cdot 10^6$	Rainfall, $t \cdot 10^6$	Ratio of rainfall to calculated value
11/V 1965	18 20 – 21 00	23.4	2.75	320	5.6	1.790	4.92	12.0	2.44
	16 20 – 19 00	23.4	3.35	140	4.6	0.645	2.16	4.4	2.04
	14 00 – 18 00	23.4	3.02	130	5.1	0.662	2.00	4.2	2.10
8/VI	14 40 – 15 40	21.6	1.10	230	8.8	2.020	2.22	8.5	3.85
	14 30 – 19 00	21.6	1.10	500	8.8	4.400	4.85	13.0	2.68
	20 00 – 23 30	21.6	0.99	500	9.8	4.900	4.85	9.2	1.90
9/VI	15 40 – 19 00	32.0	2.84	200	9.1	1.800	5.10	18.7	3.66
17/VI	*16 40 – 19 00*	*29.4*	*2.90*	*150*	*7.5*	*1.100*	*3.20*	*4.8*	*1.50*
	16 00 – 20 00	29.4	2.18	320	10.0	3.200	7.00	9.6	1.37
28/VI	14 30 – 16 00	29.4	2.76	220	9.5	2.100	5.80	4.1	0.70
1/VII	15 40 – 18 00	24.2	1.45	230	9.3	2.140	3.10	12.0	3.86
3/VII	18 25 – 19 15	39.4	4.15	54	9.6	0.520	2.16	4.5	2.08
	14 00 – 16 00	39.4	4.15	900	9.6	8.600	3.57	12.1	0.34

To determine the average precipitation per unit area during the instability-resolution time, we propose to introduce the factor τ/τ_1, which gives an estimate of the number of times water may accumulate in time τ over a certain point, assuming that the stratification is represented by τ_1.

We thus obtain the formula

$$Q_{av} \leqslant \frac{\tau}{\tau_1} \frac{\bar{w}_{l,x}^2}{2g} \rho_m. \tag{3.53}$$

Nevertheless, one is primarily interested in the maximum amount of shower-type precipitation, since it is the maximum precipitation that characterizes the process. To this end, we can use Eq. (3.51) with the factor τ/τ_1:

$$Q_m \leqslant \frac{\tau}{\tau_1} \frac{w_m^2}{2g} \rho_m. \tag{3.54}$$

Thus, Eqs. (3.53) and (3.54) enable us to calculate the average (over the area covered by the precipitation) and maximum amounts of shower-type precipitation per unit area during the entire resolution time of atmospheric instability.

3.8. OTHER METHODS FOR CALCULATING SHOWER-TYPE PRECIPITATION

N. M. Mal'bakhova of the High-Altitude Geophysics Institute has suggested a method for estimating precipitation from data concerning atmospheric stratification both prior to the formation of precipitation and after its fall to earth. The method is valid provided the area is such that the appropriate radiosonde data are representative (a radius of 100 km about the sounding point).

If there is no advection of air masses, one considers a neutral mass, i. e., a mass of air into which there is no inflow of heat (or in which the inflow is balanced by the outflow) during the entire process: development of cumulus, formation and fallout of showers. Thus the process to be considered is pseudo-adiabatic (the lowest atmospheric layer, about 500 m deep, is not involved in the calculation). Considering a layer of air of unit cross section with base at altitude 500 m and top at the convection level, let us calculate the total energy of this layer from the onset of convection till the dissipation of the cloud.

If not for precipitation, the total energy would have remained constant:

$$\frac{\partial}{\partial t}(I + \Pi + K) = 0, \qquad (3.55)$$

where I, Π and K are the internal, potential and kinetic energies of a column of air of unit cross section extending from z_0 to the convection level.

The level z_0 is selected anew for each particular case, in order to eliminate the effect of diurnal temperature variations; on the average, it is 600–800 m. Replacing Eq. (3.55) by the corresponding finite-difference equation and selecting the boundary states t_0 and t_c in such a way that the kinetic energy of the air column in these states is practically zero, we obtain $\Delta(I+\Pi)=0$, and the variation of the sum $I+\Pi$ is

$$\Delta(I + \Pi) = \Delta E + A[\Delta(P_0 z_0) - \Delta(P_H z_H)], \qquad (3.56)$$

where ΔE is the variation of the enthalpy of the air column, $A(\Delta Pz)$ is the difference in the work of expansion at the lower (z_0) and upper (z_H) boundaries of the column. The second term in (3.56) is one or two orders of magnitude smaller than the first; its neglect introduces a measurement error of from 8 to 10%.

In an adiabatic process (and this is the case under consideration), the variation of enthalpy is due to phase transitions of water in the column.

If Q' stands for the amount of water vapor condensing per unit column during the entire growth of the cloud, the heat set free thereby is

$$\Delta\theta' = Q'L. \qquad (3.57)$$

During the resolution of instability, formation of clouds and formation of cloud and rain particles, part of the condensed water falls to the surface as precipitation. Denote the amount of precipitation by Q. A quantity Q'', say, of this water evaporates at the periphery of the air column, reducing the latter's heat content by

$$\Delta\theta'' = Q''L. \qquad (3.58)$$

Thus, the quantity of heat $\Delta\Theta$ (in cal/cm^2) added to the heat content of a unit column of air owing to resolution of instability and showery precipitation is given by

$$\Delta\Theta = \Delta\Theta' - \Delta\Theta'' = L(Q' - Q'') = LQ. \tag{3.59}$$

Now, having determined the heat content of the air column before and after precipitation, E_1 and E_2, respectively, we can estimate the amount of precipitation as

$$Q = \frac{\Delta\Theta}{L} = \frac{E_2 - E_1}{L}. \tag{3.60}$$

In order to calculate the enthalpy, we need radiosonde data for the times immediately before the onset of convection and just after dissipation of the cloud(s). For a unit air column, this quantity is determined by integrating the expression

$$dE = c_p T_v dz \tag{3.61}$$

with respect to height. Assuming a layer with γ=const, this gives

$$E = \frac{c_p}{R\gamma + g}\left[T_0 P_0 - T_v P_v\right],$$

where $P_0 T_0$ and $P_v T_v$ are the pressure and temperature at the lower and upper boundaries of the layer.

Summing the heat content over all layers with γ= const, we obtain the enthalpy of the entire unit column from z_0 to z_H:

$$E = \sum_{i=1}^{n} \frac{c_p}{R\gamma_i - g}\left[T_{0_i} P_{0_i} - P_{v_i} T_{v_i}\right]. \tag{3.62}$$

Calculating the enthalpy E_1 before the onset of convection and E_2 after the resolution of instability and substituting these into Eq. (3.62), we obtain the shower-type precipitation resulting from nearly pseudo-adiabatic processes.

Some results of such calculations in the absence of advection are shown in Table 10 and Figure 41. In the table we also list some actual values of Q for comparison; these were obtained from a dense network of self-recording raingauges. The comparison, shown both in Table 10 and in Figure 41, shows that the agreement is in general quite good.

In North Caucasus, summer showers are due most frequently to frontal processes, when the advection of heat is too significant to be disregarded. The intensity and amount of precipitation from frontal clouds are usually much higher than from air-mass clouds. For such cases it is therefore necessary to correct the previous technique for advection.

The form of Eq. (3.59) for nonadiabatic processes is

$$\Delta\Theta = LQ + \Delta\Theta_{adv}, \tag{3.63}$$

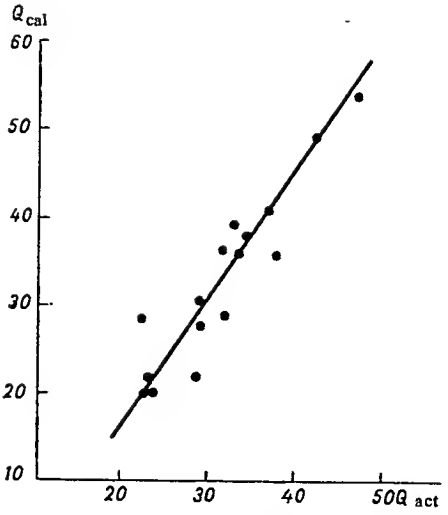

FIGURE 41. Correlation plot between Q_{cal} and Q_{act}.

where $\Delta\theta_{adv}$ is the advective increment to the heat content of unit air column during the process. Then the precipitation from frontal clouds is given by

$$Q = \frac{\Delta\theta + \Delta\theta_{adv}}{L}. \tag{3.64}$$

TABLE 10. Comparison of calculated and actual precipitation.

Date	E_1, cal/cm^2	E_2, cal/cm^2	ΔE	Q_{cal} mm	Q_{act} mm	ΔQ	$\frac{\Delta Q}{Q_{act}}$ %
27/V 1967	48 700	46 972	1728	29	31.7	2.7	8.5
28/V	46 876	45 435	1351	20	22.7	21.5	11.5
4/VI	45 313	42 898	2415	36	31.4	4.6	11
13/VI	67 743	65 199	2544	38	34.4	3.6	10
16/VI	48 058	47 160	1498	22	28.5	6.5	23
22/VI	43 388	40 960	2428	36	33.3	2.7	8 1
26/VI	48 517	46 960	1539	22,9	23.1	0.2	0.9
2/VII	54 972	53 120	1852	27,7	29.1	1.4	4.7
7/VII	46 253	42 576	3677	54	47	7	14.5
9/VII	48 046	46 680	1366	20,4	23.4	3	1.3
10/VII	43 522	40 793	2729	10,7	36.9	3.8	10.3
11/VII	49 535	47 625	1910	28.5	22.4	6.1	27
18/VII	48 108	44 806	3302	49	42.4	6.6	15
19/VII	49 164	46 767	2397	35,8	37.6	1.8	4.8
27/VII	49 152	47 098	2054	30,6	29	1.7	5.8
31/VII	50 735	48 101	2634	39,3	33	6.2	18

Since it is extremely difficult to solve the total energy equation including terms describing the divergence of forms of energy, it is more convenient to incorporate advection by using a conservative quantity such as pseudo-equivalent temperature T_p. This quantity is constant in pseudo-adiabatic processes, and its variation defines the deviation from adiabaticity /63/.

In the first case, the stratification curves before and after precipitation are divided into layers with constant lapse rate and constant relative humidity gradient. The thickness of each layer is at most 50 mb. For each layer, a graphic technique is used to determine the average pseudo-equivalent temperature T_p. One then constructs a pseudo-equivalent temperature profile for the air mass from z_0 to the upper free-convection level z_H.

The changes occurring in T_p during the development of convection and precipitation give the correction for advective heat to be introduced into the formula (3.64) for the amount of precipitation.

The increment $\Delta\theta_{adv}$ may be written as

$$\Delta\theta_{adv} = c_p \int_{z_0}^{z_v} \Delta T_p \rho dz, \tag{3.65}$$

where ΔT_p is the change in pseudo-equivalent temperature at altitude z during the process.

For unit column of air, in a layer with $\gamma = \text{const}$, use of finite differences in this equation yields

$$\theta_{adv} = \frac{c_p}{g} T_0 \left(\frac{P_c}{P_w}\right)^{\frac{R}{g}(\gamma_d - \gamma_c)} (P_1 - P_2), \tag{3.66}$$

where P_1 and P_2 are the pressures at the lower and upper boundaries of the layer, P_c is the pressure at the condensation level, P_w the pressure at the level where the dry adiabatic lapse rate γ_d is equal to the wet rate γ_w. The quantity

$$T_0 \left(\frac{P_c}{P_w}\right)^{\frac{R}{g}(\gamma_d - \gamma_w)} \tag{3.67}$$

is the pseudo-equivalent temperature of the layer.

Summing the advective heat over all layers from z_0 to z_n, we have

$$\theta_{adv} = \frac{c_p}{g} \sum_{i=1}^{n} T_{0i} \left(\frac{P_{ci}}{P_{wi}}\right)^{\frac{R}{g}(\gamma_d - \gamma_w)} (P_{1_i} - P_{2_i}). \tag{3.68}$$

Using this equation, one obtains

$$\Delta\theta_{adv} = \theta_{adv2} - \theta_{adv1} \tag{3.69}$$

which, when substituted into Eq. (3.64), gives the amount of precipitation Q, in g/cm^2, from a unit column of air.

Results of calculations with these equations in three cases are shown in Table 11.

To estimate the amount of precipitation over a given area, one needs radiosonde data pertaining to the times before and after the precipitation process. This method may be utilized to determine the average precipitation over an area within which the radiosonde data are representative.

TABLE 11. *Comparison of calculated and actual precipitation*

Date	Q_{cal}, mm	Q_{act}, mm	ΔQ mm	$\Delta Q/Q_{act}$ %
5/VI 1969	3.7	5	1.3	26
6/VI	13.8	16	2.2	13.8
11/VI	32	27	5	18.5

Moreover, having determined the average cloudiness from Eq. (3.47), one can determine the average and maximum precipitation over the territory.

The next factor we shall incorporate is the exchange of heat between the earth's surface and the air in the period elapsing between soundings; neglect of this factor is undoubtedly responsible for errors in the calculation of q.

3.9. CALCULATION OF AMOUNT OF WATER GENERATED BY CLOUD

A cumulus cloud is a system which generates solid and liquid cloud particles from water vapor. Subsequent microphysical processes within the cloud cause the small cloud particles to grow until they reach the dimensions of raindrops, graupel or hail, which can no longer be supported by the updrafts and fall from the cloud as precipitation. Large particles fall from the cloud as precipitation, while small particles evaporate at the periphery of the cloud or outside it. In order to decide whether the process of formation of large cloud particles should be modified so as to increase precipitation, it is important to determine what part of the water generated in the cloud falls as precipitation and what part remains in the atmosphere due to evaporation. If the overwhelming majority of the cloud water becomes precipitation and only a small proportion of small particles remain in the atmosphere, it is hardly worthwhile stimulating precipitation from convective clouds. On the other hand, if most of the generated water remains in the atmosphere, one should definitely consider intensifying the growth of these small droplets or ice crystals with a view to inducing precipitation. This problem may be solved by analyzing the thermodynamic conditions of convective cloud formation.

Let us try to determine the entire quantity of water generated by a cloud.

The specific humidity q of the air (in g/g) is determined from the equation $q=0.622\left(\frac{E}{P}\right)$, where E is the elasticity of the saturated water vapor (millibars) and P the air pressure.

To calculate the amount of water generated by the cloud during the development of convection, we must determine the amount of water vapor that condenses when lifted from the condensation level z_c to the maximum updraft speed level z_m during that time.

By the Clausius equation, the saturated vapor pressure at the condensation level at temperature T_c is given by

$$E_c = E_0 e^{\frac{L}{AR_0}\cdot\frac{T_c - T}{TT_c}}, \tag{3.70}$$

where R_0 is the gas constant for water vapor, E_0 the saturated water vapor pressure at temperature 0°, E_c the elasticity of saturated water vapor at the condensation level temperature T_c.

Using this equation and remembering that water vapor is saturated at each level of the cloud, one finds the following expression for the amount of water that condenses upon ascent from z_c to z_m:

$$q = 0.622\frac{E_c}{P_m P_c}\left\{P_m - P_c e^{\frac{L}{AR_0}\frac{T_m - T_c}{T_m T_c}}\right\}, \tag{3.71}$$

where T_m is the air temperature at level z_m; P_c and P_m are the air pressures at levels z_c and z_m, respectively. The total amount of water generated in the cloud (in g/cm^2) is

$$\Delta Q = q\Delta m, \tag{3.72}$$

where Δm is the mass of air displaced during the convection process. Simultaneous solution of Eqs. (3.71) and (3.72) yields the amount of water generated by the cloud in a unit air column, over a radius within which radiosonde data are representative. To obtain the amount of water generated over a horizontal surface of area 1 cm^2 in the cloud, one need only divide ΔQ from Eq. (3.72) by the convective cloudiness S.

In calculations, the quantity q represented by Eq. (3.71) must be determined directly from the aerological diagram.

Subtracting from ΔQ the amount of precipitation $\bar{Q}$, one can determine the amount of water generated by the cloud that remains in the atmosphere, Q_0. The amount of shower-type precipitation from the cloud is calculated using Eq. (3.53).

We now define the precipitation-generation coefficient K_p as the ratio of the amount of precipitation from the cloud to the entire quantity of water generated by the cloud:

$$K_p = \frac{\bar{Q}}{\Delta Q}. \tag{3.73}$$

Similarly, the water-generation coefficient K_1 represents the amount of water vapor in the column from z_c to z_m that liquefies or solidifies:

$$K_1 = \frac{q\Delta m}{q_c\Delta m} = \frac{P_m - P_c e^{\frac{L}{AR_0}\frac{T_m - T_c}{T_m T_c}}}{P_m}, \tag{3.74}$$

where q_c is the amount of water vapor at the condensation level, in grams per gram of air.

If T_m is low, K_1 tends to unity, corresponding to the case in which all the water vapor in the cloud turns into raindrops or ice.

It follows from Eq. (3.74) that the amount of generated water depends mainly on the temperature at the condensation level, which determines the saturated vapor pressure at that altitude. At level z_m, the saturated vapor pressure is usually 1—2 mb, varying only slightly with height, so that a change of 5—6° in the temperature at z_m has little effect on the water generation of the cloud. This is usually the reason for the great intensity of showers in the tropics, where the condensation level is not infrequently at the +20° isotherm, corresponding to saturated vapor pressure of 23.4 mb.

As an example, we consider the average precipitation reaching the surface from clouds on May 11, 1965, which was $\bar{Q}=1.8$ g/cm^2.

Eq. (3.71) gives $q=9\cdot 10^{-4}$ g/g.

The amount of water passing through a unit column of the cloud at level z_m was 4.6 g/cm^2, so that the amount of evaporated water was 2.8 g/cm^2 and the precipitation-generation coefficient is $K_0=0.39$, approximately 2/3 of the water having evaporated at the periphery of the cloud and a little more than 1/3 having fallen to the surface as precipitation.

At the condensation level z_c we have $q_c=1\cdot 10^{-3}$ g/g, while at z_m level $q_m=0.1\cdot 10^{-3}$ g/g. Thus, of the total quantity of water vapor passing through the cloud, $0.9\cdot 10^{-3}$ g/g, was generated as water droplets. Thus the water-generation coefficient is $K_1=0.9$.

Workers at the High-Altitude Geophysics Institute are now engaged in calculating the amount of water evaporating at the cloud periphery and the coefficients of precipitation and water generation, for all cases of precipitation recorded by the raingauge network of the Institute's Caucasus Hail-Suppression Expedition.

The precipitation-generation coefficient K_0 may well turn out to be a stable quantity. In that case calculation of the overall amount of water generated in a cloud will enable one to predict shower-type precipitation from convective clouds on the basis of atmospheric stratification data, providing yet another method of forecasting the amount of shower-type precipitation.

Continuation of these studies will expand our knowledge of the microphysical conditions governing the development of convective clouds.

Chapter 4

STORM PREDICTION

4.1. CONDITIONS INITIATING STORMS

Thunderstorms constitute one of the most dangerous weather phenomena, both for aviation and for agriculture; in the absence of suitable protective measures, they may also endanger human life.

At any one time, more than one thousand thunderstorms may be occurring in different parts of the globe. The daily "quota" of thunderstorm phenomena is 44,000. In middle latitudes, thunderstorm activity is observed mainly in the warm half of the year. The number and intensity of storms decrease with increasing latitude. Thus, in the polar regions thunderstorms are quite rare; in middle latitudes there are on the average from 20 to 30 stormy days per year, in the tropical belt from 80 to 100 (as many as 220 have been observed on the island of Java, in the region of Bogor).

Observations show that thunderstorms arise only in cumulonimbus clouds associated with atmospheric convection; they are never observed in stratified clouds. However, electrical charges are not produced in every cumulonimbus cloud — only in clouds showing relatively large vertical development, whose tops reach the level of natural crystallization (in moderate latitudes).

The chief factor in the formation of convective clouds is violent convection, produced in an unstable air mass by heating of the lower atmospheric layers during the day or by passage of a front. Thus, a first prerequisite for the development of thunderstorms is violent vertical motion, promoting the growth of convective clouds with considerable vertical development.

Research has shown that meteorological and electrical processes are intimately connected. Studies of the electrical structure of clouds have shown that positive charges are found above 7 km, where the temperatures are less than –20° /48, 162–165, 175/, while the center of negative charges is characterized by temperatures slightly below 0°. Simpson and Robinson /164/, using data from electric field measurements in thunderstorm clouds at Kew, constructed a theoretical model of a thunderstorm cloud, according to which the upper, positive charge (24 coulombs) is distributed throughout a sphere of radius 2 km centered at a height of 6 km, with temperature –30°, and the negative charge (–20 coulombs) concentrated in a sphere of radius 1 km centered at a height of 3 km, where the temperature is –8°; A second region of positive charge (4 coulombs) is concentrated in a sphere of radius 0.5 km around the 1.5° isotherm. This scheme is in good agreement with experimental data of Imyanitov /38, 39/, who concluded that clouds possess

this type of electrical structure, irrespective of their vertical extension, as long as freezing or consolidation of cloud particles has not begun. He also showed that shower and hail clouds display a reverse type of polarization /38/. The rate of accumulation of volume charge at the stage when the cloud is developing into cumulonimbus varies from 0.1 to 0.3 e. s. u. /m^3. sec, increasing quite sharply during the active stage of the cloud to 10^2 e. s. u. / /m^3. sec.

Malan and Schonland /148/, studying warm thunderstorm clouds over South Africa, established that the negatively charged regions form a single vertical column between the 0° and —40° isotherms, the upper part of which becomes progressively higher. They found that if the temperatures in the cloud are positive a positive charge is formed.

Kuettner /134/ presented important data on the nature of hydrometeors in thunderstorm clouds whose bases are in the temperature region around 0°. His observations, made inside clouds capping a mountain peak, are more reliable and definitive than those made in an airplane, for in the latter case it is difficult to distinguish graupel from snow in the precipitation on the fuselage. In most of the clouds Kuettner studied solid precipitation prevailed, being detected in 93% of all cases, while raindrops were observed only in 21%. In 75% of cases he observed graupel, accompanied by high electric field intensities, whereas large hail, by no means a necessary component of a thunderstorm cloud, was comparatively rare. Snow crystals prevailed in the later part of the storm, when the precipitation had become steady and moderate and the thunderstorm activity weaker. Kuettner establish that during high precipitation intensity, an indispensable requirement for the electrical activity of a cumulonimbus cloud, the central thunderstorm activity region is generally identical with the region of most intensive precipitation. The first thunderstorm activity is observed with the onset of heavy solid precipitation inside the cloud.

Workman and Reynolds /176—179/, corroborating Kuettner's findings, showed that the electrical separation in a cloud is closely bound up with the mechanism of precipitation and takes place after precipitation has occurred. In thunderstorm clouds over New Mexico, where they made their observations, charge separation was observed at temperatures from 0 to —15°. The first internal thunderstorm discharge was recorced 12 minutes after appearance of the initial radar echo, which had by then reached the level of the —30° isotherm and had begun to descend; simultaneously, precipitation from the cloud base began. After a few minutes, thunderbolts were heard. Workman and Reynolds noted a certain periodicity of thunderstorm activity; the period, from 25—40 minutes, corresponded to the activity period of the cell.

Data on the frequency of lightning as a function of the temperature distribution in clouds are extremely sparse. Kuettner, Workman and Reynolds affirmed that thunderstorms cannot arise unless the temperature at the level of the cloud base is above 0°. Ludlam /142/ reached a similar conclusion from studies of thunderstorms over the eastern part of the North Atlantic. Workman and Reynolds remarked that thunderstorm activity in cloud tops is rare, when the echo peaks do not reach the level of the —30° isotherm. According to data of Byers and Braham, the temperature at the level of the echo peak is less than —20°. Thus, a second necessary condition for the occurrence of a thunderstorm is the presence of crystals in the upper part of the cloud.

Any satisfactory theory must conform to certain specific features of thunderstorm clouds, which may be listed as follows.

1. Precipitation and electrical activity inside a single thunderstorm cell last on the average about 30 minutes.

2. The mean electrical moment neutralized by the thunderbolt is 110 coulombs/km, corresponding to a charge of from 20 to 30 coulombs.

3. The charge released immediately after a thunderbolt, associated with a fall speed v of precipitation elements, is of the order of $\frac{8000}{v}$ coulombs.

4. In a cumulonimbus cloud of appreciable thickness, this charge is generated and released in a region between the −5° and −40° isotherms, of average radius about 2 km.

5. The negative charge center lies near the −5° isotherm, the positive charge center several kilometers higher; near the cloud base there is an additional positive charge, centered near the 0° isotherm or slightly below it.

6. The formation and release of charges is closely bound up with the occurrence of precipitation, particularly graupel. Particles of precipitation must fall, overcoming the updrafts, at velocities of several meters per second.

7. In view of the fact that the first thunderbolt occurs 12 to 20 minutes after the appearance of precipitation in radar-detectable quantities, a sufficiently high charge should form and be released.

We now briefly survey the existing theories of the formation and separation of electrical charges.

Elster and Geitel /130/ investigated effects accompanying rainfall in a vertical electric field and the collision of raindrops with smaller cloud droplets in their path of fall. Raindrops are polarized in the electric field; if the field is directed downward, as is the case in fine weather, positive charge will accumulate on the lower half of the drop and negative charge on its upper half. Elster and Geitel conjectured that cloud droplets rebounding from the raindrops upon collision with them carry away some of the positive charge from the underside of the raindrops. In a positive field, therefore, the raindrops will acquire a negative charge, and as a result of gravitational separation of drops, the original field will be enhanced. This theory is no longer considered valid, as the modern theory of precipitation assigns a major role to coalescence of drops, which accrete smaller drops upon collision with them.

Wilson /174/ pointed out that, under certain conditions, electrically polarized raindrops falling through a cloud of ions or charged cloud droplets could acquire a negative charge by selective ion capture. If the fall speed of a drop through a downwardly directed field is much greater than that of the positive ions, the latter are repelled from the lower half of the drop and deflected to one side, while negative ions are attracted to it. However, for a thunderstorm to occur, a charge of 1000 coulombs must accumulate in a volume of 60 km^3 within 20 minutes; hence the process as suggested by Wilson cannot possibly produce the required effect within the lifetime of a typical thunderstorm cell. It may play a secondary role in charge separation at later stages, when the major process has already created strong fields and intensive ionization.

Wall /171/ also tried to explain why charge separation takes place primarily at below-zero temperatures; he suggested that not only raindrops but also ice crystals participate in selective ion capture. In his opinion,

the initial field polarizes hexagonal plate crystals, which become dipoles if they fall with their principal axes along the vertical, and their undersides are positively charged. This theory is based on the assumption that ice has a polar structure, which implies the appearance of piezo- and pyroelectrical properties in ice. However, Mason and Owston /182/ showed experimentally that asymmetric crystals grown in a vaporous medium do not possess these properties.

Frenkel /129/ pointed out that, as a dipole liquid, cloud droplets easily adsorb negative ions at their surfaces and acquire a certain negative equilibrium charge; in other words, a particle encountering positive and negative ions while falling may acquire charge by a simple process of ion discharge.

Frenkel's theory would explain why precipitation from thunderstorm clouds is predominantly positive charged. Qualitatively speaking, however, it cannot explain the high rate of charge separation in such clouds.

The phenomenon of electrification associated with the disruption of water drops upon impact with a solid surface, was first studied in detail by Lenard /136/. Simpson /162, 165/, in a series of experiments, established that breaking of drops in a strong vertical air jet could also produce a considerable electrification. Calculations of the time needed for drops to grow to sizable dimensions by coalescence yield a figure of approximately 4 minutes Since about 12 minutes elapse from the appearance of the first radar echo from a thunderstorm cloud to the first lightning stroke, this time suffices for only three consecutive disruptions of the same mass of water in the cloud. The maximum charge producible under such conditions is $9 \cdot 10^{-2}$ coulombs/km^3, two orders of magnitude lower than that required by conditions 3 and 4.

Nevertheless, experiments to determine the size of charges produced by breaking of drops in strong electric fields have shown that the prior presence of induced charges on the drops may cause the subsequent charges to be much larger than otherwise.

Simpson and Scrase /163/ conjectured that the distribution of basic charges in a thunderstorm cloud might be due to electrification upon collision and fracture of ice crystals; the latter would be negatively charged, a compensating positive charge being carried upward on cloud droplets.

Again, the main shortcoming of this hypothesis is the smallness of the electrical charge formed by fracture of ice crystals, compared with that necessary to produce a thunderstorm.

Dinger and Gunn /123/ showed that when ice containing air melts, air bubbles rise to the surface of the newly formed liquid and transfer a negative charge to the surrounding air, an equal positive charge remaining in the water. This process may be significant in the melting of graupel and snowflakes, but it does not explain the observed polarity of thunderstorm clouds. It may provide a partial explanation for the predominance of positive charge in steady precipitation and assist in the formation of the local positive charge detected near the bases of thunderstorm clouds with warm bases.

Workman and Reynolds /176—179/ conducted numerous experiments in connection with electrical effects associated with the freezing of water and dilute aqueous solutions. They found that during freezing a potential difference develops across the ice-liquid interface, of sign and magnitude dependent on the nature and concentration of the solution. On the basis

of laboratory experiments, they tried to devise a theory of charge generation and separation in thunderstorms.

The basic assumption of their theory was the existence of wet hailstones, i. e., solid particles which, having reached critical size and fall speed (which depend on the temperature and liquid water content of the cloud), begin to capture supercooled cloud drops in quantities too large to be frozen on the surface, and thus acquire a liquid coat. Workman and Reynolds suggested that this begins at temperatures between —10 and —15°, following which only a fraction of the cloud water freezes on the hailstones, the remainder being shed in the form of small drops. In addition, at the ice-liquid interface negative ions are captured preferably by the ice, so that the water drops flung off carry away a positive charge, leaving a net negative charge on the hailstone. Gravitational separation of the negatively charged hailstones and positively charged drops would then account for the observed polarity. In the supercooled region of the cloud, drops shed from the hailstones would carry an excess of negative charge, while the positively charged drops, rising in the jet to heights where they can again be captured by negatively charged hailstones, increase their charge. Thus creation of the electric field would become a cumulative process.

Workman and Reynolds considered that their theory had two main advantages. First, it provided a natural explanation for the centering of negative charge around the —10° isotherm; second, laboratory experiments show that the magnitude of the charges carried through the ice-liquid interface was sufficient to account for the charges arising in thunderstorm clouds. Nevertheless, if the Workman-Reynolds effect were the principal mechanism of charge formation, thunderstorms would normally be accompanied by hail. Factual data are at variance with this conclusion. Moreover, the cumulative nature of the process as described raises certain doubts. It seems probable that a relatively small proportion of the water collected by wet hailstones is shed from their upper surface not as small drops but as large ones; this implies a lower rate of separation of drops and hailstones, and hence a lower probability of the released drops being recaptured by hailstones at higher levels. In addition, in a positively directed field, drops from the negatively polarized upper surface of the hailstones would weaken the field.

Summarizing, one sees that all of the above theories are open to objection from the quantitative standpoint, and in addition some of them contradict known facts concerning the meteorological and electrical structure of thuderstorm clouds.

There is at present no complete theory explaining charge generation in convective clouds. Hence thunderstorm prediction remains one of the most difficult problems of modern meteorology.

4.2. THUNDERSTORM PREDICTION METHOD

Present-day weather forecasters employ more than ten different methods for thunderstorm prediction. We shall consider the most widespread ones.

In Lebedeva's method, the criterion of instability is the temperature difference between the rising air parcel and the environmental air; the humidity criterion is the sum of dew-point deficits at the basic isobaric surfaces: 850, 700 and 500 mb. An additional criterion is the temperature at the upper convection level.

In the techniques of Bailey and Whiting the instability criterion is the lapse rate in the 850—500 mb layer; Bailey's humidity criterion is the sum of dew-point deficits at 700 and 500 mb, Whiting's the vertical depth of the wet layer and the liquid water content of the lowest atmospheric layers, as indicated by the dew-point on the 850 mb surface.

Cox suggests a compound criterion of instability: first, the difference between the actual temperature at the 500 mb surface and the temperature as read off from the wet adiabat at that altitude passing through the mean wet-bulb temperature in the layer from the surface to the 900 mb level; second, the difference between the actual temperature at the 600 mb surface and the temperature of the wet adiabat through the 850 mb potential temperature surface. The indication of water content is the dew-point deficit at the 700 mb surface.

Faust's measure of instability is the difference between the actual temperature at the 500 mb surface, and the "zero evaporation" temperature.

Slavin uses as instability criterion the temperature difference between the dry and wet adiabats at the 500 mb surface, corrected for the effect of evaporation and nonadiabaticity of the rising air mass.

The most effective method under Transcaucasian conditions is that of Sosin /86/, who suggests identifying unstable stratification by analyzing the change with height of the pseudopotential temperature.

In Yakutiya, Ivanidze /37/ proposed an empirical formula:

$$I = \frac{H_{1000}^{300}}{H_{700}^{300} - H_{1000}^{700}} + 10^{-2}\tau_{700},$$

where H is the relative geopotential and τ the dew-point at the 700 mb surface. From the value of I one estimates the probability of thunderstorm phenomena.

Judging from the above list, it is evident that all the available thunderstorm-prediction methods are based on certain criteria for instability and humidity, correlated with thunderstorm phenomena.

Only in Lebedeva's method is the suggestion made to reckon with the temperature at the upper convection level, which is equivalent to incorporating the crystallization factor.

We now offer some suggestions regarding an approach to thunderstorm prediction based on the specific microstructure of thunderstorm clouds and also on a thermodynamic characterization of the state of the atmosphere necessary for their formation.

The work of Workman and Reynolds /176—179/ showed that electric charge separation is closely connected with precipitation and takes place later than fallout. This has been confirmed by experiments of Chapman /180/: examining disruption of drops of distilled water, he showed that when drops of radius $d=4$ mm are disrupted in an air jet, positive and negative charges appear; their magnitude increasing with the velocity of the jet.

In view of all the aforesaid, it seems logical to conclude that precipitation must be present in the cloud for thunderstorm charges to be generated.

Sulakvelidze /90/ showed that shower-type precipitation may occur in a cumulonimbus cloud if the updraft speed is at least 10 m/sec. It is also known that in middle latitudes one finds thunderstorm charges in cumulonimbus clouds whose tops have reached the level of natural crystallization. The importance of the crystal fraction in a cloud for the generation of

thunderstorm discharges has been confirmed by experiments conducted in California, which produced internal discharges in supercooled fine-weather cumulus clouds /152/.

Thus, in order to produce thunderstorm charges, the vertical extent of the cloud should attain a level of temperatures at which icing begins.

The observations of Selezneva /80/ have shown that in every case the temperature at which the solid phase first appears in a cloud depends on the velocity of vertical currents. According to Findeisen's data /127/, the updraft speed influences the freezing temperature of the cloud droplets. Thus, at updraft speed 10 m/sec the critical temperature is −13°, while at speed 25 m/sec it is −19 to −20°.

We thus have two criteria for the occurrence of thunderstorms: 1) updraft speeds above 10 m/sec, and 2) the upper boundary of the cloud should lie above the icing level. The immediate task is now to verify whether these conditions are sufficient to create a thermodynamic state suitable for the occurrence of thunderstorms.

With this end in view, Velentsova /7/ drew up a plot (Figure 42) featuring a curve (AO) representing the distribution of critical temperature (for the appearance of the first ice crystals) as a function of vertical velocity (according to Findeisen); to plot each concrete case, she computed the maximum updraft speed, using the method of Chapter 1, and determined the temperature at the convection level. All in all, 250 cases were analyzed, 170 with thunderstorms and 80 without. The analysis was based on actual radiosonde data pertaining to times close to the initiation of the thunderstorm or shower phenomena. On days with no thunderstorm phenomena, the data for the calculation were recorded at times after 1500 hours, when conditions were most favorable for convection to develop. The humidity of the air mass was taken into account in calculating the updraft speed by assuming entrainment of 1/3 of the environmental air into the rising air. One sees from Figure 42 that all the thunderstorm cases fall not in the zone AOB, but in $C'CB$, where the maximum updraft speed is 10 m/sec or more and the temperature at the upper convection level is 3 or 4° below the critical temperature.

For a more accurate delineation of the relationship between the temperature at the cloud top and the time of occurrence of a thunderstorm (assuming the updraft speed sufficient, i.e., $w_m \geqslant 10$ m/sec), radar data recorded by the North Caucasus Hail-Suppression Expedition in 1966–67 were processed.

Those cases analyzed were those in which thunderstorms had been recorded in clouds observed by radar (wavelength $\lambda=3.2$ cm). To avoid errors in determining the cloud top height $H_{c.t.}$, the only observations analyzed were those for which the distance L from the cloud to the radar station was at most 40 km.

The results are shown in Table 12. The data show clearly that thunderstorms first appeared when the temperature T at the cloud top was less than the "critical temperature" T_{cr} for the appearance of ice crystals. Whenever the cloud height H was below the level $H_{c.t.}$ of critical temperatures or near this level, no thunderstorms were observed.

Additional observations were undertaken on August 18, 1967, at the Kuba-Taba station, to ascertain the dependence of the occurrence of thunderstorm charges on the temperature at the cloud top. During evening hours, when it was easy to discern each internal discharge in the cloud by visual means, the height of each cloud with discharges was recorded. The growth of the tops of seven different clouds was observed. The results are shown in Table 13.

TABLE 12. Radar observations of thunderstorm phenomena

Date	w_m m/sec	T_c°	H km	Time	L, km	$H_{c.t.}$ km	T°	Time at which thunderstorm was observed
10/V 1966	21	—19	5.8	—	24	9.7	—43	Thunderstorm
13/V	15	—16	5.6	—	27	7.7	—33	"
19/V	36	—23	7.0	—	13,5	6.6	—19	—
20/V	26	—21	6.5	—	25	7.0	—19	—
1/VI	22	—19	6.6	10 14 — 13 10	32	3.7—5.2	—12	—
				15 05	42	7.8	—30	14 50
2/VI	15	—16	5.9	—	0	4.7	—9	—
14/VI	3	—	—	15 07	14	6.7	—17	—
25/VI	26	—21	6.5	18 35	42	5.7	—15	—
				19 00	—	6.5	—21	—
				19 08	39	7.2	—26	19 07
27/VI	23	—20	6.4	11 43	35	6.0	—15	—
				11 55	—	8.2	—31	12 20
23/VII	13	—15	6.6	12 08	38	6.0	—11	—
				13 55	36	8.5	—25	12 20
1/VIII	20	—18	7.4	14 15	35	6.5	—15	—
				14 32	27	5.0	—7	—
				15 17	15	8.8	—27	15 15
5/VIII	28	—20	7.0	15 30	32	6.6	—15	—
				15 33	29	5.7	—9	—
				15 36	35	7.4	—19	—
				15 38	39	9.7	—33	15 44
11/VIII	50	—23	7.9	—	35	13.9	—50	Thunderstorm
17/VIII	18	—18	7.5	—	31	5.7	—9	—
18/VIII	31	—23	7.7	10 10	36	5.8	—11	—
				11 44	22	7.0	—19	—
				11 50	20	5.8	—11	—
				12 10	30	7.6	—22	—
26/VIII	25	—20	6.9	12 32	20	10.0	—34	12 30
				12 50	37	5.7	—12	—
				13 00	36	7.7	—26	13 00

The conclusions from the data of Tables 12 and 13 and Figure 42 are as follows.

1. No thunderstorm phenomena are observed if the cloud tops lie below the critical temperature level, i. e., when conditions within the cloud are not suitable for crystallization.

2. A thunderstorm is observed when the vertical extent of the cloud reaches a level at which the temperature is several degrees less than Findeisen's critical temperature, i. e., when active crystallization begins.

3. A necessary condition for thunderstorms is that the cloud contain a large-drop fraction, made possible by maximum updraft speeds w_m in excess of 10 m/sec.

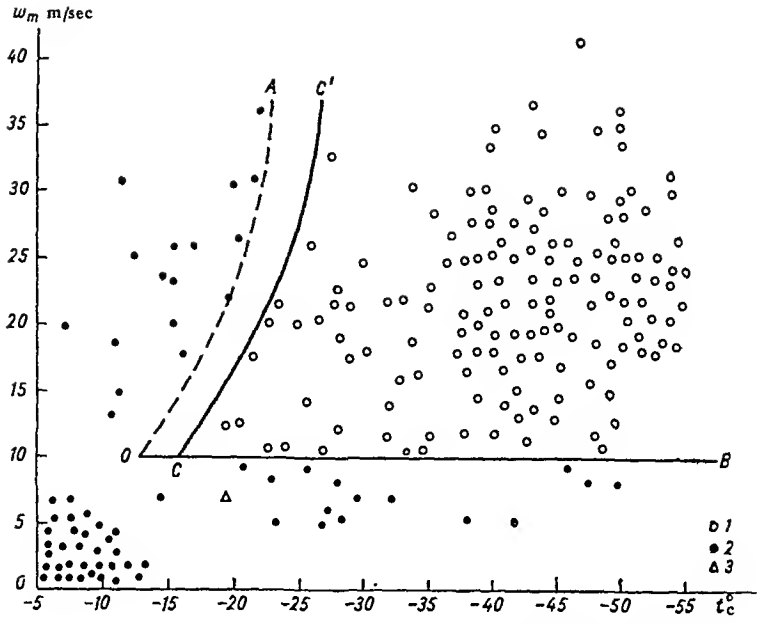

FIGURE 42. Occurrence of thunderstorms as a function of maximum updraft speed w_m and temperature t_c at convection level (cloud top).

1 – thunderstorm; 2 – showers; 3 – soft hail.

TABLE 13. Observations of thunderstorm phenomena at Kuba-Taba Station, August 18, 1967. $w_m = 23$ m/sec.

No. of cloud	Time	L, km	$H_{c.t.}$ km	T°	T_u from	T_u to	$T_l - T_{cr}$	$T_u - T_{cr}$	Thunderstorm observed
1	19 30	30	7.3	—23	—20	—26	—6	0	Thunderstorm
2	19 30	32	6.5	—17	—14	—20	0	6	—
3	19 40	18	6.8	—19	—17	—21	—2	4	—
4	20 16	41	8.2	—30	—27	—33	—13	—7	Thunderstorm
	20 25	41	9.0	—35	—32	—38	—18	—12	.
	20 35	41	7.1	—21	—18	—24	—4	2	—
	20 47	38	7.6	—25	—22	—28	—8	—2	Thunderstorm
5	20 22	41	7.7	—26	—23	—29	—9	—3	.
	20 30	40	7.8	—27	—24	—30	—6	—4	.
	20 45	—	7.7	—26	—23	—29	—9	—3	.
6	21 22	41	9.9	—40	—37	—43	—23	—17	.
7	20 50	40	7.1	—21	—18	—24	—4	2	.
	20 57	—	7.3	—23	—20	—26	—6	0	.
	21 10	—	7.1	—20	—17	—23	—3	3	—

Notation: T – temperature at cloud top: T_u and T_l – upper and lower limits of temperature at height $H_{c.t.}$; T_{cr} – critical temperature for appearance of ice crystals at $w_m = 23$ m/sec.

Chapter 5

FORECASTING TECHNIQUE. TESTING OF METHODS FOR PREDICTING HAIL, SHOWER-TYPE PRECIPITATION AND THUNDERSTORMS

5.1. INITIAL DATA FOR PREPARING FORECASTS

Preparation of a forecast of hail, thunderstorms and shower-type precipitation involves the plotting of a prognostic curve showing stratification of temperature and humidity at the time of maximum convection, using, say, the method proposed in the Handbook of Short-Range Weather Forecasts, Part II, 1965 edition. As intensive thunderstorm-hail processes are observed on frontal surfaces, success in predicting these phenomena is dependent (among other things) on successful prediction of the movement of the front. When data are available from high-frequency atmospheric soundings, one can plot an actual stratification curve for a sounding period of 6 or 7 hours, allowing for the convection temperature and the convection condensation level.

Consider a stable air column 1 near the ground (Figure 43). If an air parcel at *A* is lifted adiabatically, with constant moisture content, it must become saturated at its lifting condensation level *LCL*; to the left of the curve *AB*, there will be negative instability energy. As the surface air is heated, an adiabatic or near-adiabatic lapse rate is established in the lower atmospheric layer. By the time the surface-air temperature has reached T_c, the lifting condensation level reaches the level of *B* and coincides with the free convection level *CCL*, and there will be no negative instability energy. It is assumed here that no water evaporates into the air, so that the dew-point temperature remains constant.

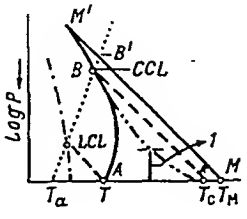

FIGURE 43. Illustrating the definition of convection temperature and convection condensation level.

As shown in /156/, the diurnal variation of the dew point is considerably less than that of temperature. With normal variations of the dew-point, the negative area disappears a short time before the temperature T_c is reached (T_m is the surface-air temperature at the time of maximum heating, T_c the convection temperature, B the convection condensation level in convection). The difference T_c—T is the temperature rise (slightly exaggerated) necessary to allow the development of convective clouds.

The temperature T_c is invaluable in the prediction of thermal convection. A good forecast depends on the forecaster's ability to estimate whether the maximum temperature will reach or exceed the critical value T_c.

The area ABT_c in Figure 43 represents the approximate quantity of heat that must be communicated to an air column of unit cross section below the B level to establish the dry adiabatic lapse rate.

5.2. TECHNIQUE FOR CALCULATION OF MAXIMUM UPDRAFT SPEED

After plotting the temperature and humidity stratification curve, one determines the convection condensation level by the method described above. If conditions are unsuitable for the development of thermal convection, the next step is to assess whether convection may develop from higher levels. The curve of state is plotted from the condensation level (point B) up to its intersection with the stratification curve. The maximum deviation of the curve of state from the stratification curve is then determined.

In case there are several layers showing the same deviation, the maximum deviation used for the calculation is that pertaining to the lowest level (Figure 44). If it is necessary to allow for entrainment, the layer extending from the condensation level to the maximum speed level is divided into 200 mb layers. The wet-bulb temperature after saturation of the mixture is then calculated for each layer, as shown in Figure 45 (see Chapter 1). Then the curve of state with allowance for entrainment of environmental air into the cloud is constructed. One now determines the maximum deviation ΔT_m of the curve of state from the stratification curve, and inserts either ΔT_m or $\Delta T_m'$ into Eq. (1.55) to calculate the maximum updraft speed.

It has been shown /147, 166/ that the rate at which the surrounding air is entrained in a cloud depends on the cloud diameter. In clouds of diameter 500 m, the entrainment rate ranges from $0.5 \cdot 10^{-5}$ to $1.0 \cdot 10^{-5}$ cm^{-1}, while if the diameter is 5 km the range is from $0.05 \cdot 10^{-5}$ to $0.01 \cdot 10^{-5}$ cm^{-1} [sic]. The entrainment rate varies by three orders of magnitude when the cloud diameter changes from 100 m to 10 km. The entrainment coefficient fluctuates considerably in different synoptic conditions. Entrainment is greater in intra air-mass processes than in frontal processes /74/. In cases of clearly expressed cold fronts, entrainment need not be taken into consideration when calculating w_m, since the actual "rarefraction" remains negligible even when the surrounding air is quite dry. In intra air-mass processes and weakly defined fronts, entrainment should be incorporated by the technique described in Chapter 1.

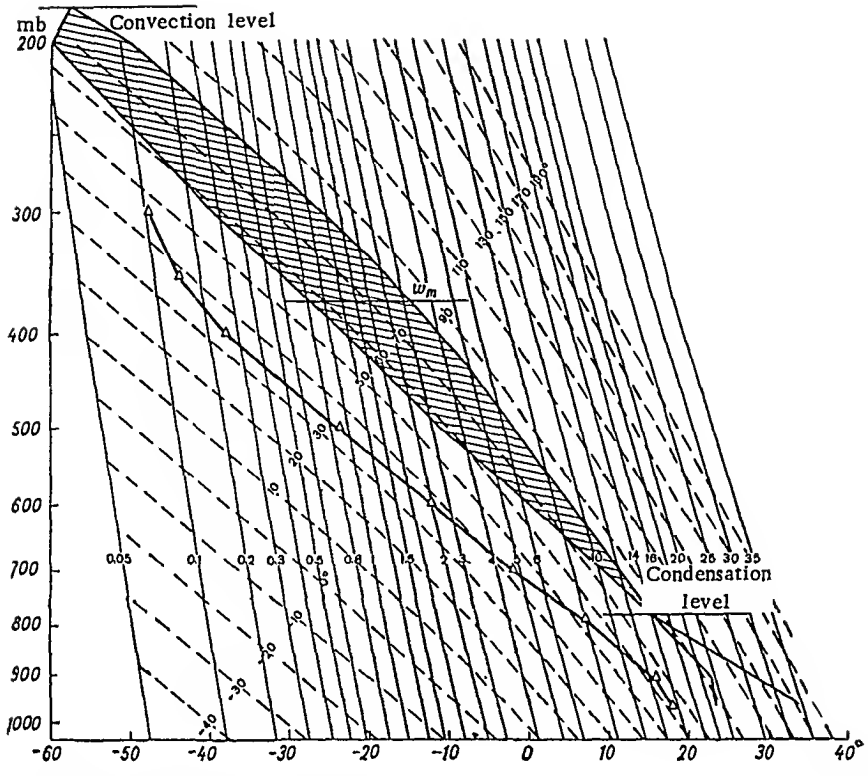

FIGURE 44. Sample calculation of maximum updraft speed w_m. (Mineral'nye Vody, radiosonde data for 0900, June 4, 1964).

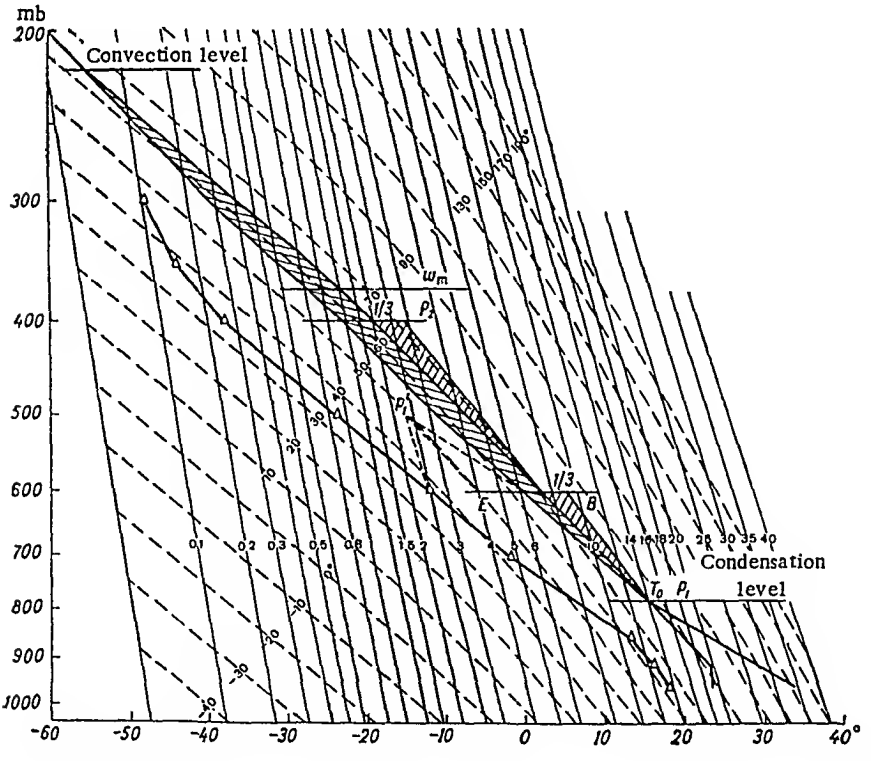

FIGURE 45. Sample calculation of maximum updraft speed w_m with allowance for entrainment.

5.3. PREPARATION OF HAIL AND THUNDERSTORM FORECASTS

Having determined w_m, t_m (the temperature at the maximum speed level) and H_0, one now uses Figure 30 to determine whether hail can form in the cloud. If the point with coordinates w_m, t_m lies in the graupel zone, the forecast should be "hail not expected"; but if the point is in the hail zone the values of w_m and H_0, via the plot of Figure 32, yield the size of hailstones that may reach the surface. If $w_m \geqslant 30$ m/sec the hail size is calculated by Eq. (2.19), as then hailstones of diameter $\geqslant 3$ cm melt only slightly when falling through the warm part of the atmosphere.

To forecast thunderstorms, one calculates the temperature at the convection level. The values of w_m and t_c° at the convection level are plotted as in Figure 42. If the point defined by w_m and t_c° falls in the thunderstorm zone, the forecast is "thunderstorm expected."

5.4. CALCULATION OF RAINFALL

It is evident from Eqs. (3.53) and (3.54) that calculation of rainfall requires a knowledge of the resolution time of instability. The latter parameter is determined from radiosonde data. Depending on the synoptic situation, one either uses actual radiosonde data or plots a prognostic stratification curve.

The instability-resolution time is determined from Eq. (3.43), where ρ_m is the density of dry air. To introduce the density of moist air Eq. (3.43) must be rewritten as

$$\tau = \tau_i + \frac{(P_0 - P_m)(P_m - P_v)(1 + 0.608 q_m)}{\rho_m S_m \bar{w}_{i.x} g (P_0 - P_v)}, \qquad (3.43')$$

where q_m is the specific humidity of the air in g/g. This may be done if one ignores the difference between the virtual temperature and the temperature of dry air, which is quite permissible at such low temperatures as are characteristic of the maximum speed level.

The factor $(1 + 0.608\, q_m)$ is generally small, so that the difference between the densities of dry and wet air at this level may be neglected.

The stages in the calculation of instability-resolution time are as follows.

1. Determine the condensation and convection levels. The convection level is determined by the point at which the stratification curve intersects the curve of state through the condensation level.

2. Calculate the maximum updraft speed from Eq. (1.55) and determine the maximum speed level.

3. Average the updraft speed over time and over the horizontal cross section of the cloud, according to the equations

$$\bar{w}_i = \frac{2}{3} w_m; \qquad (5.1)$$

$$\bar{w}_{i.x} = \frac{4}{9} w_m. \qquad (5.2)$$

4. Use density nomograms (Figure 46) to determine ρ_m for insertion in Eq. (3.43).

The value of ρ_m is determined from the temperature and pressure of the air at the maximum updraft speed level.

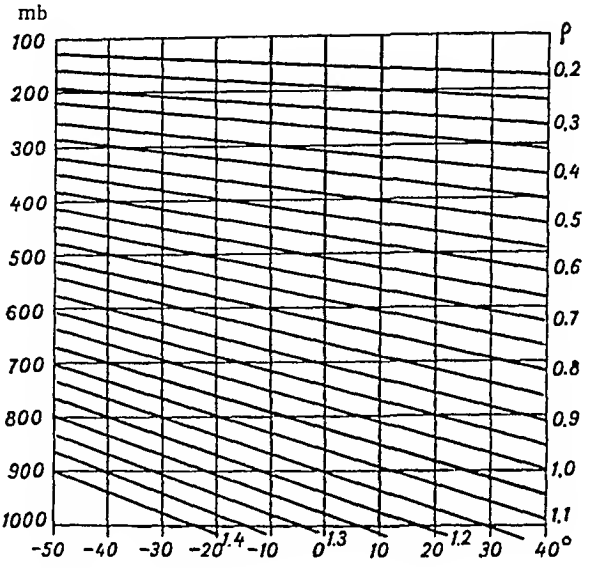

FIGURE 46. Air-density nomogram, after Smirnov.

5. Determine (P_0-P_m), (P_m-P_v), (P_0-P_v) using the aerological diagram.

6. To determine the amount of clouds at the maximum speed level from the aerological diagram, find T_m-T_{dm} and $T_{wm}-T_m$, then use Eq. (3.50') or (3.5'') to calculate S_m.

7. Using the above data and Eq. (3.43), calculate the instability-resolution time. Calculations have shown that, on the average, τ_1 is about one hour for heavy precipitation. Then calculate τ/τ_2 and insert this value in the precipitation equations (3.53) and (3.54).

A forecast prepared by these techniques applies to a representative radiosonde region (radius 100 km). To localize forecasts in North Caucasus, we have studied the aerosynoptic situations associated with intensive thunderstorm-hail processes in various parts of that area.

5.5. BASIC TYPES OF SYNOPTIC SITUATION ASSOCIATED WITH INTENSIVE THUNDERSTORMS AND HAIL IN NORTH CAUCASUS

The topography of North Caucasus is highly nonuniform. The flat region is a steppe in the west and semidesert in the east. The central region is occupied by the Stavropol' upland, to the south of which lies the Bol'shoi Kavkaz, consisting of several parallel ridges, the chief of which are the Melovoi Khrebet, Skalistyi Khrebet, Bokovoi Khrebet and Glavnyi Khrebet.

The characteristic relief is that of uplands divided into several massifs and ranges, with peaks reaching more than 5500 m. As it prevents free movement of air masses from north to south, the Bol'shoi Kavkaz constitutes a climatic barrier between the North Caucasus and Trans-Caucasia. It is a powerful source region of thunderstorms and hail /6/, and its influence on air movements reaches high altitudes. Depending on the direction of airflow, thunderstorm and hail processes are either intensified or weakened.

Over a period from 1958 to 1965, 196 incidents of thunderstorms and hail were analyzed to pinpoint the area in which convective movements are most active under different aerosynoptic conditions. Six types of situation were classified, depending on the temperature-pressure field, which make it possible to determine the areas of maximum activity and the direction of travel of thunderstorm cells.

Since the area occupied by thunderstorm activity is slightly larger than that liable to hail damage, while the distribution of these two phenomena is theoretically similar, both are governed by same types of synoptic process.

Type I. Steering flow south-westerly at the 500 mb level. The 1000—500 mb thickness chart shows a cold region over the Black Sea. Near the ground a cold front travels from the west (Figure 47).

In this case hail is observed over the Krasnodar territory, the south-west Stavropol' territory and the west of Kabardino-Balkariya. Thuderstorms occur over the entire Krasnodar and Stavropol' territories, in the south and in the mountainous regions of Kabardino-Balkariya.

Type II. On the 1000—500 mb thickness chart, a well-developed frontal zone extends from north to south perpendicular to the Caucasian Ridge. The steering flow is in the same direction (Figure 47).

In this situation, hail processes last several days. At the beginning of the process, when the westerly movement of the front along the Glavnyi Khrebet produces an orographic occlusion, hail is observed over the whole area. Source regions of hail move in three belts parallel to the Caucasian Ridge. The first belt passes through Armavir, Stavropol', Mineral'nye Vody and Novopavlovskaya; the second through Otradnaya (Krasnodar territory), Essentuki, Prokhladnaya; and the third through Karachaevsk on the Lechinkai, Nizhnii Chegem and El'khotovo.

Throughout this period, thunderstorms occur over the whole region; only toward its end do they weaken somewhat. At the end of the process the territorial distribution is the same as in Type I.

Type III. Steering flow and frontal zone in west-east direction. A cold front near the ground travels from the north over North Caucasus (Figure 47). Hail falls in isolated patches in the Krasnodar and Stavropol' territories.

Thunderstorms are observed in the Krasnodar and Stavropol' territories, and over the western parts of Kabardino-Balkariya; when air is moving in the middle troposphere with a small northerly component, thunderstorm activity is observed in the eastern regions of Kabardino-Balkariya and North Osetiya.

Type IV. Steering flow north-westerly. The 1000—500 mb thickness chart shows a cold zone over the Rostov region. Near the ground, a cold front travels north-westerly (Figure 47). Aloft over North Caucasus, there is intensive but short-lived advection of cold air. Hail falls in a belt along

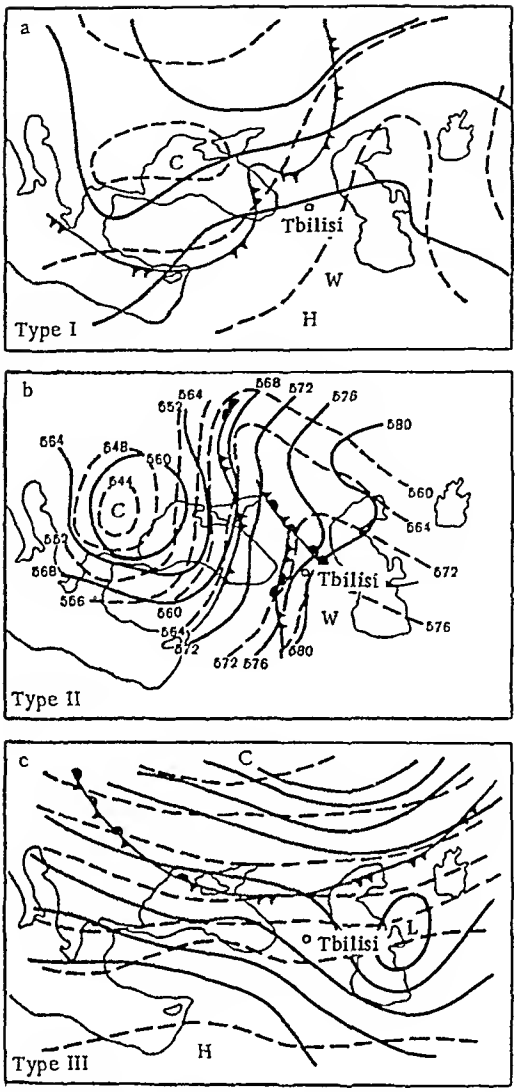

FIGURE 47 a, b, c. Temperature-pressure field in aerosynoptic situations of types I, II, III.

the southern slopes of the Caucasus, passing through Zelenchukskaya, Bermamyt, Gundelen, Nal'chik and Beslan. Thunderstorms are observed over the whole region; they are particularly heavy over the eastern parts of Kabardino-Balkariya and North Osetiya.

Type V. The temperature-pressure field shows no gradient on the 500 mb surface. The 1000—500 mb thickness chart shows a cold trough, or even a source region of cold weather, over the central part of the Caucasus (Figure 47). Hail falls only on mountains exceeding 2 km in altitud and is observed only at one or two stations. Thunderstorms extend over the whole area in isolated regions, showing a well-developed intra air-mass character. Thunderstorms sometimes begin at 1100 to 1200 hours, some outbursts continuing for the entire day. The storms end by 1900—2100 hours.

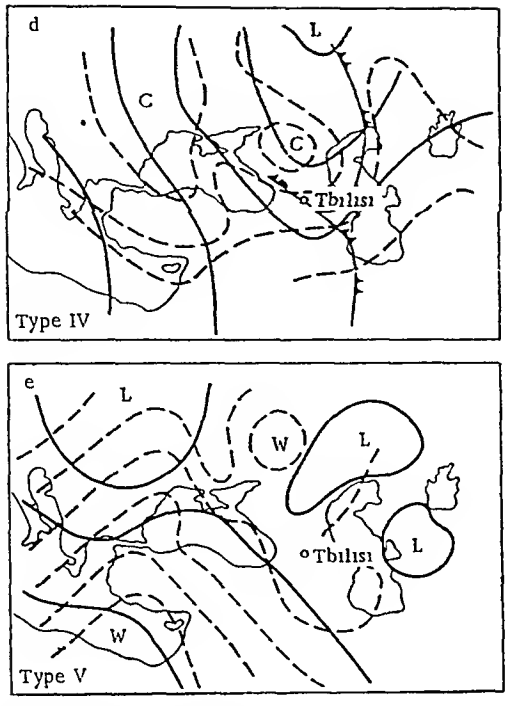

FIGURE 47 d, e Temperature pressure field in aerosynoptic situations of types IV, V

Type VI. Characterized by weak westerly transport. On the thickness chart, a heat crest lies over the eastern part of the Black Sea and West Caucasus. It is sometimes only weakly developed, but in such cases there is a well-developed cold trough over East Caucasus. The weather over North Caucasus under such conditions is relatively dry, with few clouds. Hail and thunderstorms are not observed.

The above classification may be used only to localize the prediction of hail and thunderstorm processes; in no way can it aid the actual work of forecasting. Observations have shown that such processes need not necessarily occur in synoptic situations of any of these types. The decisive factors are thermal instability and sufficient moisture reserves in the air mass, our classification only helps to determine the region in which the development of thunderstorm and hail phenomena is most probable.

5.6. SAMPLE FORECASTS OF HAIL, THUNDERSTORMS AND SHOWER-TYPE PRECIPITATION

As an example, we consider a thunderstorm-hail process that occurred in North Caucasus on June 4, 1964.

The synoptic situation was characterized by movement of a high frontal zone from west to east. The steering flow was south-westerly. In the second half of the day a secondary cold front was observed, traveling from

the north-west (Type II). The air mass was unstably stratified. According to radiosonde data over a period of 9 hours, w_m=32.8 m/sec at the 370 mb level, where the temperature t_m in the cloud, as determined by the curve of state, was −14.5°. The temperature at the convection level was t_v=−60°. The height of the zero isotherm was 4200 m. The maximum updraft speed was calculated without allowance for entrainment, since the passage was expected of a well-developed frontal zone on the 1000–500 mb thickness chart. With the help of Figure 30, the values w_m and t_m were used to determine whether hail could form in the cloud. Using Figure 32 and the values of w_m and H_0, the terminal hail size was calculated.

The calculated hailstone radius was 1.6 cm; in fact, the maximum observed radius was 1.2 cm; the hail street was about 300 km long. Figure 42 was then used to decide, according to the values of w_m and t_v, whether a thunderstorm might occur; the forecast was indeed for a thunderstorm.

To determine the precipitation, the air pressures at the surface, at the maximum speed level and at the convection level, P_0, P_m and P_v, were determined from the stratification. The respective values found were 980, 370 and 180 mb. The calculation then proceeded as follows.

1. Eq. (5.1) was used to determine the average updraft speed over time and over the cloud cross section, w_x=14.6 m/sec.

2. The nomogram of Figure 46 was used to determine the density of the air at the maximum updraft speed level from T_m and P_m:

$$\rho_m|370-27.5| = 0.55\cdot 10^{-3}\ \text{g/cm}^3.$$

3. The amount of clouds at the maximum speed level was determined from Eq. (3.50″). To this end, we first found T_m-T_{dm}=12.3 and $T_{wm}-T_m$= =13.5; Eq. (3.50″) then gave S_m=0.195.

4. Eq. (3.43) with the above data gave the value τ=1.23.

5. Finally, Eqs. (3.53) and (3.54) yielded Q_{av}=10.4 mm and Q_m=36.4 mm. The actual quantities were Q_m=39.1 mm (at the village of Zol'skoe, Kabardino-Balkar Autonomous SSR) and Q_{av}=8.9 mm.

5.7. TESTS OF THE METHODS

The hail-forecasting method described above was tested during the summers of 1964 and 1965 at the Central Forecasting Institute (TsIP, now called Gidromet-tsentr SSSR). Over the summer of 1965, the method was tried out in the hydrometeorological services (UGMS) of the following areas: Lithuania, Belorussia, North Caucasus, the Urals, Kazakhstan, the Volga, the Ukraine, the Far East, Irkutsk, Upper Volga, Central Chernozem, Turkmenistan. Some of the results of these trials are shown in Table 14. The method has been put into routine operation in some divisions of the Main Administration of the Hydrometeorological Service affiliated to the USSR Council of Ministers.

Tests of the method by the Caucasus Combined Expedition had the following results. All in all, 526 forecasts were prepared. Of these, 93% were accurate; the accuracy of "hail expected" forecasts was 91%, that of the "no-hail" forecasts 95%. Additional tests of the method at Gidromet-tsentr SSSR confirmed its high accuracy.

TABLE 14. Reliability test of hail-prediction method based on results obtained in different regions.

Forecaster	Year	Total number of forecasts				Number of "hail expected" forecasts				Number of "no hail expected" forecasts				Number of days		Percentage of phenomena occurrences predicted
		total	accurate	inaccurate	accuracy, %	total	accurate	inaccurate	accuracy, %	total	accurate	inaccurate	accuracy, %	with hail	without hail	
TsIP	1964	71	67	4	94	9	8	1	89	62	59	3	95	11	60	73
Georgian UGMS .	1964	110	97	13	88	34	29	5	85	76	68	8	89.5	37	73	79
	1965	124	103	21	83	57	48	9	84	67	55	12	82	60	64	80
Mineral'nye Vody (Civil Aviation Meteorological Station)	1965	126	118	8	97	33	29	4	88	93	89	4	95.7	33	93	88
North-Caucasian UGMS	1965	191	170	21	89	31	25	6	81	160	145	15	91	40	151	63
Moldavian UGMS .	1965	137	118	19	96	33	27	6	82	104	91	13	87.5	40	97	68
Nal'chik Hydrometeorological Service	1965	124	120	4	99	20	18	2	90	104	102	2	98	20	104	90
		883	693	90	90	217	184	33	85	666	609	57	91	241	642	76

The calculations of average and maximum amount of clouds were carried out for days with air-mass processes and thick frontal cloudiness in the years 1964—1966. The results were compared with data from the self-recording raingauge network and from meteorological posts and stations spread over the territory of the Kabardino-Balkar Autonomous SSR. The results of the comparison are shown in Table 15 and Figures 48, 49.

It should be noted that the precipitation calculations were carried out for synoptic situations of Types II, IV, V and VI, since in situations of Types I and III the maximum of the process, and sometimes even the entire thunderstorm-hail process, ultimately leaves the Kabardino-Balkar Autonomous SSR.

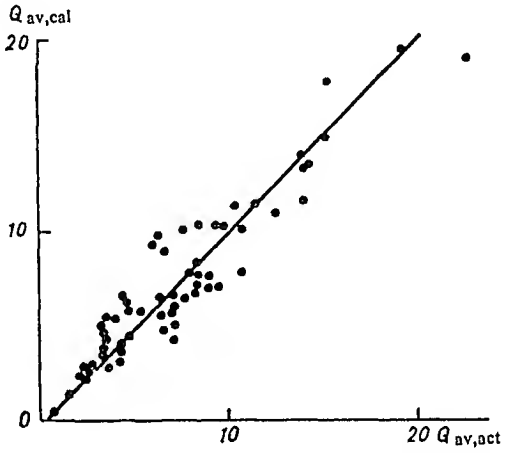

FIGURE 48. Correlation plot for $Q_{av,cal}$ and $Q_{av,act}$.

As shown by Table 16, showers exceeding 10.0 mm are observed over Kabardino-Balkariya most frequently in synoptic situations of Types II and IV; they make up respectively 58.5 and 94.0% of the total number of days on which these situations prevail. Under conditions of Types I and III, precipitation is less than 10.0 mm (when the maximum of the process leaves the area) or even zero (when the whole processes is observed outside Kabardino-Balkariya). As a rule, under Type I and III conditions shower-type precipitation may exceed 10.0 mm, but this happens outside Kabardino-Balkariya. For example, on June 9, 1964 (Type I), the maximum precipitation registered at the Ipatovo station, Stavropol' territory, was 61.7 mm; on August 24, 1965 (Type III) the maximum was 76.2 mm (registered at the Zelenchukskaya station, Stavropol' territory). Calculations for these types of situation, using radiosonde data representative as to both time and location, gave the following values for Q_m: 60.0 mm on June 9, 1964, 61.0 mm on August 24, 1965.

Analyzing the calculated figures (Figures 50 and 51, Table 17) for the average and maximum shower-type precipitations, one finds that the maximum relative error in both was ±70%; the average relative errors were ±19.8% for the average precipitation and ±18.0% for the maximum precipitation. According to Table 17, the maximum absolute error of the calculated maximum precipitation, ΔQ_m, was +24.3 mm, obtained when the actual precipitation was Q_{mact}=43.0 mm; the minimum absolute error was —16.2 mm, the actual maximum precipitation being 76.2mm.

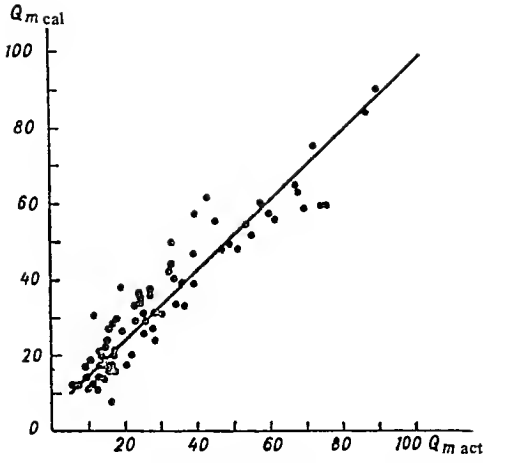

FIGURE 49. Correlation plot for $Q_{m\,cal}$ and $Q_{m\,act}$

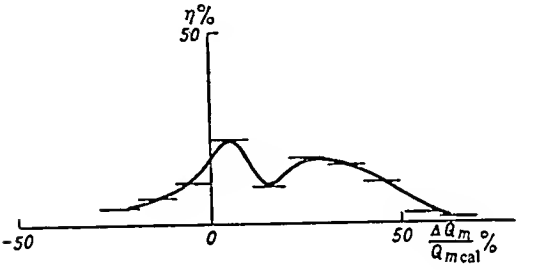

FIGURE 50. Frequency η of relative errors in calculation of average precipitation (1964–1966).

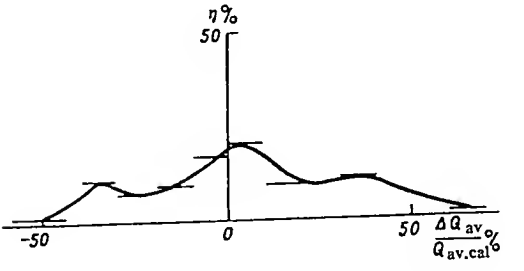

FIGURE 51. Frequency η of relative errors in calculation of maximum precipitation (1964–1966).

TABLE 15. Comparison of calculated and actual precipitation for 1964, 1965 and 1966

Date	Type	Sounding		w_m m/sec	$\bar{w}_{t,x}$ m/sec	τ hrs.	$\frac{\tau}{\tau_1}$	Q_{cal}, mm		Q_{act}, mm		ΔQ_{av}, mm	ΔQ_m, mm	$\Delta Q_{av}/Q_{av}$	$\Delta Q_m/Q_m$
		point	time of day					Q_{av}	Q_m	$Q_{av.act}$	$Q_{m\,act}$				
1964															
11/V	II	M.V.	09 00	17.3	7.6	2.1	2.1	4.2	21.4	7.1	13.1	—2.9	8.3	—69.0	8.8
25/V	V	„	15 00	16.2	5.7	3.7	3.7	3.8	20.2	3.3	9.5	0.5	10.7	11.9	3.0
2/VI	II	K.-T.	06 00	9.1	4.1	4.1	4.1	2.2	11.0	2.4	3.8	—0.2	7.2	—7.2	5.5
4/VI	II	„	06 00	30.6	13.6	1.7	1.7	7.6	38.8	8.9	39.1	—1.3	—0.3	—17.0	0.8
5/VI	II	M.V.	15 00	34.0	15.1	1.9	1.9	12 4	63.0	20.2	69.5	—7.8	—6.5	—38.6	10.3
10/VI	II	K.-T.	06 00	43.3	19.3	1.2	1.2	11.6	59.0	14.0	39.2	—2.4	—19.8	—20.7	33.6
9/VI	I	M.V.	09 00	32.0	14.2	2.0	2.0	—	60.0	—	61.7	—	—2.8	—	—2.8
12/VI	II	K.-T.	06 30	26.4	11.7	2.4	2.4	10.0	52.5	10.6	49.5	—0.6	3.0	—6.0	5.7
21/VI	IV	M.V.	03 00	31.8	14.1	1.9	1.9	10.0	53.5	7.5	32.7	2.5	20.8	25.0	39.0
25/VI	IV	K.-T.	06 00	15.2	6.7	3.7	3.7	5.3	27.3	3.4	15.0	1.9	12.3	35.8	45.0
2/VII	II	„	06 00	9.4	4.2	3.0	3.0	2.8	12.9	3.6	6.6	- 0.8	6.3	—30.4	48.7
2/VIII	IV	„	14 20	22.4	9.9	2.3	2.3	7.0	35.7	9.4	34.7	—2.4	1.0	—34.2	2.8
5/VIII	II	M.V.	03 00	19.8	8.8	3.1	3.1	7.8	39.3	10.3	27.6	—2.5	11.7	—33.0	29.8
1965															
1/V	II	K.-T.	13 20	5.9	4.4	1.7	1.7	0.4	2.0	0.8	2.0	—	—	—	—
6/V	VI	„	06 15	0	0	—	—	0	0	—	2.6	—	—	—	—
7/V	VI	„	07 00	12.8	5.7	2.4	2.4	—	13.0	—	16.2	—	—3.2		—24.6

8/V	II	M.V.	09 00	17.5	7.7	2.3	2.3	4.0	20.3	4.3	10.3	−0.3	10.0	−7.5	48.5
9/V	II	K.-T.	06 45	28.6	12.6	1.7	1.7	7.7	40.3	7.9	27.5	−0.2	12.8	−2.6	31.4
10/V	II	„	06 45	16.3	7 0	2.0	2.0	4.7	18.3	6.6	15.2	−1.9	3.1	−40.0	17.0
11/V	II	M.V.	15 00	31.2	13.8	2.3	2.3	13.5	68.8	14.2	68.6	−0.7	0.2	−0.5	0.3
12/V	V	K.-T.	06 00	0	0	—	—	0	0	—	0	—	—	—	—
16/V	II	„	07 00	22.4	10.0	1.8	1.8	6.2	31.2	4.5	17.0	1.7	14.2	27.6	45.5
19/V	V	„	07 00	8.5	3.8	3.7	3.7	—	9.5	—	4.0	—	—	—	—
20/V	V	„	07 00	0	0	—	—	0	0	—	0	—	—	—	—
21/V	V	„	07 00	7.8	0	—	—	0	0	—	0	—	—	—	—
22/V	V	„	07 00	20.5	8.9	1.5	1.5	—	17.8	—	21.2	—	−3.4	—	−12.0
23/V	V	„	06 50	10.6	4.7	3.5	3.5	—	13.0	—	10.2	—	2.8	—	21.6
26/V	V	„	06 00	0	0	—	—	0	0	—	0	—	—	—	—
28/V	V	„	06 00	0	0	—	—	0	0	—	0	—	—	—	—
29/V	V	„	06 00	0	0	—	—	0	0	—	0	—	—	—	—
30/V	V	„	06 00	0	0	—	—	0	0	—	0	—	—	—	—
1/VI	IV	„	06 20	10.8	4.8	2.4	2.4	2.2	10.1	—	7.8	—	—	—	—
2/VI	V	„	06 50	0	0	—	—	0	0	—	8.5	—	—	—	—
5/VI	IV	M.V.	15 00	18.9	8.4	2.5	2.5	6.1	25.6	7.1	28.5	−2.0	−2.9	−38.2	−11.3
6/VI	IV	K.-T.	07 00	23.8	10.6	2.0	2.0	6.6	35.4	7.0	23.6	−0.4	11.8	−6.1	33.3
7/VI	II	M.V.	09 00	12.9	5.7	2.4	2.4	2.6	13.2	—	10.8	—	2.4	—	18.2
8/VI	II	K.-T.	07 00	32.8	17.9	1.7	1.7	10.3	51.5	9.4	51.2	0.9	0.3	9.2	0.6
9/VI	II	M.V.	15 00	51.7	23.0	1.4	1.4	17.7	88.7	15.2	86.6	2.5	2.1	14.1	2.4
11/VI	VI	K.-T.	06 50	0	0	—	—	0	0	—	9.1	—	—	—	—
14/VI	II	„	13 50	27.0	12.0	3.2	3.2	13.3	67.3	14.0	43.0	−0.7	24.3	−5.3	35.8
16/VI	I	M.V.	09 00	21.6	9.6	2.1	2.1	6.7	33.8	8.2	30.4	−1.5	3.4	−22.4	10.0
17/VI	I	„	09 00	29.4	13.1	2.1	2.1	10.3	5.0	8.4	47.0	1.9	5.0	19.0	9.6

TABLE 15. (Contd.)

Date	Type	Sounding		w_m m/sec	$\bar{w}_{t,\tau}$ m/sec	τ hrs.	$\frac{\tau}{\tau_1}$	Q_{cal}, mm		Q_{act}, mm		ΔQ_{av}, mm	ΔQ_m, mm	$\Delta Q_{av}/Q_{av}$	$\Delta Q_m/Q_m$
		point	time of day					Q_{av}	Q_m	$Q_{av.act}$	$Q_{m\,act}$				
18/VI	II	K.-T.	12 30	34.6	15.4	2.8	2.8	19.3	98.0	19.1	90.0	0.2	8.0	1.0	8.1
19/VI	IV	"	13 35	26.6	11.8	2.8	2.8	11.3	58.5	10.2	53.5	1.1	5.0	9.7	8.5
20/VI	IV	M.V.	09 00	43.4	19.3	1.6	1.6	—	79.0	—	72.5	—	6.5	—	8.2
23/VI	V	K.-T.	06 45	24.2	10.7	2.3	2.3	—	38.5	—	24.2	—	14.3	—	37.0
24/VI	V	"	06 45	16.4	7.3	3.1	3.1	—	28.2	—	27.8	—	0.4	—	1.4
25/VI	IV	"	14 50	10.0	4.4	1.7	1.7	1.4	7.6	3.9	9.8	—	—2.2	—	—29.0
26/VI	IV	M.V.	09 00	24.0	10.6	2.2	2.2	8.2	44.4	8.2	33.9	0	10.5	0	23.7
27/VI	IV	K.-T.	06 15	11.5	5.1	3.5	3.5	3.7	18.4	4.2	13.4	—0.6	5.0	—17.4	27.2
28/VI	IV	"	06 15	18.5	8.2	2.8	2.8	65.5	32.8	6.4	26.6	0.1	6.2	1.5	18.9
29/VI	IV	"	06 15	7.9	3.5	2.2	2.2	1.2	5.9	1.5	4.0	—	—	—	—
30/VI	V	"	06 45	19.0	8.4	3.5	3.5	—	35.8	—	36.0	—	—0.2	—	0.6
1/VII	IV	"	06 10	35.0	15.5	1.7	1.7	11.4	58.2	11.4	45.0	0	13.2	0	22.6
2/VII	V	"	06 20	39.6	17.6	1.5	1.5	—	59.5	—	60.4	—	—0.9	—	—1.5
3/VII	V	"	13 00	32.2	14.3	1.7	1.7	—	49.5	—	39.0	—	10.5	—	21.2
4/VII	V	M.V.	09 00	15.5	6.9	2.1	2.1	—	8.9	—	10.0	—	—1.1	—	—12.3
5/VII	IV	"	15 00	20.4	9.1	2.3	2.3	5.6	27.7	6.5	25.4	—0.9	2.3	—16.9	8.3
6/VII	IV	K.-T.	06 20	12.2	5.4	2.9	2.9	3.0	15.5	4.2	9.0	—1.2	6.5	—40.0	42.0
7/VII	II	"	06 20	35.0	15.6	2.1	2.1	14.0	70.0	13.9	67.2	0.1	2.8	0.8	4.0
9/VII	V	"	06 00	0	0	—	—	0	0	—	0	—	—	—	—
10/VII	V	"	12 50	0	0	0	0	0	0	—	1.5	—	—	—	—
11/VII	II	"	06 10	20.0	8.9	2.3	2.3	6.6	33.2	4.3	28.3	2.2	10.3	34.0	31.0

15 /II	II	.	06 10	0	0	—	—	0	0	—	0	—	—	—	—
16/VII	II	.	06 10	0	0	—	—	0	0	—	1.2	—	—	—	—
17/VII	II	.	06 10	0	0	—	—	0	0	—	10.0	—	—	—	—
19/VII	IV	.	11 50	31.4	13.9	1.3	1.3	6.4	32.6	7.6	25.0	1.2	7.6	—18.8	23.3
20/VII	II	M.V.	03 00	23.7	10.5	2.0	2.0	6.8	36.6	8.9	24,0	—2,1	12.6	29.0	34.4
24/VII	V	K.-T.	06 20	0	0	—	—	0	0	—	10.0	—	—	—	—
25/VII	V	.	06 20	14.8	0.6	5.2	5.2	—	32.4	—	23.2	—	9,2	—	28.4
26/VII	V	M.V.	03 00	0	0	—	—	0	0	—	5.0	—	—	—	—
27/VII	V	K.-T.	12 35	19.3	8.6	1.8	1.8	—	21.4	—	17.2	—	4,2	—	19.6
30/VII	V	.	06 20	0	0	—	—	0	0	—	0	—	—	—	—
2/VIII	V	.	06 20	0	0	—	—	0	0	—	0.6	—	—	—	—
3/VIII	V	.	06 20	0	0	—	—	0	0	—	0	—	—	—	—
4/VIII	II	.	06 20	0	0	—	—	0	0	—	3.2	—	—	—	—
5/VIII	II	.	06 20	0	0	—	—	0	0	—	7.3	—	—	—	—
8/VIII	II	.	06 25	0	0	—	—	0	0	—	2.4	—	—	—	—
9/VIII	VI	M.V.	09 00	0	0	—	—	0	0	—	5.5	—	—	—	—
10/VIII	IV	K.-T.	06 05	0	0	—	—	0	0	—	0	—	—	—	—
12/VIII	V	.	06 20	0	0	—	—	0	0	—	1.5	—	—	—	—
13/VIII	II	.	06 20	0	0	—	—	0	0	—	10.0	—	—	—	—
14/VIII	II	.	06 20	0	0	—	—	0	0	—	10.0	—	—	—	—
23/VIII	V	.	13 02	0	0	—	—	0	0	—	0	—	—	—	—
24/VIII	III	M.V.	03 00	45.6	20,3	1.2	1.2	—	61.0	—	76.2	—	—15.2	—	—25.0
25/VIII	V	.	09 00	0	0	—	—	0	0	—	9.1	—	—	—	—
26/VIII	V	K.-T.	06 15	12,4	5,5	2,6	2,6	—	13.7	—	11.1	—	2.6	—	19.0
28/VIII	VI	.	08 45	0	0	—	—	0	0	—	1.8	—	—	—	—
30/VIII	II	M.V.	09 00	49.0	21.7	1,4	1.4	—	76.0	—	86.4	—	—10.4	—	—13.7

TABLE 15. (Contd.)

Date	Type	Sounding		w_m m/sec	$\overline{w_t}$, x m/sec	τ hrs.	$\frac{\tau}{\tau_1}$	Q_{av}, mm		Q_{act}, mm		ΔQ_{cp}, mm	ΔQ_m, mm	$\Delta Q_{av}/Q_{av}$	$\Delta Q_m/Q_m$
		point	time of day					Q_{av}	Q_m	$Q_{av.act}$	$Q_{m\,act}$				
31/VIII	V	K.-T.	06 25	0	0	—	—	0	0	—	34.0	—	—	—	—
1966															
2/V	IV	M.V.	15 00	24.0	10.6	1.5	1.5	5.0	27.0	3.2	19.8	1.8	7.2	56.0	36.4
4/V	IV	K.-T.	06 00	13.5	6.0	2.0	2.0	2.6	72.3	2.5	7.6	0.3	4.7	12.0	62.0
10/V	II	"	12 10	19.0	8.4	1.4	1.4	3.4	17.5	3.3	16.1	0.1	1.4	23.5	8.7
13/V *	II	"	12 10	16.0	7.1	1.6	1.6	2.8	14.2	2.3	13.0	0.5	1.2	3.0	9.2
21/V	II	"	06 40	0	0	—	—	0	0	—	9.4	—	9.4	—	—
22/V	II	"	12 05	23.0	10.2	2.1	2.1	6.3	32.4	3.9	18.9	2.4	13.5	61.5	71.5
23/V	II	"	06 05	16.8	7.5	2.3	2.3	4.4	22.1	4.8	17.3	—0.4	4.8	8.3	27.8
24/V	II	M.V.	15 00	15.7	7.0	2.0	2.0	3.3	16.7	5.2	15.8	—	—	—	—
30/V	II	"	09 00	7.8	3.5	1.6	1.6	0.9	4.4	small	7.9	—	—3.5	—	—
31/V	II	"	09 00	18.3	8.1	2.0	2.0	4.7	23.5	3.3	15.0	1.4	8.5	42.5	56.5
4/VI	II	K.-T.	12 35	0	0	—	—	0	0	0	0	0	0	—	—
5/VI	II	"	12 35	0	0	—	—	0	0	—	1.0	—	—1.0	—	—
6/VI	II	"	11 00	0	0	—	—	0	0	1	14.5	—	—14.5	—	—
7/VI	II	M.V.	15 00	27.2	12.9	1.4	1.4	8.9	45.5	6.6	32.7	2.3	12.8	35.0	39.0
8/VI **	II	K.-T.	06 00	0	0	—	—	0	0	—	0	0	0	—	—
14/VI	IV	"	06 00	0	0	—	—	0	0	—	6.9	—	—6.9	—	—
15/VI	IV	"	12 45	23.5	10.4	1.6	1.6	5.8	31.0	4.6	17.8	1.2	13.2	26.2	74.0

26/VI	IV	"	10 55	27.6	12.3	2.1	2.1	9.1	46.5	6.0	33.1	3.1	13.4	34.5	28.8
28/VI	IV	"	12 45	0	0	—	—	0	0	0	0	0	0	0	0
3/VII	II	"	12 45	30.4	13.5	1.9	1.9	10.9	54.8	12.4	55.0	−1.5	−0.2	−12.1	−0.36
4/VII	II	M.V.	03 00	15.7	7.0	2.6	2.6	6.2	21.0	9.8	21.7	−3.6	−0.7	−36.8	−3.2
10/VII	II	K.-T.	06 00	0	0	—	—	0	0	—	0	0	0	0	0
11/VII	II	"	06 00	0	0	—	—	0	0	—	0	0	0	0	0
20/VII	IV	"	06 00	0	0	—	—	0	0	—	0	0	0	0	0
24/VII	II	"	06 00	0	0	—	—	0	0	—	0	0	0	0	0
25/VII	II	"	06 00	0	0	—	—	0	0	—	0	0	0	0	0
27/VII	II	"	06 00	22.2	9.5	2.5	2.5	7.6	41.6	8.1	29.7	−0.5	11.6	−6.2	39.0
31/VII	II	"	06 00	0	0	—	—	0	0	—	1.4	—	1.4	—	—
2/VIII	II	M.V.	09 00	27.7	12.3	2.0	2.0	9.7	42.6	6.2	35.2	3.5	7.4	51.5	20.4
3/VIII	II	K.-T.	06 20	18.4	8.2	1.6	1.6	3.2	16.0	2.7	14.2	0.5	1.6	18.5	11.3
11/VIII	II	"	15 00	33.6	14.9	1.9	1.9	13.2	67.4	21.4	57.6	−9.2	9.8	−43.0	17.0
12/VIII	II	"	13 00	0	0	—	—	0	0	—	0	0	0	0	0
13/VIII	II	"	13 50	0	0	—	—	0	0	—	0	0	0	0	0
14/VIII	II	"	13 50	0	0	—	—	0	0	—	0	0	0	0	0
15/VIII	II	"	13 50	0	0	—	—	0	0	—	0	0	0	0	0
16/VIII	II	"	06 00	0	0	—	—	0	0	—	0	0	0	0	0
17/VIII	II	"	06 00	0	0	—	—	0	0	—	0	0	0	0	−0.7
18/VIII	II	"	06 00	16 0	7.1	1.5	1.5	2.7	14.0	—	14.1	—	−0.1	—	−0.7
19/VIII	IV	"	06 00	11.2	5.0	2.4	2.4	2.3	11.3	2.2	12.5	0.1	1.2	4.5	−9.6
24/VIII	II	"	06 00	25.0	21.1	1.6	1.6	5.7	29.2	5.1	16.7	0.6	12.5	11.8	75.0

* May 14, 15, 16 and 25 — steady rain.

** June 9, 10 and 13, July 5 and 28 — steady rain.

TABLE 16. Frequency of showers over Kabardino-Balkariya in different types of synoptic situation

Type	Number of days with showers						
	total	> 10 mm		< 10 mm		no precipitation	
		days	%	days	%	days	%
I	20	6	30.0	14	70.0	0	0
II	24	14	58.5	8	33.4	2	8.1
III	29	1	5.2	14	73.6	4	21.2
IV	16	15	94.0	1	6.0	0	0
V	33	12	36.4	11	33.3	10	30.3
VI	6	1	16.7	4	66.6	1	16.7

TABLE 17. Results of comparison of calculated and actual precipitation

Year	ΔQ_m mm		$\frac{\Delta Q_m}{Q_m}$ %		ΔQ_{av} mm		$\frac{\Delta Q_{av}}{Q_{av}}$ %	
	max. ($Q_{m\,act}$)	min. ($Q_{m\,act}$)	max.	av.	max. ($Q_{m\,act}$)	min. ($Q_{av.\,act}$)	max.	av.
1964	+20.8 (32.7)	−6.5 (69.5)	+65.5	± 21.9	2.5 (7.5)	−7.8 (20.2)	− 69.0	± 21.3
1965	+24.3 (43.0)	−16.2 (76.2)	+48.5	± 17.6	2.5 (15.2)	−2.1 (8.9)	− 40.0	± 15.3
1966	+21.6 (19.7)	−1.9 (2.2)	+52.0	± 15.6	3.5 (6.2)	−9.2 (21.4)	+ 70.0	± 22.9
Max. over 3 years	+24.3 (43.0)	−16.2 (76.2)	+65.5	± 18.0	+3.5 (6.2)	−9.2 (21.4)	+ 70.0	±19.8

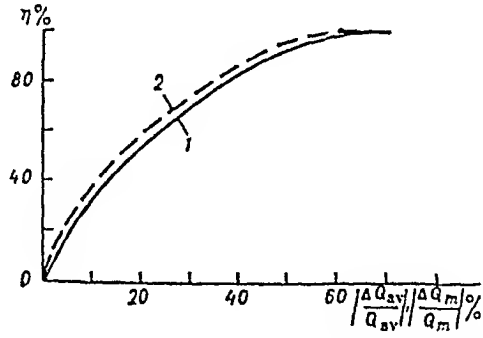

FIGURE 52. Frequency η of relative errors in calculation of mean (1) and maximum (2) amount of precipitation.

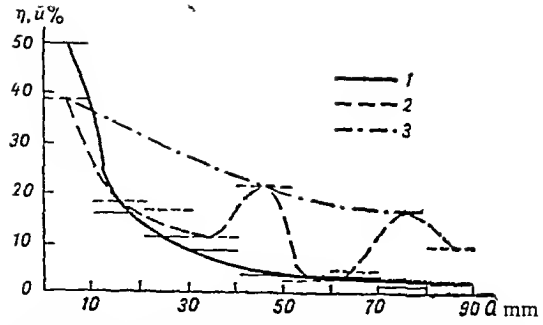

FIGURE 53. Frequency η and mean relative error $\bar{u}$ in calculation of Q_m as a function of amount of precipitation Q.

1 — mean relative error in the calculation of precipitation;
2 — frequency distribution of amount of precipitation;
3 — averaged frequency.

TABLE 18. Q_m values calculated with and without allowance for τ, compared with actual precipitation, for days with heavy showers

$\frac{\Delta Q_m}{Q_m}$ % with allowance for τ		$\frac{\Delta Q_m}{Q_m}$ % with allowance for τ	
max.	av.	max.	av.
+ 37.0	+ 14.5; −3.2%	−252.0	−94.6; + 20%

TABLE 19. *Frequency η of relative errors in calculation of maximum and average precipitation for 1964, 1965 and 1966*

$\frac{\Delta Q_m}{Q_{m\,cal}}$ %	$\eta = \frac{N_l}{N}$ %	$\frac{\Delta Q_{av}}{Q_{av,cal}}$ %	$\eta = \frac{N_l}{N}$ %
±10	33	±10	37
±20	50	±20	55
±30	72	±30	73
±40	90	±40	95
±50	96	±50	97
±60	99	±60	99
±70	100	±70	100

TABLE 20. Frequency η of relative errors and average relative error $\bar{u}$ in calculation of precipitation, as function of precipitation Q_m

Q_m, mm	$\eta = \frac{N_{Q_i}}{N}$ %	$\bar{u} = \frac{\Delta Q_m}{Q_m}$ %
0.0 − 10.0	50.3	±39.0
10.1 − 20.0	16.0	±18.0
20.1 − 30.0	11.5	±16.7
30.1 − 40.0	8.4	±11.5
40.1 − 50.0	3.8	±21.9
50.1 − 60.0	3.1	±2.7
60.1 − 70.0	3.1	±4.3
70.1 − 80.0	1.5	±16.6
80.1 − 90.0	2.3	±9.4

The maximum absolute error ΔQ_{av} was +3.5 mm, obtained when the actual figure was +6.2 mm; the minimum was −9.2 mm, the actual figure being −21.4 mm.

The average relative error in the calculated maximum precipitation for days with heavy showers, without allowance for the instability-resolution time, was −94.6% (see Table 18; one case, in which the error was +20.0%, has been excluded).

However, calculation of the maximum and average errors does not provide a reliable characterization of the method. Accordingly, Figures 50, 51 and 52, and Table 19 describe the distribution of the relative errors found in calculation of the average and maximum amounts of precipitation. One sees from Table 19 that approximately 75% of all the forecasts were accurate to within ±30% (this estimate applies to the calculated figures for both average and maximum precipitation).

It is also interesting to examine the variation of the average relative error as the precipitation increases.

Table 20 and Figure 53 present data on the variation of the average relative error as a function of the precipitation. Figure 53 is based on the data of Table 20. Plotted against the amount of precipitation Q are the relative frequency η of days with different precipitation amounts and the average relative error $\bar{u}$ in the calculation of Q_m.

In the calculations of the maximum (see Figure 51), the predicted precipitation is generally greater than the actual figure: in 80% of the cases $Q_{mcal} > Q_{mact}$. This may be because the instrument is not always capable of registering the maximum precipitation, as the probability that the maximum will occur precisely at the location of the instrument is of course extremely small (the distance between the instruments was on the average from 6 to 10 km). As for the error in the calculated average precipitation, the distribution is almost symmetric (same frequency of overestimates as underestimates). The reason for this is possibly that the updraft speeds are assumed to behave similarly over quite a wide range; in particular, we assume that the distribution of w_m across the cloud is parabolic, while Shishkin's data apply primarily to the time variation of the maximum updraft speed. However, these data were derived for speeds $10.0 < w_m < 20.0$ m/sec, and it is therefore quite possible that Shishkin's curve of w_m plotted against time is valid only under restricted conditions. In case of cumulonimbus clouds with $w_m > 20$ m/sec, the time distribution of w_m may be different, requiring a sizable correction in the precipitation calculations.

5.8. ESTIMATED EFFICIENCY OF METHODS

Bagrov /3/ has shown that data on the accuracy of a method are in themselves inadequate to provide an idea of its efficiency. He proposes the following criterion:

$$H = \frac{u - u_r}{1 - u_r}, \tag{5.3}$$

TABLE 21. Calculation of accuracy of method for prediction of shower-type precipitation

Year	Total number of forecasts				Number of shower forecasts												Actual number of days with precipitation			Percentage of phenomena occurrences predicted		
					0.0 – 3.5 mm				3.6 – 8.0 mm				> 8.0 mm									
	total	accurate	inaccurate	accuracy, %	total	accurate	inaccurate	accuracy, %	total	accurate	inaccurate	accuracy, %	total	accurate	inaccurate	accuracy, %	0.0 – 3.5 mm	3.6 – 8.0 mm	> 8.0 mm	0.0 – 3.5 mm	3.6 – 8.0 mm	> 8.0 mm
1964	13	13	0	100.0	0	0	0	–	0	0	0	–	13	13	0	100.0	0	0	13	–	–	100.0
1965	78	65	13	83.5	34	23	11	67.0	2	1	1	50.0	42	40	2	95.3	23	7	48	100.0	14.3	83.5
1966	40	36	4	90.0	19	16	3	84.2	1	1	0	100.0	20	19	1	95.0	16	3	21	100.0	33.4	90.5
	131	114	17	87.0	53	39	14	73.6	3	2	1	66.6	75	72	3	96.0	39	10	82	100.0	20.0	88.0

where H is the reliability, u_r is the total accuracy of all random forecasts (i. e., forecasts obtained unmethodically, guesses), u the total accuracy of the method. To estimate the accuracy of random forecasts, one defines the frequency of an event as the ratio of the number of its actual occurrences to the total number of cases:

$$\varphi_1 = \frac{N_1}{N};\ \varphi_2 = \frac{N_2}{N},$$

where φ_1 and φ_2 are the natural frequencies, N_1 and N_2 the numbers of cases in which the event occurs and does not occur, respectively, and N is the total number of cases.

The total accuracy of the random forecasts is

$$u_r = \varphi_1\pi_1 + \varphi_2\pi_2, \tag{5.4}$$

where π_1, π_2 are the frequencies of forecasts of the event in question, relative to the total number of forecasts. The data of Table 21 yield a value of 0.74 for the reliability of our hail-prediction method. Similar calculations give the reliability of the thunderstorm-prediction method as 0.86.

In order to determine the reliability of the method for predicting shower-type precipitation, a three-phase gradation of precipitation was used, in analogy with that employed at Gidromet-tsentr SSSR /79/: 0.0 – 3.5 mm (slight rain), 3.6 – 8.0 mm (rain), > 8.0 mm (heavy rain). Moreover, if the actual precipitation was seen to be greater or less than the predicted amount, the forecast was considered inaccurate.

The value of H, and also $\varphi_1, \varphi_2, \varphi_3, \pi_1, \pi_2, \pi_3$, may be calculated from the data in Table 21.

Use of Eq. (5.4) gave the total accuracy of random forecasts as 0.499. According to the data of Table 21, the total accuracy of the method, based on 131 forecasts, was 0.87. The reliability of the shower-precipitation method, based on the above gradation, was then found from Eq. (5.3) to be 0.74

To be efficient in practice, a prediction method should have reliability of at least 0.2 – 0.3. Thus, the figures obtained above for the efficiency of our methods for prediction of hail, thunderstorms and showers show that they are quite effective and may be recommended for practical and routine use.

CONCLUSION

The work carried out at the High-Altitude Geophysics Institute from 1960 to 1968 has shown that methods based on the mechanism of shower formation and on the thermodynamic state of the atmosphere yield highly reliable forecasts of the weather phenomena associated with the development of convective clouds. The conclusions drawn from this research are as follows.

1. The potential development of convective clouds depends not only on the lapse rate and relative humidity of the air, but to a large extent on the ratio of the masses of air in the active layer and in the penetrating convection layer.

2. The development of convection is influenced by vertical wind shear.

3. Analysis of the distribution of vertical velocities with respect to time and with respect to the horizontal cross section of the cloud shows that the most favorable distribution curve of velocities across the cloud is a parabola with parameter $p = 4.5 \cdot 10^8$ cm/sec.

4. The level at which the updraft speed reaches a maximum coincides with the level of the maximum radar reflection from the cloud. This level is characterized by maximum deviation of the curve of state from the stratification curve.

5. The major hail-producing factor is the existence of conditions for wet growth in a convective cloud; this in turn depends on the maximum updraft speed and on the temperature at that level, calculated from atmospheric stratification data.

6. A necessary condition for the initiation of a thunderstorm is that the cloud contain large-drop and crystal fractions.

7. Prediction of the amount of heavy shower precipitation requires consideration of the resolution time of atomspheric instability and of the time necessary for moisture to collect in the accumulation zone.

8. The calculations have shown that in intensive processes the accumulation time is on the average one hour.

9. The maximum amount of shower-type precipitation depends on the maximum updraft speed and on the instability-resolution time. The latter in turn depends on the updraft speed, averaged over time and over the horizontal cross section of the cloud, and also on the relative masses of the stratification layers. The average precipitation depends on the average updraft speed.

10. Accumulation of moisture in the atmosphere may be a recurrent process.

11. Calculations have shown that the instability-resolution time may be as long as two hours, in keeping with the conclusion that accumulation of moisture due to stratification of air masses may be a recurrent process.

12. Our methods for prediction of hail, thunderstorms and showers are applicable to the territory in which the radiosonde data are representative

(a radius of 100—150 km from the sounding point). The earliness of the forecast depends on whether a prognostic stratification curve may be constructed.

13. The accuracy of the methods depends to a large degree on how well the prognostic stratification curve represents the changes of state of the atmosphere when air transport aloft is considerable and there are significant changes of pressure at the surface.

14. Since our methods are based on the physical essence of the phenomena involved, they should be applicable regardless of the physico-geographical features of the territory.

15. Localization of the forecasts requires a study of the distribution of intensive processes over territory, depending on the synoptic situation.

The accuracy of the hail and shower forecasts is more than 90%, furnishing confirmation of the assumed mechanism underlying the method. At any rate, the implication is that in 90% of cases the hail-formation process corresponds to the theories developed at the High-Altitude Geophysics Institute.

The earliness of the forecast depends on the length of time for which the atmospheric stratification is predicted, allowing for advection as determined from pressure charts; it is at most 24 hours.

The authors believe that the immediate problem is now how to predict precipitation from frontal clouds over the entire area of passage of the front, thus eliminating the restriction to the representative sounding area. An indispensable requirement for solution of this problem is to increase the length of time elapsing before occurrence of the predicted phenomena. This may probably be done by devising a suitable thermodynamic model of a cold front and determining the conditions for resolution of atmospheric instability over a large area in frontal processes.

The complications that arise in this context are due to the need to allow for horizontal airflow and for the specific time-dependence of the various atmospheric parameters. It may be possible to eliminate the time factor, as has been done in the solution of actual problems, but the question is as yet far from clear. All that one can say with certainty is that the problem is far from solution.

BIBLIOGRAPHY

1. Anchugova, R.A. K voprosu o dinamike razvitiya radioekho ot kuchevo-dozhdevykh oblakov (On the Dynamics of Development of Radar Echos from Cumulonimbus Clouds). — Trudy Glavnoi Geofizicheskoi Observatorii, No. 224. 1968.
2. Balabuev, A.G. K voprosu formirovaniya moshchno-kuchevykh oblakov v gornykh usloviyakh (On the Formation of Cumulus Congestus in Mountainous Areas). — Trudy Instituta Geografii AN Gruz SSR, Vol. 25, No.1. 1967.
3. Bagrov, N.A. K voprosu otsenki gidrometeorologicheskikh prognozov (On the Estimation of Hydrometeorological Forecastings). — Meteorologiya i Gidrologiya, No. 6. 1958.
4. Bachurina, A.A. Sovremennoe sostoyanie metoda prognoza osadkov (Present State of the Procedure for Forecasting Precipitation). — Meteorologiya i Gidrologiya, No. 6. 1962.
5. Barukova, Yu. A. et al. O kolichestve i intensivnosti osadkov iz konvektivnykh oblakov (On the Amount and Intensity of Precipitation from Convective Clouds). — Trudy Glavnoi Geofizicheskoi Observatorii, No. 104. 1960.
6. Belentsova, V.A. and N. I. Glushkova. Aerosinopticheskie usloviya obrazovaniya grozovo-gradovykh ptotsessov na severnom Kavkaze (Aerosynoptic Conditions of Formation of Thunderstorm and Hail Processes in North Caucasus). — Trudy Vysokogornogo Geofizicheskogo Instituta, No. 11. 1968.
7. Belentsova, V.A. Prognoz groz v usloviyakh Severnogo Kavkaza (Forecasting of Thunderstorms in North Caucasus). — Trudy Vysokogornogo Geofizicheskogo Instituta, No.5. 1966.
8. Bibilashvili, N. Sh. Nekotorye voprosy struktury konvektivnykh potokov v kuchevykh i moshchno-kuchevykh oblakakh (Some Aspects of the Structure of Convective Flow in Cumulus and Cumulus Congestus). — In: Fizika oblakov i osadkov, Vol. 2. Moskva, Izdatel'stvo AN SSSR. 1961.
9. Bibilashvili, N. Sh. Osobennosti koagulyatsionnogo rosta gradin, svyazannye s izmeneniem skorosti vertikal'nykh potokov po vysote (Features of the Coalescence Growth of Hailstones Associated with the Change of Vertical Current Velocity with Height). — Izvestiya AN SSSR, Seriya Geofizicheskaya, No. 4. 1960.
10. Bibilashvili, N. Sh., V. F. Lapcheva, and G.K. Sulakvelidze. Vodnost' v kapel'nykh oblakakh i nekotorye voptosy prognoza livnevykh osadkov (Liquid-Watet Content in Droplet Clouds and Some Problems in the Fotecasting of Showers). — Doklady AN SSSR, Vol. 131, No.3. 1960.
11. Bibilashvili, N. Sh. et al. Vliyanie izmeneniya vertikal'noi sostavlyayushchei skorosti vetra na obrazovanie livnevykh osadkov i grada (Effect of Variation in the Vertical Component of Wind Speed on the Formation of Showers and Hail). — Doklady AN SSSR, Vol. 128, No.3. 1959.
13. Bogatyr', L.F. and A.I. Romov. Svoistva atmosfery i nekotorye aerosinopticheskie usloviya pri grozakh i livnyakh na territorii Ukrainy (Properties of the Atmosphere and Some Aerosynoptic Conditions in Thunderstorms and Showers over the Territory of the Ukraine). — Trudy Kievskoi Glavnoi Fizicheskoi Observatorii, No. 1. 1952.
14. Bordovskaya, L.I. Nekotorye kharakteristiki sostoyaniya atmosfery pri vnutrimassovykh livnevykh osadkakh v gornykh raionakh (Some Characteristics of the State of the Atmosphere in Intra Air-Mass Shower-Type Precipitation over Mountainous Regions). — Trudy Vysokogornogo Geofizicheskogo Instituta, No. 3(5). 1966.
15. Budilova, E.P. and N.S. Shishkin. Raschety kolichestva skondensirovannoi vlazi v konvektivnykh oblakakh (Calculation of the Amount of Condensed Moisture in Convective Clouds). — Trudy Glavnoi Geofizicheskoi Observatorii, No. 47 (109). 1954.
16. Budilova, E.P. and V.G. Lenshin. O prognoze intensivnosti atmosfernoi konvektsii po metodu sloya (Forecasting of the Intensity of Atmospheric Convection by the Slice Method). — Trudy Glavnoi Geofizicheskoi Observatorii, No. 202. 1967.
17. Bel'tishchev, N.F. K voprosu ob interpretatsii mezostruktury polya oblachnosti (Interpretation of the Mesostructure of the Field of Cloudiness). — Trudy MMTs, No. 8. 1965.

18. Vinnichenko, N.K. et al. Turbulentnost' v svobodnoi atmosfere (Turbulence in the Free Atmosphere). — Leningrad, Gidrometeoizdat. 1968.
19. Vorob'eva, E.F. and B. N. Trubnikov. Yacheikovaya konvektsiya pri anizotropnoi turbulentnosti i nalichii polya otnositel'no vikhrya (Cellular Convection in Anisotropic Turbulence in the Presence of Relative Vortex Field). — Trudy Tsentral'noi Astronomicheskoi Observatorii, No. 75, 1967.
20. Vul'fson, N. I. Kompensatsionnye niskhodyashchie techeniya, obuslovlennye razvivayushchimsya kuchevymi oblakami (Compensatory Downdrafts Due to Developing Cumulus Clouds). — Izvestiya AN SSSR, Seriya Geofizicheskaya, No.1. 1957.
21. Vul'fson, N.I. Issledovanie konvektivnykh dvizhenii v svobodnoi atmosfere (Investigation of Convective Movements in the Free Atmosphere). — Izdatel'stvo AN SSSR. 1961.
22. Gandin, L.S. Ob ustoichivosti voin u poverkhnosti razdela potokov napraviennykh pod uglom drug k drugu (On Stability of Waves at the Surface Separating Flows at an Angle to Each Other). — Izvestiya AN SSSR, Seriya Geofizicheskaya, No.3. 1957.
23. Gandin, L.S. Ob obrazovanii turbulentnykh dvizhenii na frontakh (On the Formation of Turbulent Motions at Fronts). — Trudy Glavnoi Geofizicheskoi Observatorii, No. 76. 1958.
24. Glushkova, N.I. and V.F. Lapcheva. K voprosu prognoza livnevykh i gradovykh osadkov, voznikayushchikh vo vnutrimassovykh moshchno-kuchevykh oblakakh (Forecasting of Showers and Hail in Intra Air-Mass Cumulus Congestus Clouds). — Trudy ELE, Vol. 2 (5). Moskva, Izdatel'stvo AN SSSR. 1961.
25. Glushkova, N.I. Metod prognoza grada i livnya (A Method for Forecasting Hail and Showers). — Trudy Vysokogornogo Geofizicheskogo, Instituta, No. 3(5). 1966.
26. Glushkova, N.I. Nekotoryc utochneniya prognoza grada (Some Improvements in Hail Forecasting). — Trudy Vysokogornogo Geofizicheskogo Instituta, No.5. 1966.
27. Goral', G.G. Opredelenie vremeni razvitiya zony akkumulyatsii do nachala obrusheniya (Determination of the Time of Development of the Accumulation Zone up to the Beginning of its Collpase). — Trudy Vysokogornogo Geofizicheskogo Instituta, No.5. 1966.
28. Gritsenko, M.V. and A.F. Dyubyuk. Polnyi zapas energii neustoichivosti vozdushnykh mass nad Moskvoi (The Complete Reserves of Instability Energy of Air Masses over Moscow). — Meteorologiya i Gidrologiya, No. 5. 1939.
29. Gigineishvili, V.M. Gradobitiya v Vostochnoi Gruzii (Hail Damage in East Georgia). — Leningrad, Gidrometeoizdat. 1960.
30. Grigor'eva, A.S. and O.A. Drozdov. K voprosu o primenenii kharakteristik vlagooborota k kolichestvennomu prognozu osadkov (On Application of the Characteristics of the Hydrological Cycle to Quantitative Forecasting of Precipitation). — Trudy Glavnoi Geofizicheskoi Observatorii, No. 89. 1959.
31. Gutman, L.N. K teorii kuchevoi oblachnosti (On the Theory of Cumulus Clouds). — Izvestiya AN SSSR, Seriya Geofizicheskaya, No.7. 1961.
32. Dovgalyuk, Yu. A. Nekotorye osobennosti razvitiya konvektivnykh oblakov (Some Features of the Development of Convective Clouds). — Meteorologiya i Gidrologiya, No. 6. 1968.
33. Drozdov, O.A. O razlichiyakh v znacheniyakh temperatury i vlazhnosti v svobodnoi atmosfere v dni s osadkami i vdni bez osadkov (On Differences in Temperature and Humidity Figures in the Free Atmosphere on Days with Precipitation and on Days without Precipitation). — Trudy Glavnoi Geofizicheskoi Observatorii, No. 50 (112). 1955.
34. Drozdov, O.A. O korrelyatsionnoi forme svyazi vlagosoderzhaniya s osadkami pri izuchenii vlagooborota (On the Correlation of Moisture Content and Precipitation in Studying the Hydrological Cycle). — Trudy Glavnoi Geofizicheskoi Observatorii, No. 62 (124). 1956.
35. Zavertnev, M.P. and L.M. Lapteva. O korrelyatsionnoi svyazi mezhdu vlagosoderzhaniem oblaka i kolichestvom vypadayushchikh livnevykh osadkov (On the Correlation of the Moisture Content of a Cloud and the Amount of Showery Precipitation). — Trudy Vysokogornogo Geofizicheskogo Instituta, No. 11. 1968.
36. Zverev, A.S. et al. Kurs meteorologii (A Course of Meteorology). — Leningrad, Gidrometeoizdat. 1951.
37. Ivanidze, T.G. O prognoze groz s ispol'zovaniem indeksa neustoichivosti (Thunderstorm Forecasting Using an Instability Index). — Trudy Tsentral'nogo Instituta Prognozov, No. 158. 1966.
38. Imyanitov, I.M. Elektricheskaya struktura moshchnykh konvektivnykh oblakov i ee svyaz' s dvizheniem vozdukha v oblakakh (Electrical Structure of Thick Convective Clouds and its Connection with Air Motion in Clouds). — In: Issledovaniya oblakov, osadkov i grozovogo elektrichestva. Moskva, Izdatel'stvo AN SSSR. 1961.

39 Imyanitov, I M and T V Lobodin Issledovanie elektricheskoi struktury livnevykh i grozovykh oblakov (Investigation of the Electrical Structure of Shower and Thunderstorm Clouds) — Trudy Glavnoi Geofizicheskoi Observatorii, No 196 1962

40 Ivanov, V V and V A Zimenkov Raschet tayaniya gradin v estestvennykh protsessakh (Calculation of the Melting of Hailstones in Natural Processes) — Trudy Vysokogornogo Geofizicheskogo Instituta, No. 3(5) 1966

41 Kasatkin, I I Mikrosinopticheskie nablyudeniya nad dozhdyami, proizvedennye v Moskve v 1919, 1921, i 1922 gg (Microsynoptic Observations of Rain Carried Out in Moscow in 1919, 1921 and 1922) — Zapiski Meteorologicheskogo Obshchestva, No 3. 1927

42 Kasatkin, I I Sinopticheskie nablyudeniya nad dozhdyami, proizvedennye v Moskve s 23 po 27/VII 1912 g. (Synoptic Observations of Rain Carried Out in Moscow from 23 to 27 July, 1912) — Meteorologicheskii Vestnik, No 4 1919

43 Kasatkin, I I Nablyudeniya nad oblakami v Moskve letom 1905 g (Observations of Clouds in Moscow during the Summer of 1905). — Meteorologicheskii Vestnik, Nos 17—18 1906

44. Kartsivadze, A I et al. Nekotorye kharakteristiki radiolokatsionnykh otrazhenii ot livnevykh osadkov i grada (Some Characteristics of Radar Reflections from Showers and Hail) — Trudy Vsesoyuznogo soveshchaniya po aktivnym vozdeistviyam na gradovye protsessy Tbilisi 1964

45. Kachurin, L G Zamerzanie polidispersnykh vodyanykh aerozolei (Freezing of Polydisperse Water Aerosols). — Izvestiya AN SSSR, Seriya Geofizicheskaya, No 2 1951

46. Koval'chuk, A N Pole vetra i grad (Field of Wind and Hail) — Trudy Vysokogornogo Geofizicheskogo Instituta, No. 11 1968

47 Krichak, O G Sinopticheskaya meteorologiya (Synoptic Meteorology) — Leningrad, Gidrometeoizdat 1956.

48. Krasnogorskaya, N V Issledovanie protsessov elektrizatsii chastits i osadkov (Investigation of Electrification Processes of Particles and Precipitation). — Izvestiya AN SSSR, Seriya Geofizicheskaya, No. 1. 1960

49. Lapteva, L.M and N.M Mal'bakhova Nekotory voprosy prognozirovaniya konvektivnoi oblachnosti metodom sloya (Some Aspects of the Prediction of Convective Cloudiness by the Slice Method) — Trudy Vysokogornogo Geofizicheskogo Instituta, No. 3(5) 1966.

50 Lapteva, L M Otsenka vremeni razresheniya neustoichivosti (Estimation of the Resolution Time of Instability). — Trudy Vysokogornogo Geofizicheskogo Instituta, No. 3(5) 1966

51 Lapteva, L.M Raschet ball'nosti konvektivnykh oblakov s pomoshch yu metoda sloya (Calculation of the Amount of Convective Clouds by the Slice Method) — Trudy Vysokogornogo Geofizicheskogo Instituta, No 5 1966.

52. Lapteva, L M and G K Sulakvelidze Nekotorye utochneniya k voprosu rascheta prodolzhitel nosti razresheniya neustoichivosti v atmosfere (Some Improvements in Methods for Calculating the Resolution Time of Instability in the Atmosphere). — Trudy Vysokogornogo Geofizicheskogo Instituta, No 11. 1968

53. Lapteva, L M Metod prognozirovaniya kolichestva livnevykh osadkov (Method of Forecasting the Amount of Shower-Type Precipitation) — Trudy Vysokogornogo Geofizicheskogo Instituta, No 5 1966.

54. Laikhtman, D L O volnovykh dvizheniyakh na poverkhnosti razdela v atmosfere (On Wave Motions on the Boundary Surface in the Atmosphere). — Trudy Glavnoi Geofizicheskoi Observatorii, No 2 (64) 1947

55. Lebedev, S L. O vozniknovenii i evolyutsii konvektivnogo oblaka (On the Formation and Evolution of Convective Clouds). — Trudy Vysokogornogo Geofizicheskogo Instituta, No 3 (5) 1966

56. Lebedeva, N V Postroenie modeli konvektsii i raschet kolichestva livnevykh osadkov (A Model of Convection and Calculation of the Amount of Shower-Type Precipitation) — Trudy Tsentral'nogo Instituta Prognozov, No. 31 (58) 1954

57. Lebedeva, N V., E M Orlova, and V M Cherkasskaya K prognozu livnevykh osadkov i groz (Forecasting of Showers and Thunderstorms). — Metodicheskoe Ukazanie Tsentral'nogo Instituta Prognozov, Vol. 14. 1951

58 Lebedeva, N V Prognoz livnei i groz (Forecasting of Showers and Thunderstorms) — In Sbornik metodicheskikh ukazanii po aviatsionnoi meteorologii Tsentral nyi Institut Prognozov 1959

59. Lebedeva, N V Konvektsiya na frontakh i v tsiklonicheskikh oblastyakh (Convection at Fronts and in Cyclone Regions) — Trudy Tsentral'nogo Instituta Prognozov, No. 38(65). 1955

60 Lenshin, V G, G.I. Osipova, and N S Shishkin O prognoze kolichestva vnutrimassovykh livnevykh osadkov (Forecasting of the Amount of Intra Air-Mass Shower-Type Precipitation) — Trudy Glavnoi Geofizicheskoi Observatorii, No. 126 1962

61. Mamina, E.F. and E.K. Fedorov. O vodnom balanse oblachnoi sistemy (On the Water Balance of a Cloud System). — Izvestiya AN SSSR, Seriya Geofizicheskaya, No. 5. 1959.
62. Muchnik, V.M. K prognozirovaniyu posleporudennykh livne i groz (Forecasting of Afternoon Showers and Thunderstorms). — Trudy Kievskoi Glavnoi Fizicheskoi Observatorii, No.1. 1952.
63. Matveev, L.T. Osnovy obshchei meteorologii (Principles of General Meteorology). — Leningrad, Gidrometeoizdat. 1965.
64. Nakorenko, N. F. and F.G. Tokar'. Raspredelenie temperatury i vlazhnosti v oblakakh (Temperature and Humidity Distribution in Clouds). — Trudy NIG Glavnogo Upravleniya Gidrometeorologicheskoi Sluzhby, Ser. 1, No.21. 1946.
65. Orlova, E.M. and N.V. Petrenko. Usloviya tsirkulyatsii, blagopriyatnye dlya razvitiya vnutrimassovykh groz i livnei (Circulation Conditions Favorable for the Development of Intra Air-Mass Thunderstorms and Showers). — Trudy NIU Glavnogo Upravleniya Gidrometeorologicheskoi Sluzhby, Ser. 2, No. 6. 1943.
66. Orlova, E.M. Konvektivnye vnutrimassovye osadki (Convective Intra Air-Mass Precipitation). — Trudy NIU Glavnogo Upravleniya Gidrometeorologicheskoi Sluzhby, Ser. 2, No. 14. 1946.
67. Orlova, E.M. K voprosu ob izmenenii stratifikatsii vozdukha (On the Problem of Changes in Stratification of the Air). — Trudy Tsentral'nogo Instituta Prognozov, No. 19. 1949.
68. Orlova, E.M. K voprosu ob opredelenii izmenenii stratifikatsii vozdukha (On the Determination of Changes in Stratification of the Air). — Trudy Tsentral'nogo Instituta Prognozov, No. 25 (52). 1951.
69. Orlova, E.M. K voprosu o roli fronta v voznikonovenii livnevykh osadkov (On the Role of Fronts in the Formation of Showers). — Trudy Tsentral'nogo Instituta Prognozov, No. 38. 1955.
70. Orlova, E.M. Raschet kolichestva i prodolzhitel'nosti livnevykh osadkov (Calculation of the Amount and Duration of Shower-Type Precipitation). — Trudy Gidromettsentra SSSR, No. 13.·1967.
71. Pavlovskaya, A.A. Aerologicheskie kharakteristiki termicheskoi konvektsii razlichnoi intensivnosti (Aerological Characteristics of Thermal Convection of Different Intensities). — Trudy Tsentral'nogo Instituta Prognozov, No. 79. 1959.
72. Pastushkov, R.S. O razvitii kuchevykh oblakov v atmosfere s vertikal'nym sdvigom vetra (On the Development of Cumulus Clouds in an Atmosphere with Vertical Wind Shear). — Meteorologiya i Gidrologiya, No. 4. 1969.
73. Pastushkov, R.S. and S.M. Shmeter. Vliyanie vertikal'nykh dvizhenii v moshchnykh konvektivnykh oblakakh na pole vetra (Effect of Vertical Motions in Thick Convective Clouds on the Wind Field). — Izvestiya AN SSSR, Fizika Atmosfery i Okeana, Vol. 4, No. 3. 1968.
74. Peskov, B.E. Raschet maksimal'noi vysoty verkhnei granitsy kuchevo-dozhdevykh oblakov s uchetom vovlecheniya v razlichnykh sinopticheskikh usloviyakh (Calculation of Maximum Height of the Tops of Cumulonimbus Clouds with Allowance for Entrainment under Various Synoptic Conditions). — Trudy Vysokogornogo Geofizicheskogo Instituta, No. 11. 1968.
75. Peskov, B.E. and A.I. Snitkovskii. K prognozu sil'nykh shkvalov (Forecasting of Heavy Squalls). — Meteorologiya i Gidrologiya, No. 7. 1968.
76. Pinus, N.Z. Vertikal'nye dvizheniya v grozovykh oblakakh (Vertical Motions in Thunderstorm Clouds). — Doklady AN SSSR, Vol. 150, No.4. 1963.
77. Ponomarenko, S.I., G.A. Kashel'kova, and P.A. Mukhina. Rezul'taty ispytaniya razlichnykh sposobov prognoza groz (Results of Trials of Various Thunderstorm-Forecasting Methods). — Trudy Tsentral'nogo Instituta Prognozov, No. 149. 1966.
78. Rukovodstvo po kratkosrochnym prognozam pogody (Handbook of Short-Range Weather Forecasting). Parts 1 and 2. — Leningrad, Gidrometeoizdat. 1964.
79. Ponomarenko, S.I. and N.V. Abramicheva. O prognozakh kolichestva livnevykh osadkov (Forecasts of the Amount of Shower-Type Precipitation). — Meteorologiya i Gidrologiya, No. 2. 1967.
80. Selezneva, E.S. Ogranitsakh i vertikal'noi moshchnosti konvektivnykh oblakov (On the Boundaries and Vertical Thickness of Convective Clouds). — Trudy Glavnoi Geofizicheskoi Observatorii, No. 93. 1959.
81. Selezneva, E.S. and M.P. Churinova. Nekotorye kharakteristiki sostoyaniya atmosfery pri razvitii kuchevykh i kuchevo-dozhdevykh oblakov (Some Characteristics of the State of the Atmosphere in the Development of Cumulus and Cumulonimbus Clouds). — Trudy Glavnoi Geofizicheskoi Observatorii, No. 102. 1960.
82. Selezneva, E.S. Usloviya obrazovaniya kuchevykh oblakov po nablyudeniyam letom 1946 g. (Conditions for the Formation of Cumulus Clouds according to Observations Carried out in the Summer of 1946). — Trudy Glavnoi Geofizicheskoi Observatorii, No. 7 (69). 1948.

83. Selezneva, E.S. Raspredelenie temperatury i vlazhnosti vdni s kuchevoi oblachnost'yu (Temperature and Humidity Distribution on Days with Cumuliform Clouds). — Trudy Glavnoi Geofizicheskoi Observatorii, No. 13 (75). 1948.
84. Skvortsov, A.A. O teplovoi konvektsii i obmene v prizemnom sloe atmosfery (On Thermal Convection and Heat Transfer in the Lowest Layer of the Atmosphere). — Izvestiya AN SSSR, Seriya Geofizicheskaya, No. 6. 1951.
85. Slavin, I.A. Metod otsenki konvektivnoi neustoichivosti i opredelenie raionov (A Method for Estimation of Convective Instability and Determination of Regions). — Informatsionnyi Sbornik Nauchno-Issledovatel'skogo Otdela Akademii im. A.F. Mozhaiskogo, No. 43. Leningrad. 1959.
86. Sosin, G.L. K prognozu groz v Zakavkaz'e (Thunderstorm Forecasting in Transcaucasia). — Meteorologiya i Gidrologiya, No. 8. 1963.
87. Sulakvelidze, G.K., N.Sh. Bibilashvili, and V.F. Lapcheva. Obrazovanie osadkov i vozdeistvie na gradovye protsessy (Formation of Precipitation and Modification of Hail Processes). — Leningrad, Gidrometeoizdat. 1965.
88. Sulakvelidze, G.K. Fizicheskie osnovy vozdeistviya na oblachnost' s tsel'yu predotvrashcheniya gradovykh yavlenii (Physical Principles of Cloud Modification for the Suppression of Hail). — Doklady AN SSSR, Vol. 144, No.4. 1962.
89. Sulakvelidze, G.K. and N.Sh. Bibilashvili. O vozmozhnosti izmereniya vodnosti oblakov i intensivnosti osadkov s pomoshch'yu RLS, rabotayushchei na dvukh dlinakh voln (Possibility of Measuring the Liquid-Water Content of Clouds and Precipitation Intensity by Operating Radar Stations on Two Wavelengths). — Trudy Vysokogornogo Geofizicheskogo Instituta, No. 3 (5). 1966.
90. Sulakvelidze, G.K. Livnevye osadki i grad (Showety Ptecipitation and Hail). — Leningrad, Gidrometeoizdat. 1967.
91. Sulakvelidze, G.K. Energiya razvitiya konvektivnogo oblaka (Enetgy of Development of a Convective Cloud). — Meteorologiya i Gidrologiya, No. 10. 1967.
92. Tkachenko, A.V. O moshchenosti konvektsii i ee ispol'zovanii pri lokal'nykh prognozakh (On the Depth of Convection and its Use in Local Forecasts). — Trudy Glavnoi Geofizicheskoi Observatorii, No. 69. 1957.
93. Ttubnikov, B.N. Issledovaniya vozdushnykh potokov nad gornymi raionami s uchetom termicheskoi neodnorodnosti podstilayushchei poverkhnosti (Investigations of Airflow over Mountainous Regions with Allowance for the Thermal Inhomogeneity of the Underlying Surface). — Izvestiya AN SSSR, Seriya Geofizicheskaya, No.2. 1964.
94. Shishkin, N.S. Oblaka osadki i grozovoe elektrichestvo (Clouds, Precipitation and Thunderstorm Electricity). — Leningtad, Gostekhizdat. 1954.
95. Shishkin, N.S. Ispol'zovanie metoda sloya dlya prognoza vertikal'noi moshchnosti konvektivnykh oblakov (Utilization of the Slice Method for Forecasting the Vertical Thickness of Convective Clouds). — Trudy Glavnoi Geofizicheskoi Observatorii, No. 54 (116). 1955.
96. Shishkin, N.S. O prognoze groz i livnei po metodu sloya (Forecasting of Thunderstorms and Showers Using the Slice Method). — Meteorologiya i Gidrologiya, No.7. 1957.
97. Shishkin, N.S. K raschetu skorosti vertikal'nogo razvitiya konvektivnogo oblaka (Calculation of the Vertical Growth Rate of Convective Clouds). — Trudy Glavnoi Geofizicheskoi Observatorii, No. 104. 1960.
98. Shishkin, N.S. Oblaka, osadki i grozovoe elektrichestvo (Clouds, Precipitation and Thunderstorm Electricity). — Leningrad, Gidrometeoizdat. 1961.
99. Shishkin, N.S. O prognoze maksimal'nogo kolichestva osadkov v gornykh raionakh (Forecasting of Maximum Precipitation in Mountainous Regions). — Trudy Glavnoi Geofizicheskoi Observatorii, No. 186. 1966.
100. Shishkin, N.S. O roste i raspade konvektivnykh oblakov pri neustoichivoi stratifikatsii atmosfery (Growth and Dissipation of Convective Clouds in an Unstably Stratified Atmosphere). — Trudy Glavnoi Geofizicheskoi Observatorii, No. 82. 1958.
101. Shishkin, N.S. and N.I. Glushkova. Sposoby prognoza grada (Methods of Hail Forecasting). — Metodicheskoe Pis'mo Tsentral'nogo Instituta Prognozov, Edited by A.A. Bachurina. Moskva. 1965.
102. Shmeter, S.M. and V.I. Silaeva. Vertikal'nye potoki vnutri kuchevo-dozhdevykh oblakov (Vertical Flows Inside Cumulonimbus Clouds). — Meteorologiya i Gidrologiya, No. 10. 1966.
104. Khrgian, A. Kh. Raspredelenie udel'noi vlazhnosti nad Moskvoi (Distribution of Specific Humidity over Moscow). — Trudy Tsentral'noi Astronomicheskoi Observatorii, No. 1. 1947.
105. Khrgian, A. Kh. Raspredelenie udel'noi vlazhnosti v svobodnoi atmosfere (Distribution of Specific Humidity in the Free Atmosphere). — Izvestiya AN SSSR, Seriya Geograficheskaya i Geofizicheskaya, Vol. 11, No.2. 1947.

106. Cherkasskaya, V.M. Osobennosti vozniknoveniya i razvitiya vnutrimassovykh konvektivnykh osadkov pri raziichnykh sinopticheskikh poiozhenlyakh (Features of the Formation and Development of intra Air-Mass Convective Precipitation in Different Synoptic Situations). — Trudy Tsentrai'nogo instituta Prognozov, No. 31 (58). 1954.
107. Chepovskaya, O.i. Predvaritci'nye rezul'taty issiedovaniya raspredeienlya grada na poverkhnosti zemii (Preliminary Results of an Investigation of Hail Distribution at the Earth's Surface). — Trudy Vysokogornogo Geofizicheskogo instituta, No. 3(5). 1966.
108. Appleman, H.S. Investigation of Hail Formation. Dynamics of Cumuius Clouds [Russian Transiation.] 1964.
109. Pastukh, V.N. and R.F. Sokhrina. Grad na territorii SSSR (Hail over the Territory of the USSR). — Trudy Giavnoi Geofizicheskoi Observatorii, No. 74. 1967.
110. Riehi, H. Tropicai Meteorology. — New York, McGraw-Hiil. 1954.
111. Shmeter, S.M. Polc vctra v okrestnostyakh kuchevo-dozhdevykh obiakov (Wind Ficid in the Vicinity of Cumulonimbus Clouds). — Meteorologiya i Gidrologiya, No. 11. 1962.
112. Atlas, D. Thc Baiancc Lcvci in Convcctive Storms. — Atmosph. Sci., Voi. 23, No.6. 1966.
113. Austin, Y.E. — J. Met., Voi. 5, No. 3. 1948.
114. Beckwith, W.B. Hail Observations in the Denver Area. — United Air Lines Circular, No. 40. 1956.
115. Bergeron, T. On the Physics of Clouds and Precipitation. — Proc. 5th Assembiy U.G.G.I. 2. Lisbon. 1935.
116. Bjerkncs, J. Saturatcd-Adiabatic Ascent of Air through Dry-Adiabatically Descending Environment. — Q. Ji. R. Met. Soc., Voi. 64, No. 275. 1938.
117. Berry, F.A., E. Boiiay, and H.R. Byers. Handbook of Meteorology. — New York, McGraw-Hili Book Company. 1945.
118. Bigg, E.K. The Supercooling of Water. — Proc. Phys. Soc., Vol. 66. 1953.
119. Brunt, D. Natural and Artificiai Clouds. — Q. Ji. Met. Soc., Vol. 63. 1937.
120. Byers, H. R. and R. R. Braham. Thunderstorm Structure and Circulation. — J. Met., Vol. 5, No. 3. 1948.
121. Browning, K.A. and F. H. Ludiam. Airflow in Convective Storms. — Q. Ji. R. Met. Soc., Voi. 88. 1962.
122. Dessens, H. La grêie et sa prévention. — Association d'études des moyens de lutte conue ies fléaux atmosphériques, No. 13. Toulouse. 1965.
123. Dinger, J.E. and R. Gunn. Electrical Effects Associated with a Change of State of Water. — Terr. Magn. Atmos. Elect., Voi. 51. 1946.
124. Dougias, R.H. and W. Hitschfeid. Studies of Alberta Hailstorms. — Sci. Rep. No. 27, Montreai Univ. 1958.
125. Doi, K. Formation and Movement of Precipitation Clouds. — Geophys. Mag., Vols. 1,2. 1962.
126. Fawbush, E.J. and R.C. Miller. — Buil. Am. Met. Soc., Voi. 34, No.6. 1953.
127. Findeisen, W. and H. Schulz. Experimental Study of Formation of icy Particles [Russian Transiation.] — in: Physics of Precipitation Formation, Moscow, Inostrannaya Literatura. 1951.
128. Fiohn, H. Hochgebirge und aiigemeine Zirkuiation. — Arch. Met. Geophys. Bioklim., Voi. 3. 1953.
129. Frenkel, J. A Theory of the Fundamentai Phenomena of Atmospheric Eiectricity. — J. Phys. USSR, Voi. 8. 1944.
130. Eister, J. and H. Geitei. Zur Influenztheorie der Niederschiagscicktrizitat. — Phys. Z., Voi. 14. 1913.
131. Haman, K. On the Accumuiation of Liquid Water in a Buoyant Jet and its Reiation to Hail Phenomena. — Acta geophys. poi., Voi. 15, No.1. 1967.
132. Haurwitz, B. The Perturbation Equations in Meteorology. — Compend. met. Boston. 1951.
133. Karaip, R. A New Theory of Hail. — In: Geographical Survey (Russian Transiation. 1960).
134. Kuettner, J. The Electrical and Meteorological Conditions inside Thunder Clouds. — J. Met., Voi.7. 1950.
135. Kessler, E. The Kinetic Correlation between the Wind and the Distribution of the Precipitation. — J. Met., Vol. 18. 1961.
136. Lenard, P. Über Regen. — Met. Z., Vol. 21. 1904.
137. List, R. Zur Aerodynamik von Hageikörner. — Z. angew. Math. Phys., Voi. 10. 1959.
138. List, R. Zur Thermodynamik teiiweise wässeriger Hageikörner. — Z. angew. Math. Phys., Voi. 11, 1960.
139. Ludiam, F.H. The Composition of Coagulation Elements in Cumuionimbus. — Q. Ji. R. Met. Soc., Voi. 76. 1950.

140. Ludlam, F.H. The Production of Showers by the Coalescence of Cloud Droplets. — Q. Jl. R. Met. Soc., Vol. 77. 1951.
141. Ludlam, F.H. The Production of Showers by the Growth of Ice Particles. — Q. Jl. R. Met. Soc., Vol. 78. 1952.
142. Ludlam, F.H. Hailstorm Studies. — Nubila Anno, No. 1. 1958.
143. Ludlam, F.H. and W.K. Macklin. Some Aspects of Severe Storm in SE England. — Nubila Anno, No. 2. Verona. 1959.
144. Malkowski, G. Zum Zusammenhang von Höhenströmung und Niederschlagsmende am Boden. Gerlands Beitr. Geophys., Vol. 74, No. 1. 1965.
145. Malkus, J. S. — Trans. Am. Geophys. Un., Vol. 30. 1949.
146. Malkus, J. S. — Q. Jl. R. Met. Soc., Vol. 78. 1952.
147. Malkus, J.S. and C. Ronne. On the Structure of Some Cumulonimbus Clouds which Penetrated the High Tropical Troposphere. — Tellus, Vol. 6. 1954.
148. Malan, D. J. and B. F.J. Schonland. The Distribution of Electricity in Thunder Clouds. — Proc. Phys. Soc. A, Vol. 209. 1951.
149. Mason, B. J. The Physics of Clouds. — Oxford Univ. Press. 1957.
150. Moore, C.B. et al. Gushes of Rain and Hail after Lightning. — J. Atmosph. Sci., No. 6. November. 1964.
151. Muller, W. Prévision de l'etendue des chutes de grêle, aide apportee à la grêle. — Bull. Observ. Puy-de-Dome.
152. MacCready, P.B. Jr., K.M. Beesmer, and T.J. Lockhart. Cloud Electrification Study. — Met. Res. J. Pasadena Calif. 1959.
153. Naito, K. Internal Gravity-Shear Waves in the Troposphere. — Can. J. Phys., Vol. 44. Toronto. 1966.
154. Newton, C.W. and S. Katz. — Bull. Am. Met. Soc., Vol. 39. 1958.
155. Newton, C.W. Hydrodynamic Interactions with Ambient Wind Field as a Factor in Cumulus Development. — 2nd Conference on Cumulus Convection, Portsmouth, New Hampshire, May. 1959. Proceedings, New York, Pergamon Press. 1960.
156. Pettersen, S. Weather Analysis and Forecasting. — New York, McGraw-Hill. 1968.
157. Prohasko, K. Die jahrliche und tägliche Periode der Gewitter und Hagelfalle in Steinmark und Kaerten. — Met. Z., Vol. 17. 1900.
158. Rossi, V. Aerologische Untersuchungen über die Feuchtlabilität der Luft in Finland besonders in Gewitter und Schauerwetterlagen. — Mitt. Met. Inst. Univ. Helsing., No. 44. 1940.
159. Saha, K.R. Hailstorms and their Effects on Aircraft. — Indian J. Met. Geophys., Vol. 12. 1961.
160. Sarrica, O. La grandine a Roma il 3 e 4 Cennoio. 1959. Italiane. — Atti Conv. Ass. geofis. ital. Feb. 1959.
161. Sekera, Z. Helmholtz Waves in a Linear Temperature Field with Vertical Wind Shear. — J. Met., Vol. 5, No.3. 1948.
162. Simpson, G. C. On Electricity of Rain and its Origin in Thunderstorms. — Phil. Trans. R. Soc. A, Vol. 209. 1909.
163. Simpson, G.C. and F. J. Scrase. Distribution of Electricity in Thunder Clouds. — Proc. R. Soc. A, Vol. 161. 1937.
164. Simpson, G.C. and G.D. Robinson. The Distribution of Electricity in Thunderclouds, I. — Proc. R. Soc. A, Vol. 177. 1941.
165. Simpson, G.C. The Electricity of Cloud and Rain. — Q. Jl. R. Met. Soc., Vol. 68. 1942.
166. Stommel, H. Entrainment of Air into a Cumulus Cloud. — J. Met., Vol. 8, 1947.
167. Schumann, T. E. W. The Theory of Hailstone Formation. — Q. Jl. R. Met. Soc., Vol. 64. 1938.
168. Schenk, G. Wassergehaltmessungen in Unwettern. — Met. Abh. Inst. Met. Geophys. Berl., Vol. 92, No. 2. 1968 — 1969.
169. Skuars, P. Mixing Processes in Convective Clouds and their Application to the Cumulonimbus Anvils. — In: Dynamics of Cumulus Clouds (Russian translation. 1964).
170. Vittori, O., Di Suiliano and Caporicco. The Density of Hailstones. — Nubila Anno, 2. Verona. 1959.
171. Wall, E. Das Gewitter. — Wett. Klima, Vol. 7. 1948.
172. Weickmann, H.K. The Language of Hailstorms and Hailstones. — Nubila Anno, VI, No.1. 1964.
173. Weickmann, H.K. Observational Data of the Formation of Precipitation in Cumulonimbus Clouds. Chicago. 1953.
174. Wilson, C.T.R. Some Thunderstorm Problems. — J. Franklin Inst., Vol. 1. 1929.